UNIVERSITY OF OKLAHOMA

GRADUATE COLLEGE

PALEOMAGNETISM AS A TOOL FOR DETERMINING DIAGENETIC, DEPOSITIONAL, AND EROSIONAL EVENTS AS RECORDED IN SEDIMENTARY AND IGNEOUS ROCKS

A DISSERTATION

SUBMITTED TO THE GRADUATE FACULTY

in partial fulfillment of the requirements for the

Degree of

DOCTOR OF PHILOSOPHY

By

SHANNON ANN DULIN
Norman, Oklahoma
2014

PALEOMAGNETISM AS A TOOL FOR DETERMINING DIAGENETIC, DEPOSITIONAL, AND EROSIONAL EVENTS AS RECORDED IN SEDIMENTARY AND IGNEOUS ROCKS

A DISSERTATION APPROVED FOR THE
CONOCOPHILLIPS SCHOOL OF GEOLOGY AND GEOPHYSICS

BY

_____
Dr. R. Douglas Elmore, Chair

_____
Dr. Gerilyn Soreghan

_____
Dr. Michael Engel

_____
Dr. Susan Postawko

_____
Dr. John Geissman

Acknowledgements

Eternal gratitude goes to my advisor Doug Elmore for his many years of guidance, prodding, and friendship. I cannot thank him enough for all the opportunities he has provided me in my long scholastic journey. I would also like to thank my committee members for their endless discussions about life, the universe and everything. Their personal and academic support has been invaluable to me.

Thanks to my fellow graduate students for all of their companionship, discussions, and endless trips to the coffee shop. Thanks also to my many, many field assistants—particularly Earl and Andrew who scouted the first trip to drill the clastic dikes, Stacey for all her help in Nevada and Colorado, and John, who had to endure a trip to Scotland. The undergraduates in the paleomagnetics laboratory worked tirelessly on processing core and last minute rock magnetic procedures. I was also fortunate enough to have many outside discussions and guidance during sampling trips and I am forever grateful to Jay Temple, Christine Siddoway, John Parnell, and Chuck Kluth, for their knowledge and friendship.

Lastly, I would like to thank my family for inspiring me to be a scientist, for my son who provided copious distractions and hilarity, and to my husband whose endless patience and support are what made this entire journey possible.

Table of Contents

List of Tables

List of Figures

Chapter 1

Chapter 2

Chapter 3

Abstract

Paleomagnetism is a useful means to study the depositional and diagenetic history of any formation. If a formation holds a geologically stable, ancient magnetization, the magnetization, and thus its origin, relates a specific event that the rock has undergone. Accurate dating of such events is difficult, particularly in the absence of stratigraphic controls, and re-creation of the history of a formation is crucial in understanding its importance in the rock record. Paleomagnetic information can be used to assess the timing of deposition of a unit or the timing of a diagenetic event that may have affected the formation of interest.

This study consists of three independent components that uses the timing of magnetization acquisition to characterize a specific event in the history of the formation of interest. The first study addresses clastic dikes of previously unknown age and origin that are exposed in the Pikes Peak Granite along nearly 175km of the Front Range in Colorado. These dikes are spatially associated with north- and northwest-striking thrust faults along the east margins of the range. Paleomagnetic demagnetization data from the dikes indicate the presence of a complex, multicomponent magnetization. A characteristic remanent magnetization (ChRM) with easterly declinations and moderate to steep inclinations resides in hematite and corresponds to a late Precambrian to early Cambrian pole position when compared to the apparent polar wander path of North America. This early magnetization was probably acquired at or soon after emplacement of the dikes and is therefore interpreted as a primary magnetization. A southeast and shallow magnetization, also residing in hematite, yields a grouping of poles of late Paleozoic age. This magnetization is interpreted as a chemical remanent

remagnetization (CRM), possibly associated with fluid flow driven by Ancestral Rocky Mountain orogeny. The second study investigates the origin of a CRM in zebra dolomite of the Devonian Guilmette Formation in Nevada. Zebra dolomite is common in Paleozoic carbonate platform sequences of the Basin and Range, and is linked to migration of warm basinal brines. The zebra dolomite of the Guilmette Formation holds a magnetization carried by magnetite that is inferred to be late Triassic in age. The timing of this magnetization may be associated with fluids driven eastward during the Triassic Sonoma orogeny. The third study evaluates a widespread late Paleozoic magnetization associated with hematite formation in concert with albitization of Precambrian crystalline rocks. This Permo-Triassic aged magnetization has been reported at several localities in Europe and in North America, and is associated with hematite precipitation by weathering-related fluids. The paleoclimate at the end of the late Paleozoic represented a shift to greenhouse conditions and probable enhanced chemical weathering. Determining the extent of this remagnetization can help to identify the paleotopographic surface, understand the Permo-Triassic paleoclimate, as well as determine the widespread extent of this chemical weathering remagnetization event.

Chapter 1: Clastic dikes in the Pikes Peak Granite, Front Range, Colorado

Abstract

Clastic dikes of unknown age and origin occur within the Pikes Peak Granite (1.09 Ga) and are spatially associated with thrust faults that define the present-day Front Range in Colorado. The dikes parallel major north- and northwest-trending thrust faults which are inherited structural lineaments dating from the Precambrian. Dikes were sampled for paleomagnetic analysis near the Ute Pass Fault in Colorado Springs and Woodland Park, Colorado, and near the Pine Gulch Fault near Pine, Colorado. Thermal demagnetization of paleomagnetic specimens reveals that the dikes have a complex magnetization history, with multiple-aged magnetizations held in hematite. The magnetizations are interpreted as chemical remanent magnetizations (CRM) likely acquired as a result of fluid-related alteration during episodic reactivation of faults from the Neoproterozoic through the early Cenozoic. Three remanent magnetizations are defined: a characteristic remanent magnetization (ChRM I) that has easterly declinations and moderate positive inclinations and a reversed direction that has westerly declinations and moderate negative inclinations, a component II that has southeasterly declinations and moderate up inclinations, and a component III that has northwesterly declinations and moderate-steep down inclinations. Some dikes have streaked directions that represent multiple magnetic components that cannot be resolved. The dikes contain detrital hematite grains as well as abundant authigenic hematite. ChRM I was acquired as a detrital remanent magnetization (DRM) or as an early CRM during the Neoproterozoic. Component II is interpreted as a CRM that was acquired during the late Paleozoic, and component III is also interpreted as a CRM that

was acquired during the late Mesozoic and the Cenozoic. In contrast to some previous studies, the paleomagnetic analysis indicates the dikes are Neoproterozoic in age.

Introduction

Clastic dikes of unknown age and origin occur within the Pikes Peak Granite along nearly 175km of the Front Range of Colorado. These dikes are spatially associated with north- and northwest-striking thrust faults along the eastern margins of the range; they parallel the predominately north-trending Ute Pass Fault near Colorado Springs and Woodland Park, Colorado, and the northwest-trending Pine Gulch Fault near Pine, Colorado (Fig. 1). The dikes vary in size from a few centimeters across to tens of meters wide (Fig. 2). Most dikes are near-vertical to sub-vertical in orientation. The dikes are predominately composed of quartz arenite, with fine- to medium-grained, well-rounded quartz, with varying degrees of induration. Both the origin and age of the dikes and the emplacement mechanism have been debated since the original discussion of the dikes appeared in the literature in the late 19th century (Cross, 1894; Crosby, 1897; Vitanage, 1954; Harms, 1965).

Paleomagnetism is a useful tool for dating sediments whose age cannot be stratigraphically determined. For example, clastic dikes within Precambrian basement rocks in Scotland that are used as paleostress indicators (Beacom et al., 1999) have been dated using paleomagnetism (Dulin et al., 2005). Paleomagnetic analysis was also successfully used to constrain the timing of poorly dated impact craters along the 38th parallel in Missouri (Dulin and Elmore, 2007; Elmore and Dulin, 2007).

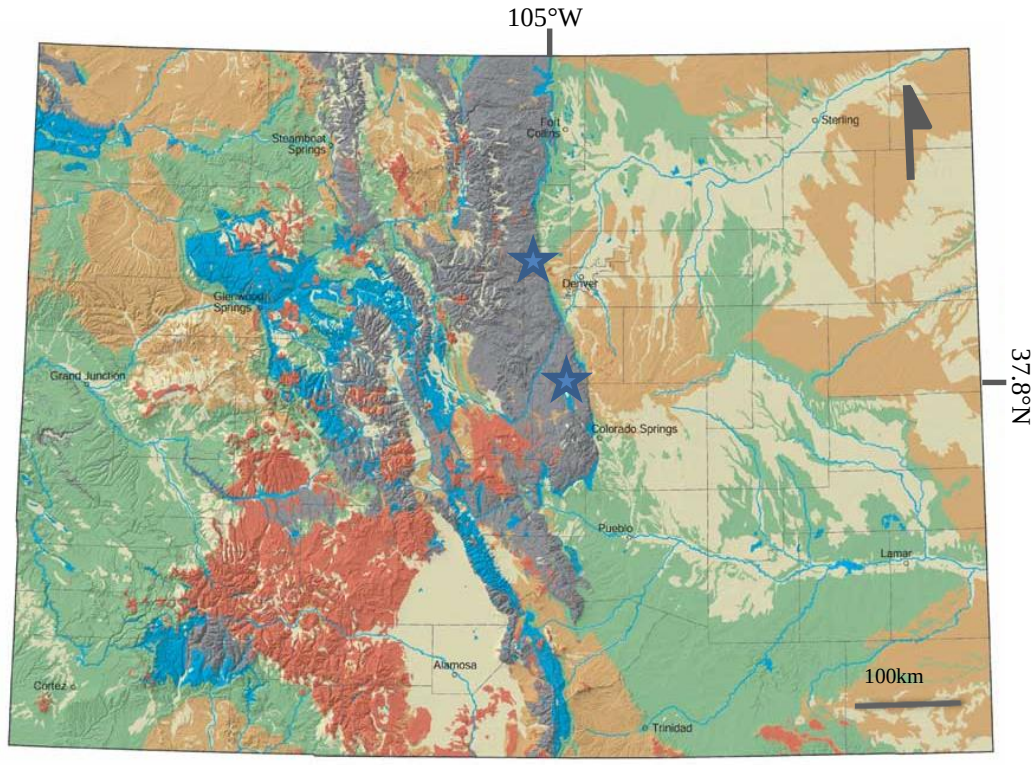

Figure 1: Geologic map of Colorado that shows Precambrian sedimentary and metamorphic rocks (gray), Paleozoic (blue), Mesozoic (green), and Cenozoic (tan) sedimentary rocks, and igneous intrusions of various ages (red). The two stars represent the study areas where clastic dikes were sampled. Image modified from www.geosurvey.state.co.us.

This study uses paleomagnetic analysis of the dikes to determining timing of emplacement within the Proterozoic Pikes Peak Granite. Paleomagnetic sampling and subsequent demagnetization of the clastic dikes indicates the presence of a complex multicomponent magnetization residing in hematite. Paleomagnetic, rock magnetic, and petrographic analysis will help constrain the origin of the dikes. If the magnetizations present are primary magnetizations, then the ages determined will date dike formation. If the magnetizations are secondary, they may date remagnetization events related to fault movements and will provide a new age constraint for the dikes; the dikes can be no

younger than the age of the magnetization acquired during tectonic processes. This is especially important in reconstructing the tectonic history of the Front Range and possibly dating the age of the thrust faults.

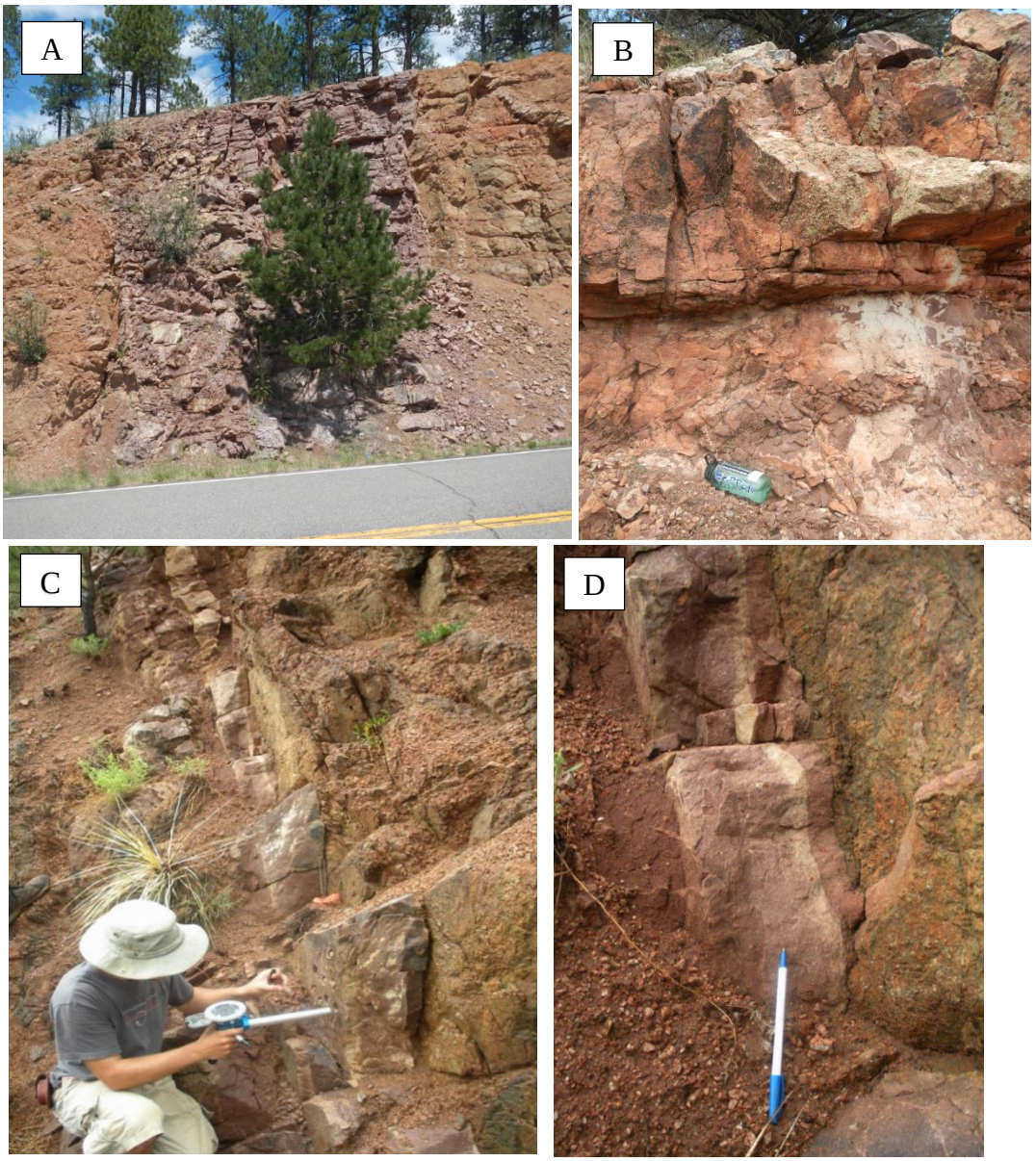

Figure 2: Sandstone dikes. A) Dike BC-D, near Buffalo Creek. Dike is obliquely cut; dike is trending roughly perpendicular to the road. B) Dike IT, in Manitou Springs. C) Dike SSD3 near Pine. D) Dike SSD4 near Pine. Pen is vertical. Note the sharp contacts between the dikes and the granite.

Geologic Background and Previous Studies

The tectonic history of the Front Range in Colorado is complex. Interactions between initial fault formation, reactivation during subsequent orogenic episodes, and deposition and subsequent erosion related to each orogeny add to the complexity of recreating the tectonic history of the study area. Major fault trends throughout Colorado are thought to originate along pre-existing zones of weakness that were present in the Precambrian (Tweto, 1980a).

During the Precambrian, three major igneous intrusions (1.7 Ga, 1.4 Ga, and 1.0 Ga) formed the basement of Colorado (Tweto, 1980a). The Pikes Peak Granite is the youngest of three major Precambrian igneous intrusions, and was emplaced as a single batholith at shallow depths (Tweto, 1980a; Hedge, 1986). The age of the granite is 1.09 Ga (Schärer and Allégre, 1982), determined by U-Pb dating of zircons. The Pikes Peak granite is an A-type granite with the potassic phase consisting of a biotite-hornblende syenogranite (Smith et al., 1999). The granite is coarse-grained and red-pink in color and weathers to a pink-orange grus.

There is no record of geologic activity in Colorado for nearly 400 My following the emplacement of the Pikes Peak Granite (Tweto, 1980b), although sedimentation, erosion, and fault movement likely occurred in this interval. Sedimentary rocks of the Uinta Mountain Group, which consists of dark red interbedded sandstone and shale, were deposited in northwestern Colorado between 770-740 Ma (Yonkee et al., 2014), with provenance of these sedimentary rocks from the Wyoming craton and possibly from westward-flowing river systems that originated near South Dakota (Condie et al., 2001).

Despite over a century of study, the origins, age, and emplacement mechanisms of the Front Range clastic dikes within the Pikes Peak Granite remain enigmatic. In the original description of the clastic dikes in the literature, Cross (1894) describes a colleague, Professor Stone, who has identified clastic dikes near the Turkey Creek Mining District in El Paso County, Colorado. Professor Stone describes the dike as follows:

"To the unassisted eye this so-called lode rock presents the appearance of an igneous rock, but under [microscopic] examination…it is plainly a fine-grained sandstone…made of quartz…with an iron-rusty cement."

The original designation of the clastic dikes as "lode rock" made a connection between hydrothermal and tectonic activity of the Colorado Mineral Belt and the age of the clastic dikes. The association does not imply an age for the dikes—mineralization within the Colorado Mineral Belt spans from Precambrian veins to Oligocene alteration associated with volcanics in the San Juan Mountains (Romberger, 1980).

Crosby (1897) related the sandstone dikes to movement along the major Front Range fault, the Ute Pass fault, and suggested the Cambrian Potsdam (now known as Sawatch) sand as the source for the clastic dike material. He postulated that the unconsolidated sand flowed into fissures created by fault displacement which occurred before lithification of the Cambrian Sawatch. The close proximity of the dikes to Front Range faults has led nearly all investigators to make a connection between fault movement and dike emplacement, but different episodes of faulting have been suggested for the timing of dike formation, such as during the Laramide or Ancestral Rockies orogenies (Harms, 1965; Vitanage, 1954). Vitanage (1954) favored an injection

of dike material from above into fissures. Harms' (1965) model of dike formation creates void space in the Pikes Peak granite due to vertical uplift, with the sand then flowing into voids due to overpressure in overlying clastic sediments. Nearly all researchers (Crosby, 1897; Harms, 1965; Kost, 1984, and others) have concluded the likely source of the sandstone dikes is the Cambrian Sawatch sandstone.

In the southern study area near Woodland Park, Colorado, there are sandstone dikes as well as large sand bodies that lack sedimentary structures. Siddoway et al. (2013) interpreted the large sand bodies as being deposited in a narrow basin with large amounts of accommodation space along the Ute Pass fault. In this model, formation of the associated dikes occurred by liquefaction of overlying sediment during tectonic events or by overpressure and filling of previous fractures that were in place in the Pikes Peak granite. Siddoway et al. (2009) and Freedman et al. (2013) reported alignment of magnetic grains that parallel the dike walls, implying an injection-type mechanism of emplacement that is in agreement with the model. Detrital zircon data from dikes in and south of Woodland Park and Colorado Springs have Grenville-aged peaks that correlate to Neoproterozoic formations in the western US, such as the Uinta Mountain Group and middle Big Cottonwood Formation, Perry Canyon and Kelly Canyon Formations, and the Nankoweap Formation (Siddoway and Gehrels, 2014). The detrital zircon signatures in the dikes are not similar to detrital zircon signatures of Paleozoic sediments, which were thought by Harms (1965) to be the source of some rock fragments within the dikes.

A petrographic and paleomagnetic study of the dikes near both Pine and the Ute Pass Fault Zone near Colorado Springs was the subject of an unpublished master's

thesis (Kost, 1984). Kost (1984) found poorly defined magnetizations interpreted to be early and late Paleozoic, late Mesozoic, Cenozoic, and recent in age. Petrographic analysis concluded the dikes were likely sourced from the Sawatch due to the presence of quartz and extensive hematite authigenesis in both units.

Methods

Twenty-two sites (8-12 specimens per site) were sampled from ten dikes along Deckers Road (SH 126) between the towns of Pine and Buffalo Creek, Colorado, southwest of the Denver metropolitan area. Twenty-nine sites from thirteen dikes were sampled in the Woodland Park, Manitou Springs, and Colorado Springs, Colorado, areas (Fig. 3). Samples were collected using a gasoline-powered modified chainsaw equipped with a Pomeroy coring device. In-situ samples were oriented in the field using a Brunton compass and inclinometer. For some dikes, slabs of dike material were oriented using a Brunton compass and transported to the Oklahoma Petroleum Information Center where the slabs were sampled using a drill press.

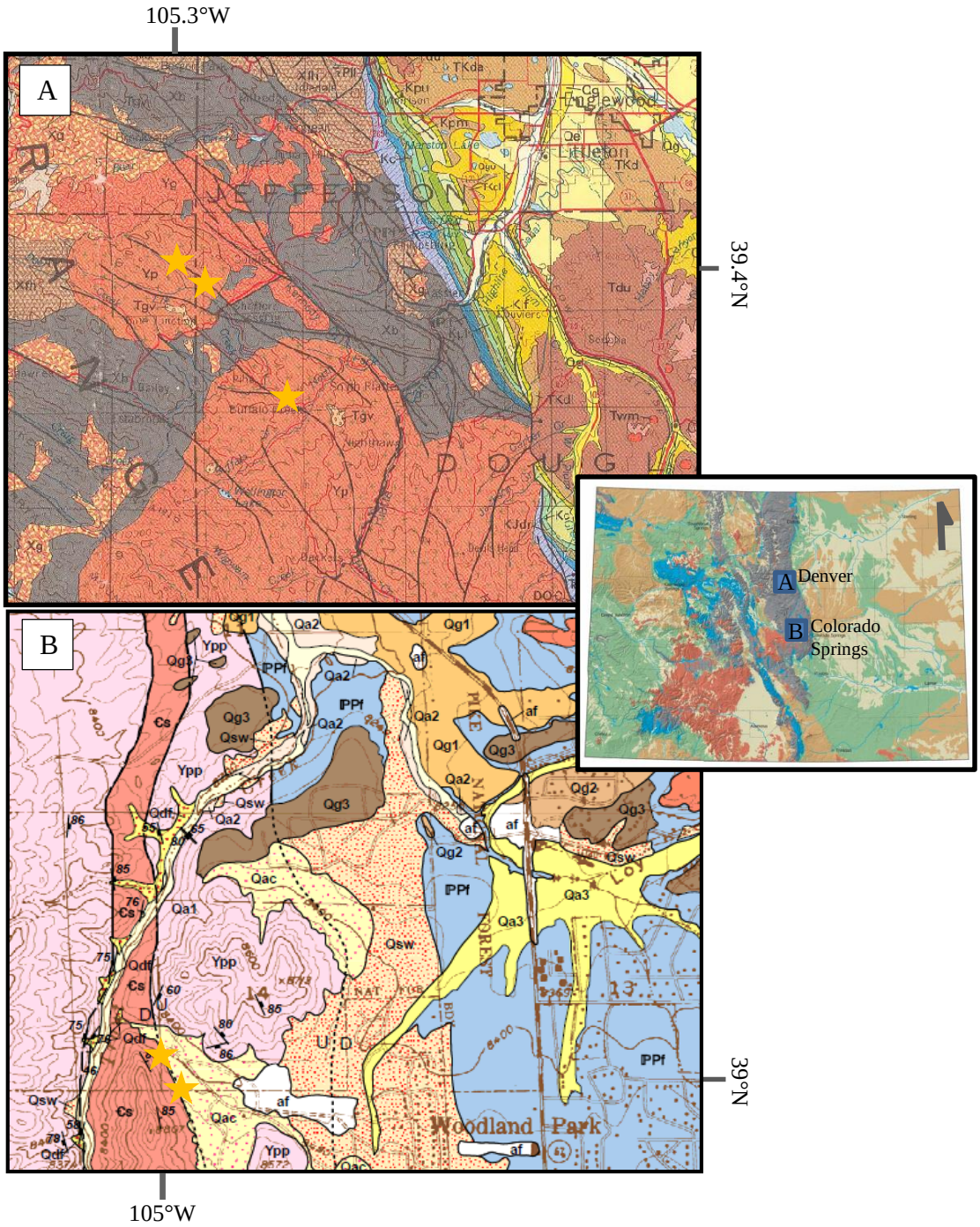

Figure 3: Sampling locations shown on state map to the right. The enlarged boxes show detailed geologic maps of the study areas. The stars show approximate sampling locations. A) The northern study area near the town of Pine. The faults are shown in grey. The pink color (Yp) is the Proterozoic Pikes Peak Granite. B) The southern study area near the town of Woodland Park. Dark pink (Ꞓs) delineates large sandstone dike. Maps from http://coloradogeologicalsurvey.org/ and Temple et al. (2007).

In the laboratory all samples were cut into standard 2.2cm length specimens for paleomagnetic analysis using an ASC Scientific rock saw. The natural remanent magnetizations (NRMs) were measured with a three-axis 2G Enterprises cryogenic magnetometer with DC squids in a magnetically shielded room. Twelve samples were subjected to alternating field (AF) demagnetization to determine the presence of low coercivity minerals. Remaining specimens were thermally demagnetized in a stepwise fashion from 100-700°C (20°C steps) in an ASC thermal demagnetizer. The demagnetization data was analyzed to determine stable magnetic components using the Super-IAPD program (http://www.ngu.no/geophysics/soft32.htm). Thermal demagnetization data were plotted as orthogonal projection diagrams (Zijderveld, 1967) and analyzed using principal component analysis (Kirschvink, 1980) to determine the magnetic components within each sample. Mean angular deviations (MAD) of 16° or less were deemed acceptable, though most samples have a MAD angle of less than 11°. Means were computed using Fisher (1953) statistics, and the mean direction was then used to determine a pole position.

Nineteen samples were imparted with an isothermal remanent magnetization (IRM) at room temperature using an ASC Scientific impulse magnetizer to determine magnetic mineralogy. Samples were first subjected to AF demagnetization to remove the remanent magnetizations. An IRM was then imparted in a stepwise fashion from 0 to 2500mT. The samples were subjected to a second AF demagnetization and subsequently imparted with three perpendicular IRMs (120mT, 500mT, and 2500mT). The samples were then thermally demagnetized in a stepwise fashion to yield tri-axial decay curves (Lowrie, 1990). Cumulative log-Gaussian (CLG) analysis was performed

using IRMUNMIX2.2 software (Heslop et al., 2002) on the IRM acquisition data to model the magnetic components within the dikes by comparing individual coercivity contributions (Kruiver et al., 2001).

A total of 75 thin sections were analyzed to determine dike composition and magnetic mineralogy. Reflected light microscopy was used to identify opaque minerals. Cathodoluminescence microscopy was performed on thin sections using a CiTL CCL 8200 MK4 stage mounted on an Olympus BX50 microscope. Scanning electron microscope (SEM) analysis of thin sections and rock samples supplemented the thin section analysis. The SEM analysis was completed using an environmental scanning electron microscope (FEI Quanta 200) with energy dispersive capabilities at the University of Oklahoma Mewbourne College of Earth and Energy IC^3 lab.

Results and Interpretations

Paleomagnetic Data

Thermal demagnetization at low temperatures (<200°C) removes a northerly and steep down component in some specimens (Fig. 4), which is interpreted as the Modern viscous remanent magnetization (VRM). At higher temperatures, the characteristic remanent magnetizations (ChRMs) can be divided into four different groupings. The magnetization history of the sandstone dikes along the Front Range is complex. The presence of multiple ages of magnetizations both in separate dikes and within the same dike makes isolation of a characteristic remanent magnetization problematic.

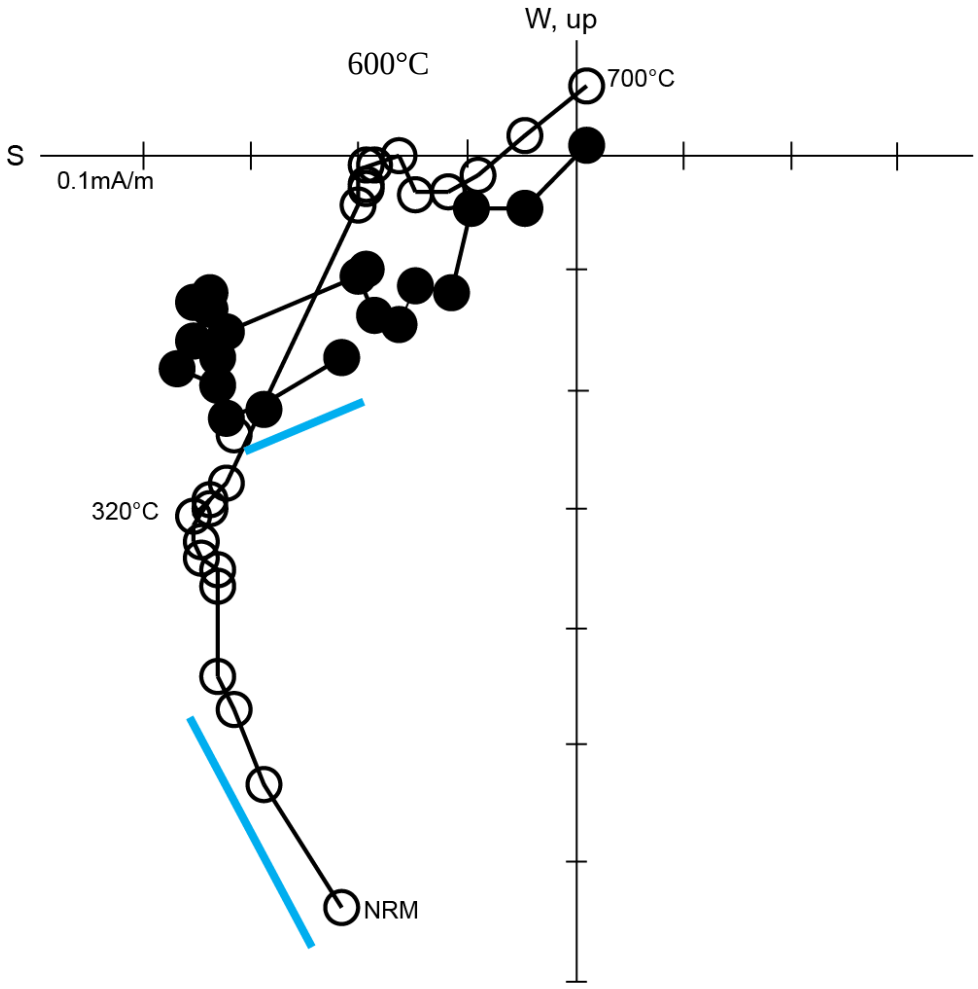

Figure 4: Orthogonal projection diagram (Zijderveld, 1967) of specimen BC4-5, a clastic dike near Buffalo Creek, Colorado. Closed (open) circles represent the horizontal (vertical) component of the magnetization. The blue line shows the Modern VRM, which is present in many of the dike specimens. The ChRM is present above 600°C.

AF demagnetization of 10 specimens resulted in between 10-30% decay of the NRM in most dike specimens. There was no straight-line decay of the magnetization observed on the orthogonal projection plots (Fig. 5); a component could not be isolated from AF demagnetization.

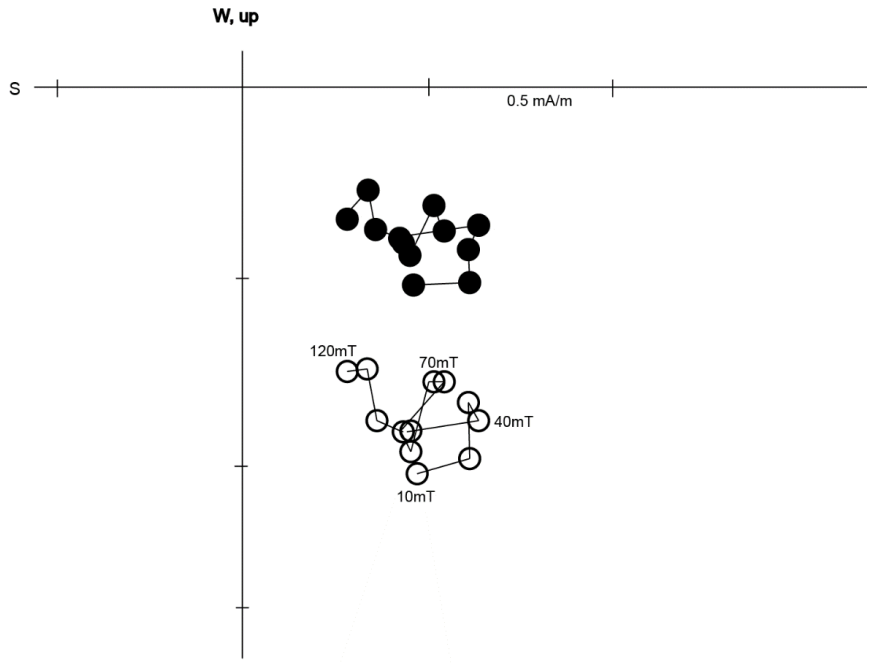

Figure 5: Orthogonal projection diagram showing AF demagnetization of a representative specimen from dike SSD10 near Pine, Colorado. Closed (open) circles represent the horizontal (vertical) component of the magnetization. Less than 30% of the NRM was removed by 120m, and no magnetic component could be resolved from the AF treatment.

ChRM I

During thermal demagnetization most specimens with ChRM I (dikes SSD-A [sites SSD1, SSD2, and SSD7], SSD3, MP2, SF and IT3; Table 1) show removal by 680°C of magnetization with an easterly declination and moderate positive inclination (Fig. 6). The magnetization in specimens from site SSD3 decay with an easterly and shallow up magnetic direction (Table 1). The ChRM in specimens from site MP2 displays decay with a southwesterly declination and inclination of moderate negative inclination (Fig. 6D) and the reversed direction was used to calculate the mean for ChRM I (Table 1). The magnetization in the specimens from all sites decay to zero intensity by 680-700°C; ChRM I is interpreted as residing in hematite.

Site	Dec (°)	Inc (°)	N/N_o	k	α95	VGP lat (°N)	VGP long (°E)	d_p(°)	d_m(°)
ChRM I									
SSD-A	77.3	42.9	23/33	8.88	44.1	-24.7	151.5	33.8	54.6
SSD3	98.5	-10.6	6/9	11.5	20.6	10	163.4	10.6	20.9
MP2	237.2	-33.3	6/9	16.57	17	-36.6	170.7	11	19.3
SF	90	57.4	4/8	9.72	31.1	-22.7	133.8	33.2	45.5
IT3	103.4	28.7	7/7	20.07	13.8	0.5	144.9	8.3	15.2
Mean	*86*	*32*		*7.54*	*29.8*	*-13.9*	*153.6*	*18.9*	*33.5*
Component II									
TCI	154	-27	6/9	7.95	25.3	56.3	125	15	27.5
TC2	136.4	-3.5	11/19	11.72	13.9	35.6	132.9	7	13.9
MP1	324.9	-15.6	7/7	57.76	8	32.9	117.6	4.2	8.2
Component III									
IT2	13.5	42.3	5/5	14.31	20.9	71.6	32.7	15.8	25.7
IT5	326.8	48.3	5/7	13.57	21.5	61.1	156	18.5	28.2
SSD10	26.5	52.7	5/6	47.44	11.2	67.9	352.5	10.7	15.5
Streaked									
BC-D	121.5	16	18/29	4.45	18.5	18	137.3	9.8	19.1
MP5	305.6	1	7/12	9.02	21.2	27.2	141.1	10.6	21.2
Granite									
PG	155.2	-16.1	4/10	44.05	14	51.7	116.7	7.4	14.4
BG	108.4	9.7	9/11	7.61	20	10.9	149.1	10.2	20.2
Other									
BC1_IT	256.8	-6.3	14/16	46.76	5.9	-12.2	170.7	3	5.9
BC1_HT	148.3	-9.6	9/14	43.46	7.9	45.2	122.7	4	8
SW	168.6	-36.6	6/9	105.22	6.6	68.9	106	4.5	7.7

Table 1: Paleomagnetic data of sites from sandstone dikes, surrounding granite, mafic dike, and Sawatch sandstone. The sites are grouped by like directions. Dec and Inc are the in situ declination and inclination of the mean magnetic direction; N/N_o represents the number of samples used to calculate the mean with respect to the number of samples measured in total; precision parameter, k, represents grouping; α95 represents 95% cone of confidence around pole; virtual geomagnetic pole (VGP) latitude and longitude; d_p/d_m represent minor/major ellipse axis of the α95 cone.

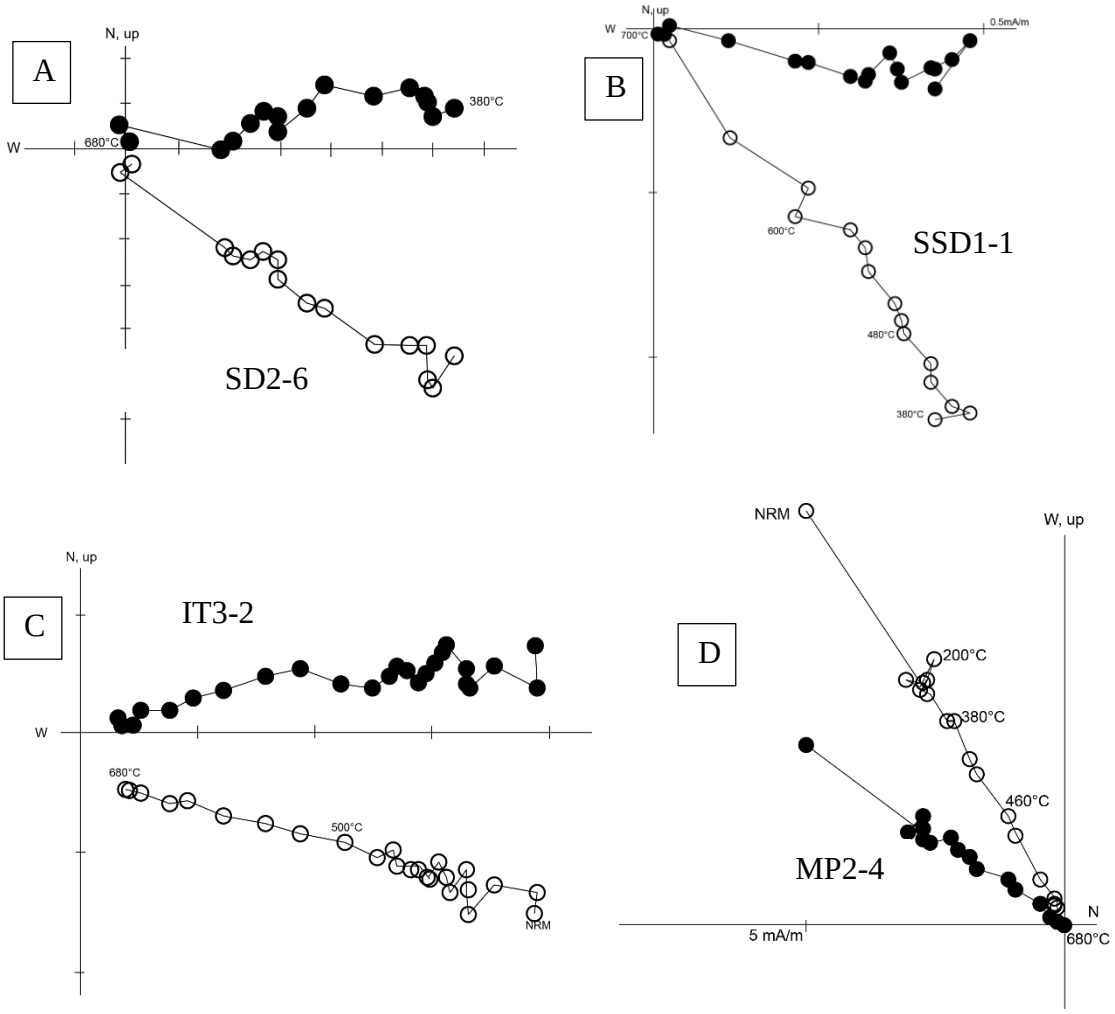

Figure 6: Orthogonal projection diagrams of representative samples of ChRM I (A-C). D) Specimen MP2-4 showing reversed direction of the ChRM. Closed (open) circles represent horizontal (vertical) component of the magnetic component.

Site MP1 is part of a larger dike, which includes site MP2. It is noteworthy that these two sites are less than 10m apart, and yet MP1 holds component II, and MP2 holds ChRM I. MP5, a discrete dike that is less than 500m away from the larger dike containing sites MP1 and MP2, holds a magnetization that is in-between MP1 and MP2 on the APWP (Fig. 8).

One site (BG) from the Pikes Peak Granite taken near Buffalo Creek, Colorado, ~15km south of Pine, Colorado, contains a similar direction to ChRM I (Table 1). Specimens from this site show removal of an east-southeasterly component with moderate positive and negative inclinations. In contrast to the dikes, this component is removed by 580°C, and is interpreted to reside in magnetite.

The equal area plot (Fig. 7) shows the means for the dike sites. The mean of the means for ChRM I is also plotted (Dec = 86°, Inc = 32°, k = 7.5, α_{95} = 29.8). The mean for site BG was not used to calculate the overall mean for ChRM I. The calculated VGP for the mean (13.9°S 153.6°E; d_p = 18.9° d_m = 33.5°) plots south of the late Cambrian/early Ordovician on the APWP for North America (Fig. 8).

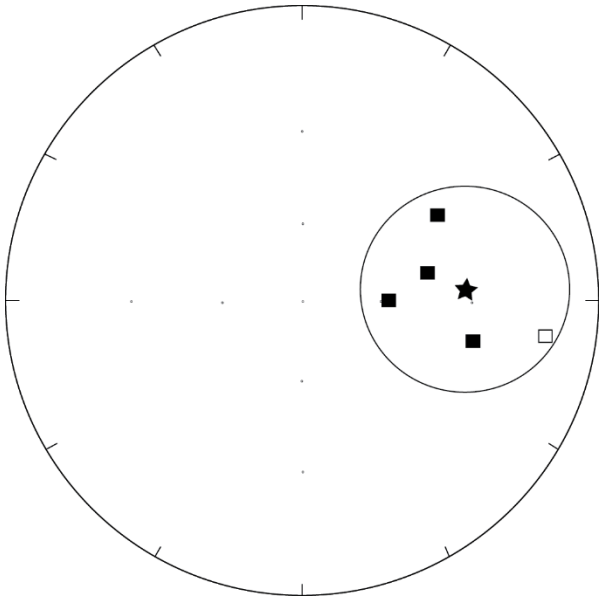

Figure 7: Equal area plot showing site means (squares) for six dikes that contain ChRM I. Closed (open) symbols represent positive (negative) inclinations. The star is the mean of means for ChRM I, and the ellipse is the error associated with the mean of means.

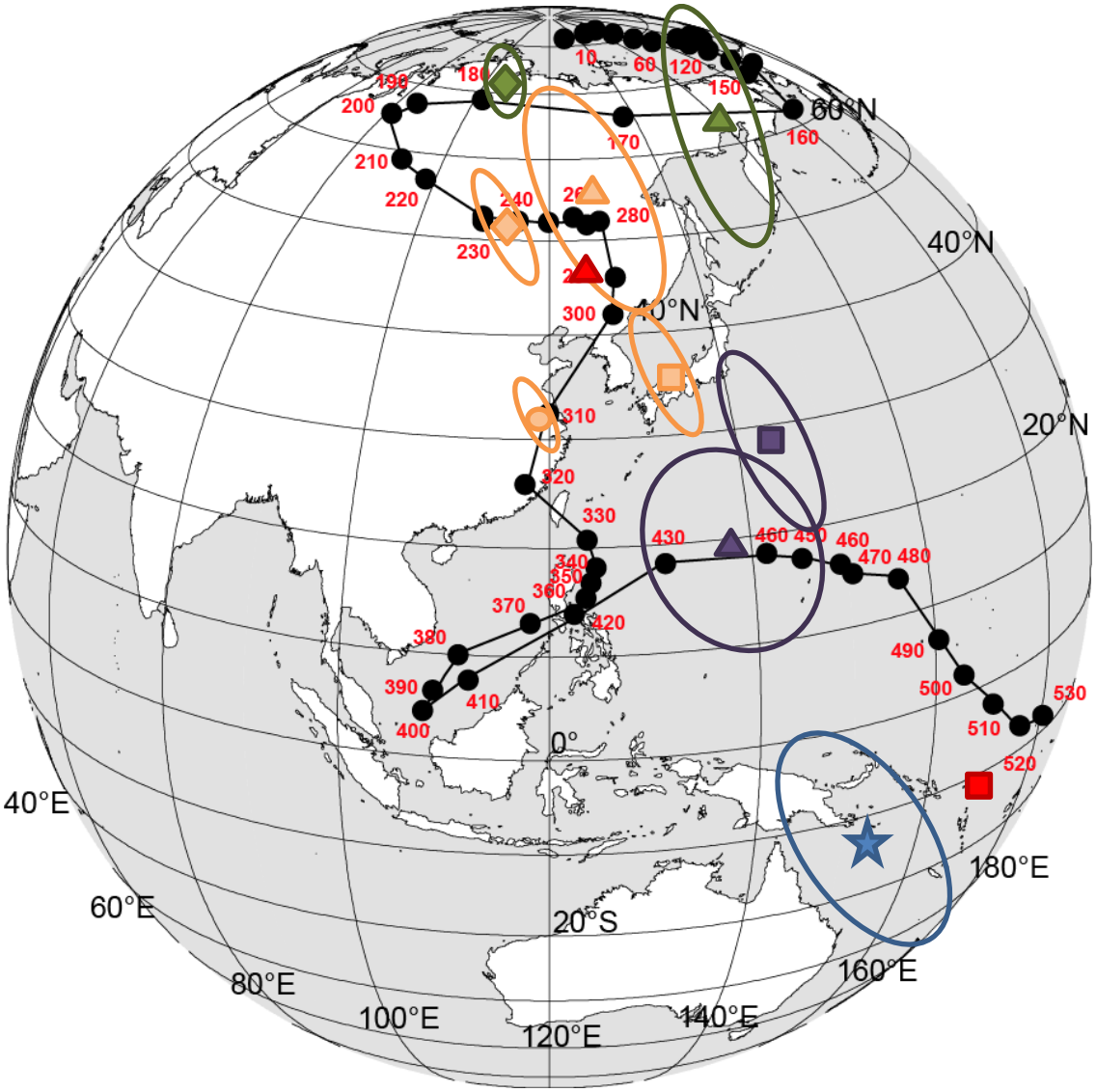

Figure 8: Apparent Polar Wander Path for North America (Torsvik et al., 2012). The VGPs are shown with their associated confidence ellipses. If no ellipse is shown, the error is smaller than the symbol. Blue Star = ChRMI mean of means. Orange = component II site means (triangle = TC1; square = TC2; circle = MP1; diamond = Pikes Peak Granite [PG]). Green = component III site means; triangle = IT5; diamond = Sawatch sandstone. Purple = streaked directions; triangle = BC-D; square = MP5. Red = BC1; square = BC1-IT component; triangle = BC1-HT component.

Component II

Component II is found in dikes TC1, TC2, and MP1 (Table 1). Figure 9 shows the orthogonal projection diagrams for representative specimens from these sites.

Specimens from sites TC1 and TC2 show removal during stepwise thermal demagnetization of a component with southeasterly declinations and moderate up inclinations, which decays by 700°C (Fig. 9). Specimens from site MP1 show removal of a magnetization with northwesterly declinations and moderate-shallow inclinations that decays by 680°C (Fig. 9). Component II is interpreted to reside in hematite based on unblocking temperatures above 580°C.

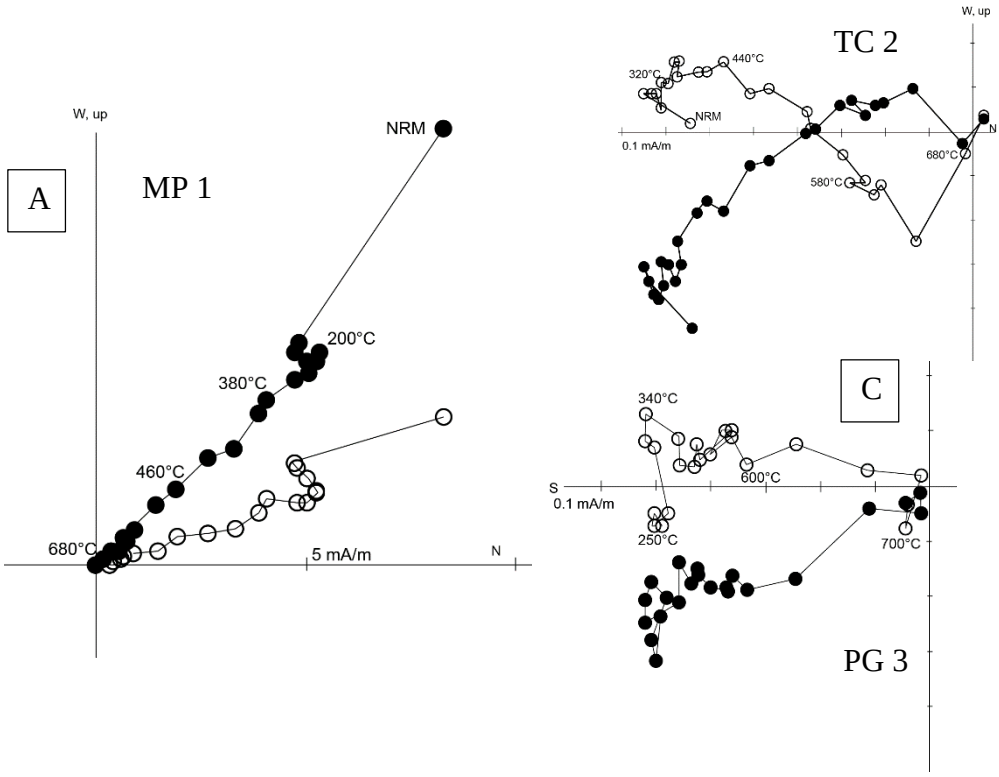

Figure 9: Orthogonal projection diagrams showing representative samples of Component II (MP1 and TC2) and of the Pikes Peak Granite (PG3). Closed (open) circles represent horizontal (vertical) component of the magnetic component.

The site means for TC1, TC2, and the antipode of MP1 (Table 1) are shown in the equal area projection (Fig. 10; Table 1). The VGPs for sites TC1 (56.3°N, 125°E; d_p = 15, d_m = 27.5), TC2 (35.6°N, 132.9°E; d_p = 7, d_m = 13.9), and MP1 (32.9°N, 117.6°E; d_p = 4.2, d_m = 8.2) are plotted on the APWP (Fig. 8). The mean of means was not

calculated for component II since the VGPs for each site do not represent a grouping, but instead span the late Paleozoic portion of the APWP.

Specimens of the Pikes Peak Granite from sites near the dikes at Pine also yield a similar magnetization in hematite as the dikes that hold component II (Fig. 9; Table 1). The mean of Pikes Peak Granite (sites PPG1 and PPG3) at these localities (Dec = 155.2°, Inc = -16.1°, N = 4 of 10, k = 44.05, α_{95} = 14; Table 1) yield a pole position of 51.7°N, 116.7°E (d_p = 7.4, d_m = 14.4), which plots in the late Paleozoic part of the APWP for North America (Fig. 8).

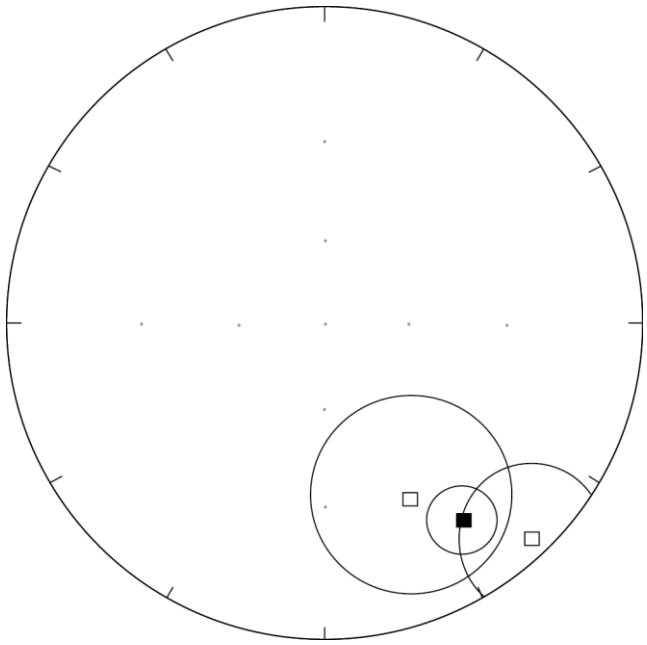

Figure 10: Equal area plot showing site means for the sites that hold Component II. No mean was calculated because the VGPs for the sites span the Paleozoic. Closed (open) symbols represent positive (negative) inclinations.

Component III

Component III is held by specimens in sites IT2, IT5, and SSD10. These sites have a north-northwesterly declination and moderate to steep down inclination (Fig. 11; Table 1). The IT sites represent different sites within the same dike in Manitou Springs,

Colorado. Also included is site SW, collected in the Cambrian Sawatch sandstone near Woodland Park, Colorado. Specimens from this site contain a component with south-southeasterly declination and moderate to steep up inclination, the antipode of which has a northwesterly declination and moderate down inclination. Other Sawatch localities sampled did not yield a stable magnetization. Similar to the previously discussed magnetizations, component III is also held in hematite, as seen by decay to 680-700°C in all specimens.

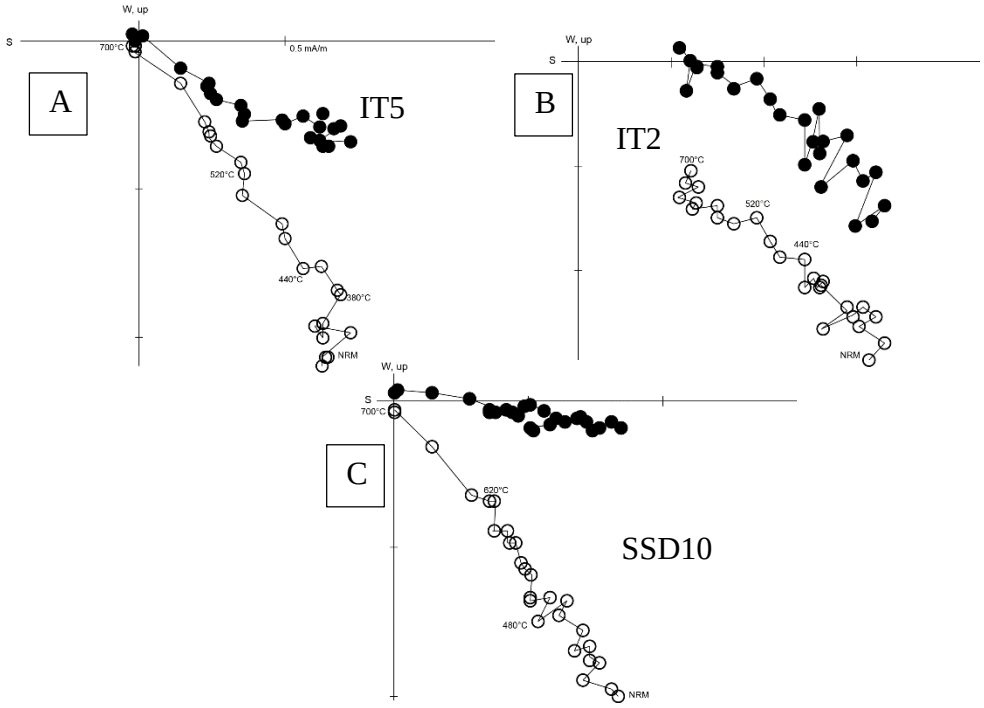

Figure 11: Orthogonal projection diagrams showing representative samples of Component III. Closed (open) circles represent horizontal (vertical) component of the magnetization.

Figure 12 is the equal area projection showing the means for each dike or site, along with the modern magnetic field (Dec = 8.5°, Inc = 65.7°) for Pine, Colorado. The modern magnetic field for Manitou Springs (where sites IT were collected) is similar (Dec = 8.4°, Inc = 65.6°). IT2 and SSD10 have directions similar to the modern

magnetic field. Site IT5 has a more northwesterly declination; the VGP for IT5 plots near the middle Jurassic of the APWP (Fig. 8). Site SW, the Cambrian Sawatch sandstone, yields a VGP of similar age, plotting near the early Jurassic portion of the APWP (Fig. 8).

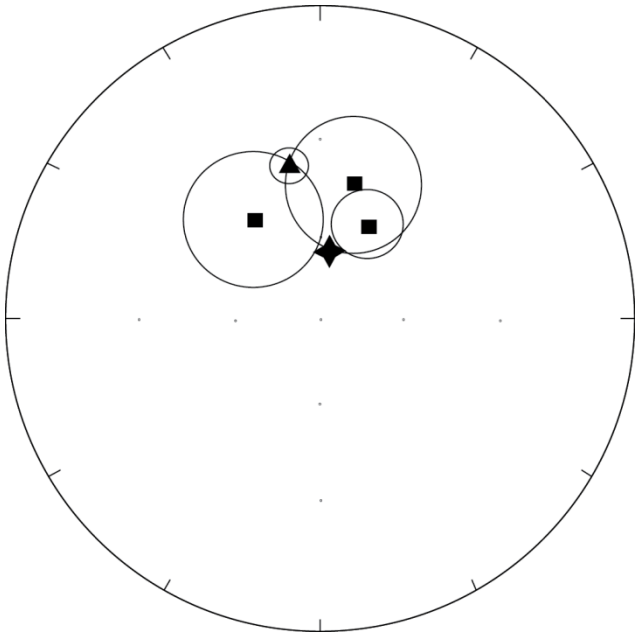

Figure 12: Equal area plot showing site means for the sites that hold Component III. No mean was calculated because the VGPs for the sites span the Mesozoic and Cenozoic. Closed (open) symbols represent positive (negative) inclinations. The triangle is the Cambrian Sawatch sandstone. The star represents the Modern magnetic field at Pine and Manitou Springs, Colorado.

Streaked Data

Some dikes yield a streaked distribution of specimen directions. Dike BC-D (sites BC3, BC4, BC9, and BC10), and dikes MP5, SSD6, MD, and CD, along with site IT6 all show streaked distributions on equal area projections. For example, dike BC-D shows a distribution of southeasterly declinations but the inclinations are streaked from moderate up (-46°) to moderate down (56°) (Fig. 13). Although the calculated VGP falls on the Ordovician part of the APWP, the pole also falls between ChRM I and

component II poles (Fig. 8). Dike SSD6 shows a streak from north-northeasterly declinations and moderate inclinations to northwesterly declinations and moderate inclinations. The streaked distributions are interpreted to represent vector additions between multiple magnetizations held within the specimens.

Great-circle analyses (Halls, 1976; Bailey and Halls, 1984, McFadden and McElhinny, 1988) were performed on streaked distributions of directions to determine if one of the magnetic components could be resolved. The demagnetization paths for the magnetizations in specimens did not produce well-defined great circle paths. The data for the streaked distributions were also analyzed using Kent (1982) statistics to determine if the data distribution were elliptical. This analysis indicated that the streaked data distributions were not unimodal.

The streaked distributions for SSD6, MD, CD and IT6 are interpreted to be magnetizations that represent unresolvable vector additions between early Cenozoic and Modern components. The VGPs for BC-D and MP5 are plotted on Figure 8. The complex magnetizations in these two dikes are interpreted to represent vector additions between Neoproterozoic/early Paleozoic and late Paleozoic magnetizations.

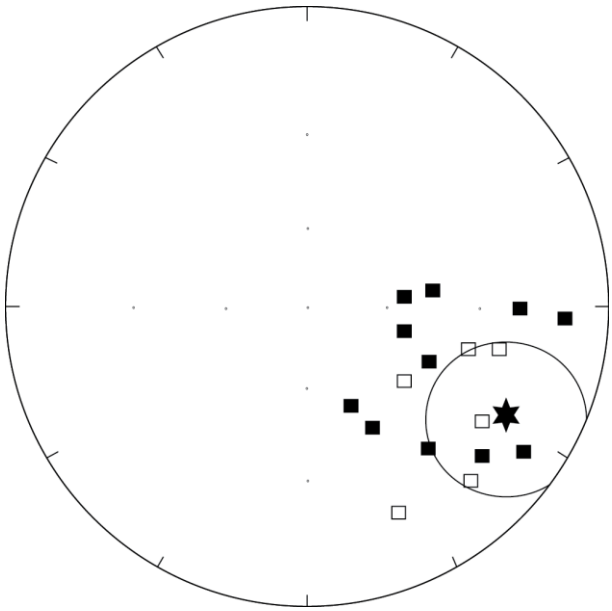

Figure 13: Equal area plot showing specimen directions for dike BC-D. Closed (open) symbols represent positive (negative) inclinations. Declinations are scattered from easterly to southeasterly, with streaked inclinations (-46° to 56°). The star represents the mean of means and the ellipse is the α95 cone of confidence.

Dike BC1

Site BC1, an intermediate composition igneous sill approximately 12km south of dike BC-D, contains magnetizations similar to ChRM I and Component II. Figure 14A shows a representative orthogonal projection diagram from BC1. At intermediate temperatures, a magnetization with westerly declinations and shallow up inclination is removed between 440-560°C. This magnetization is interpreted to reside in magnetite. AF demagnetization confirms the presence of a low-coercivity phase with a west-southwesterly declination and shallow inclination (Fig. 14B). At higher temperatures (580-700°C), a magnetization with southeasterly declinations and moderate up inclination is removed, and is interpreted to reside in hematite. The equal area plot showing means of each component is also shown in Figure 14C. On the APWP (Fig. 8),

the intermediate temperature component is plotted as BC1-IT; the high temperature component is plotted as BC1-HT. The HT pole plots near the poles for ChRM I whereas the IT pole plots on the late Paleozoic part of the APWP (Fig. 8).

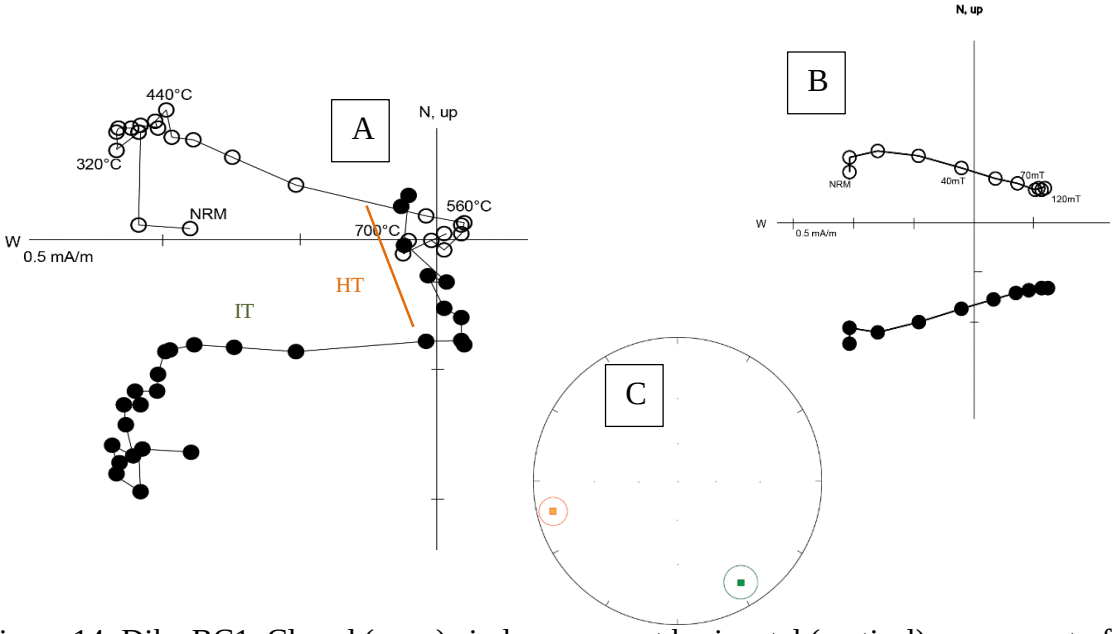

Figure 14: Dike BC1. Closed (open) circles represent horizontal (vertical) component of the magnetic component. A) Orthogonal projection diagram of specimen BC1-4. The orange (green) line outlines the HT (IT) component. B) AF demagnetizations of specimen BC1-2. C) Equal area plot. Orange (green) square represents the HT (IT) component. Solid squares represent positive inclinations, and ellipses show the cones of confidence.

Magnetic Mineralogy

Cumulative log-Gaussian (CLG) analysis (Kruiver et al., 2001) was performed to determine the coercivity ranges of the carriers of the magnetization within the dikes. Modeling yielded a 1-component (100% contribution) of a high-coercivity magnetic mineral phase (Fig. 15). When compared to coercivity ranges of magnetic minerals outlined by Peters and Dekkers (2003), the coercivity range of the magnetic contributor in the dikes lies solely within the coercivity range for hematite.

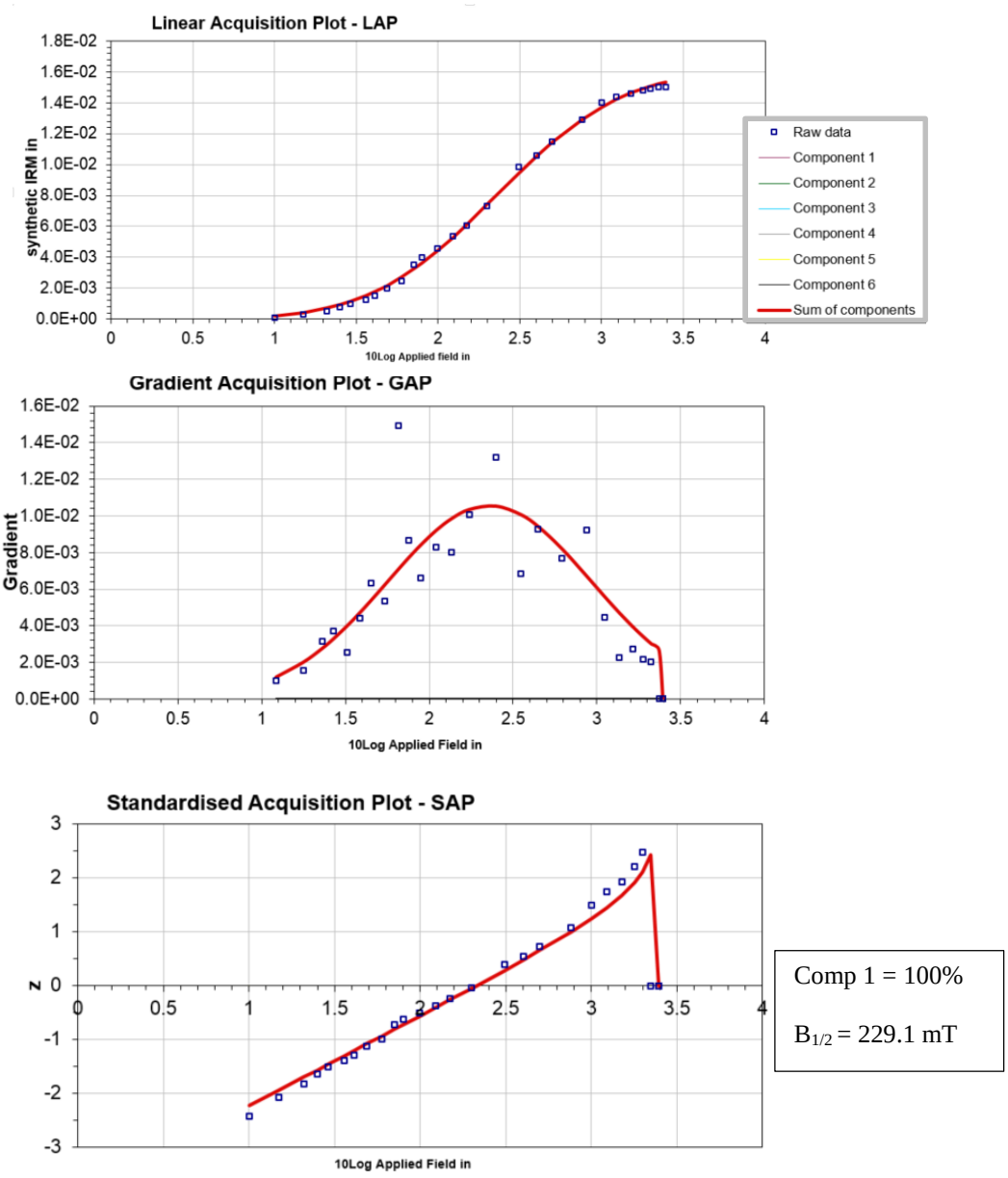

Figure 15: Modeling of IRM acquisition curve using CLG analysis for a representative specimen. The model shows a best-fit to the acquisition curve is by 100% contributions of one magnetic component. The coercivity of the component is shown on the inset box, and is wholly within the coercivity range for hematite.

Tri-axial decay of the isothermal remanent magnetization (IRM) reveals that a high-coercivity component is the highest intensity magnetic phase in most dikes samples (Fig. 16). All the ChRMs are interpreted to be held in hematite due to the high unblocking temperatures (above 580°C) of the magnetizations. AF decay of specimens shows less than 30% reduction in NRM intensity.

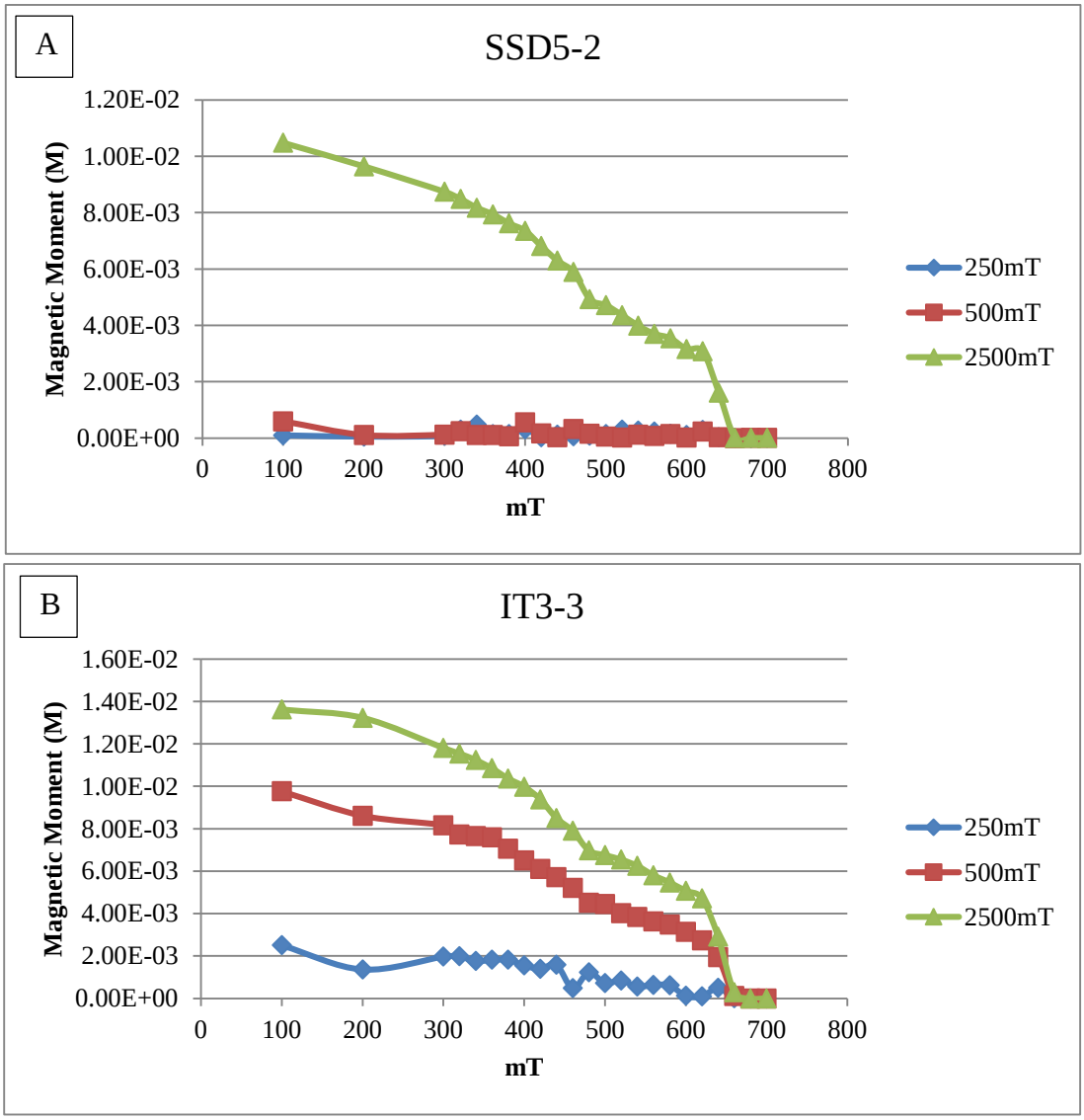

Figure 16: Tri-axial decay of the IRM for two representative dike samples. The highest coercivity component holds most of the magnetization in specimen IT3-3 (B), while it holds all of the magnetization in specimen SSD5-2 (A).

Dike BC1 shows AF decay of a low-coercivity component, with further thermal decay to 680°C revealing a magnetization in hematite. IRM acquisition suggests that more both low- and high-coercivity components are present as the sample does not reach full saturation by 1500mT (Fig. 17). Tri-axial decay of the IRM of dike BC1 shows that a higher proportion of the NRM is held in mid- and low-coercivity minerals in comparison to the other dikes (Fig. 17).

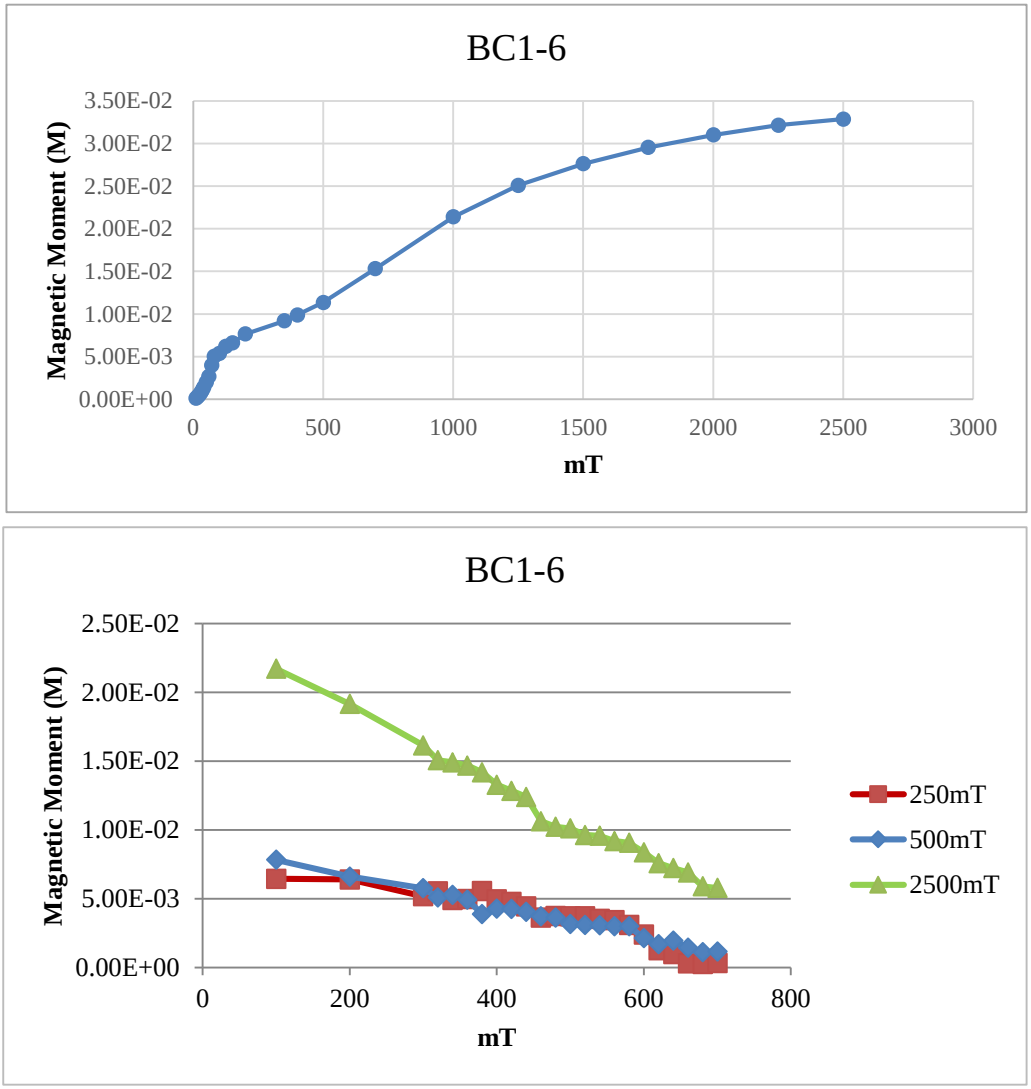

Figure 17: Top shows IRM acquisition curve for BC1-6. Bottom shows tri-axial decay of the same sample. BC1 holds a two-component magnetization in magnetite and hematite.

Petrography

The dikes are primarily (>90%) composed of well-rounded to subangular quartz, with moderate to poor sorting. The most common grain size of quartz within the dikes is below 1mm; most grains measure between 0.2-0.33mm (e.g., Vitanage, 1954). There are few larger, very well-rounded quartz grains, that measure up to 4mm. Dust lines and quartz overgrowths occur on grains in most of the dikes (Fig. 18A). The prescence of rounded quartz overgrowths suggests that the sands are second cycle. The quartz is primarily monocrystalline, although some undulose extinctions, indicative of strain, occurs. Some of the dikes display fractured and offset quartz boundaries, recording cataclastic movement within the dikes (Fig. 18B).

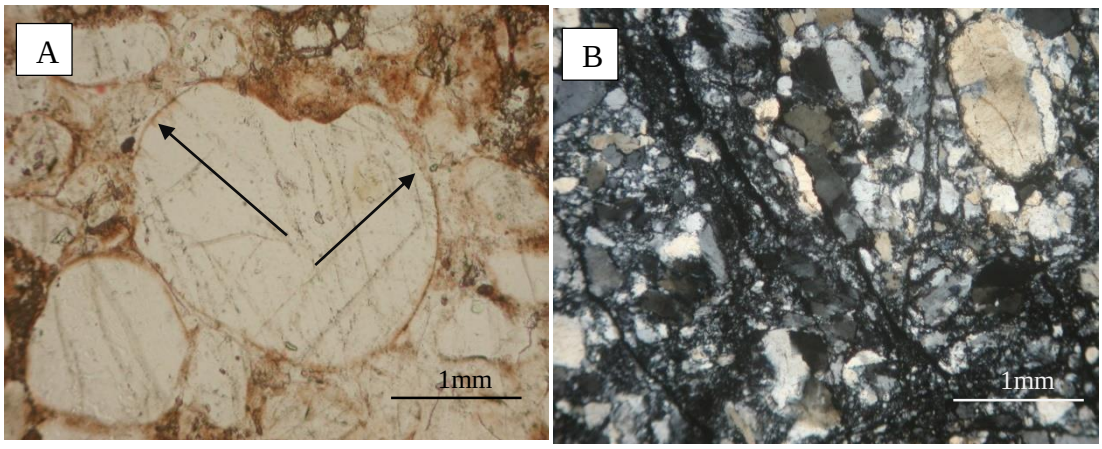

Figure 18: Photomicrographs of sandstone dikes. A) PPO light showing large quartz grain with hematite-rimmed dust lines (arrow). Abundant hematite is seen in the matrix/cement as well as quartz overgrowth cement. Many quartz grains show strain lines. B) CPO light showing cataclasis bands that indicate post-lithification structural deformation internal to the dikes. Small offsets are visible within individual quartz grains in many dikes.

Many of the dikes contain granitic fragments of varying size, ranging from sand sized (Fig. 19) to pebble and cobble-sized (Fig. 20). The granitic fragments are suspended within the dike material, and are angular. The fragments are generally found near the dike walls, but some smaller dikes (<1m across) show granitic fragments throughout the dike. Harms (1965) noted that long, angular granitic fragments are oriented with their long axes parallel to the dike walls (also seen in thin section).

The remaining constituents compromise feldspar, clay, and minor accessory minerals such as zircon and apatite. Feldspar sizes within the dikes range from <1mm to >10mm. All feldspars show extensive alteration (Fig. 20B). Clays are common within the matrix of the dikes. Authigenic copper (Fig. 21A) is found within dike SSD-A.

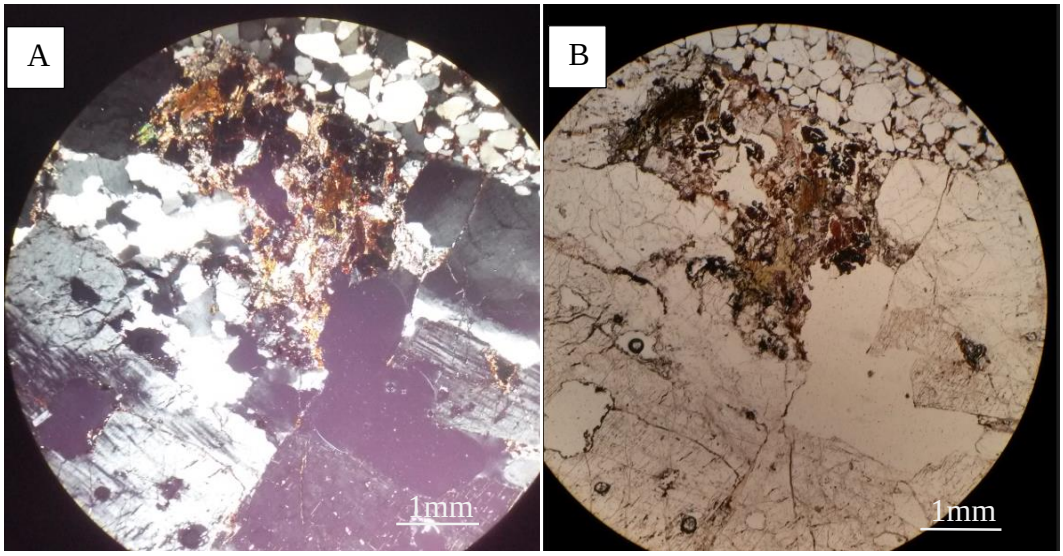

Figure 19: Photomicrograph in A) CPO light and B) PPO light of a dike showing large feldspars (microcline) that are incorporated pieces of granite wall rock. The feldspars are altering to sericite, and there is hematitic clay seen in the matrix.

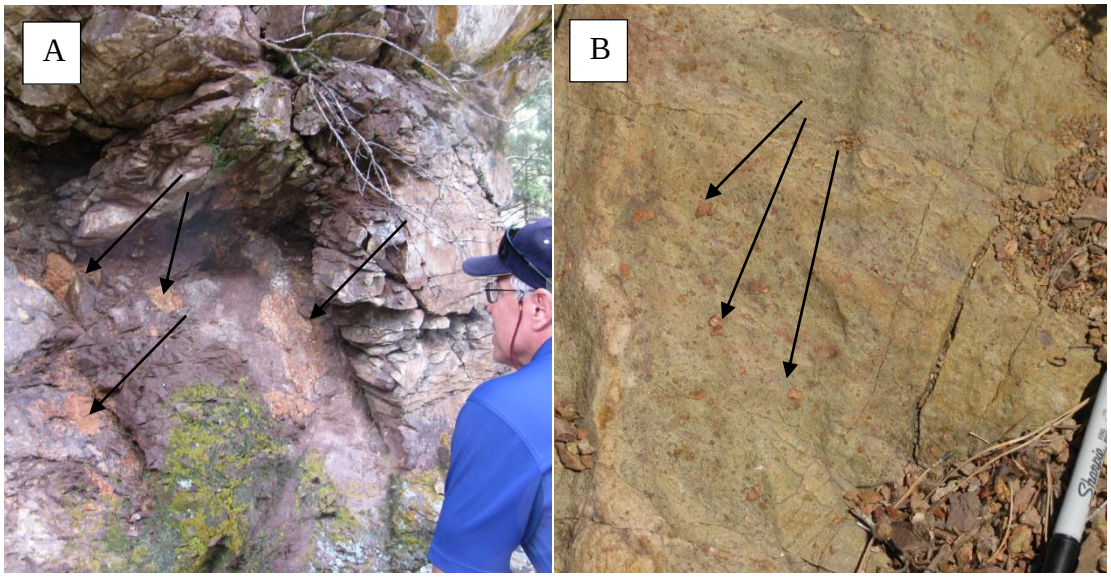

Figure 20: Granitic clasts of A) boulder-cobble size and also of B) pebble size entrained within the sandstone dikes. Arrows point out some clasts of granite.

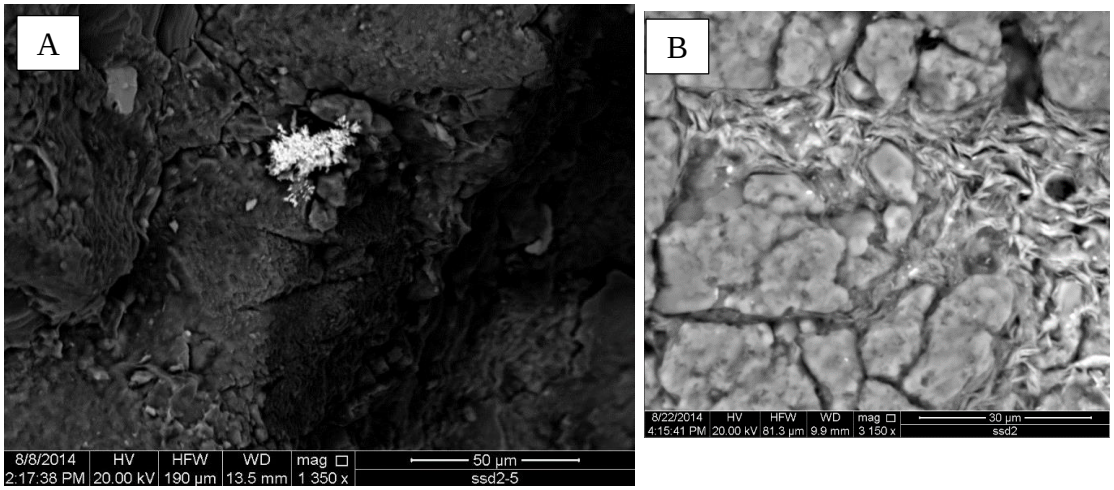

Figure 21: SEM backscattered electron images. A) Authigenic copper is the bright reflective material between two quartz grains; the copper was identified using EDS analysis. B) Clay cement infilling between grains with iron-rich (bright spots) interpreted as hematite based on EDS analysis.

The cement in the dikes is primarily clays and quartz cement (Figs. 18-21), with significant hematite and some limonite. Carbonate cements were reported by Harms (1965) and Kost (1984), as well as shale fragments within the dikes that were attributed to the Fountain Formation, although no carbonate cements or shale fragments were observed in the dikes in this study.

The most abundant iron-oxide phase within the dikes is hematite. Hematite occurs as authigenic hematite pigment, detrital specularite grains (including hematite replaced biotite; Fig. 22A and 23A), and as alteration products of detrital iron oxides (titanomagnetite) and in-situ biotite (Fig 24A). Kost (1984) also found these same types of hematite within the dike specimens.

Hematite rims many of the quartz grains and fills much of the interstitial spaces within the dikes (Fig. 22A). Hematite pigment (Fig. 22B) is abundant, and is seen within all the dikes, although to varying degrees. The hematite is commonly associated with clay and is found within the matrix, and is more abundant in finer-grained dikes. Crystal aggregates of hematite, also found in abundance by Kost (1984), were observed in many of the dikes.

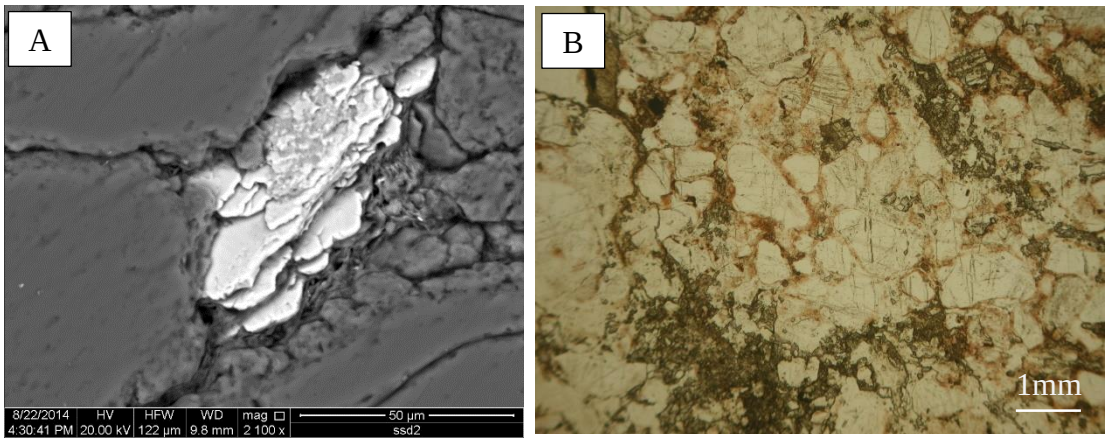

Figure 22: A) SEM backscattered electron image of bladed hematite rimming quartz grains with abundant hematite clay. B) PPO light image of sandstone dike BCD showing abundant hematite pigment.

Detrital specularite was also seen in the dikes. Figure 23A shows detrital specularite crystals within dike SSD-A. The specularite contains titanium, which was seen in EDS analysis. Detrital hematite grains that exhibit "tiger stripe" intergrowths with ilmenite were reported by Kost (1984). Figure 23B shows a reflected light photomicrograph of detrital hematite. Abundant pigment can also be seen in the image.

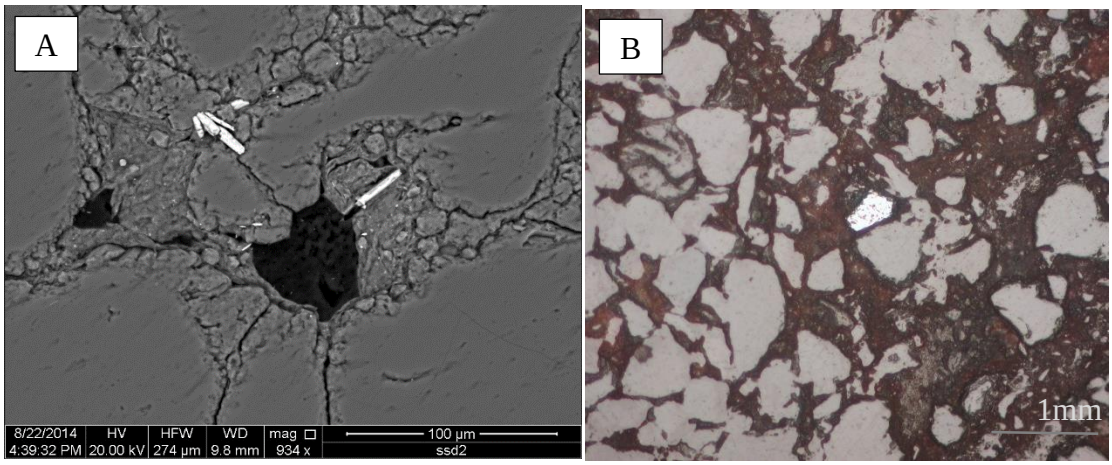

Figure 23: Detrital hematite phases within the sandstone dikes. A) SEM backscattered electron image showing bladed specularite (possibly replaced biotite). B) Reflected light photomicrograph showing abundant hematite pigment as well as a reflective grain of detrital hematite.

Replacement textures were observed both petrographically and in the SEM. Figure 24A shows hematite replacing biotite preferentially along cleavage planes which is common in the dikes. The biotite is probably the source of the iron for the authigenic hematite growth. Replacement of detrital titanomagnetite also occurs within the dikes (Fig. 24B).

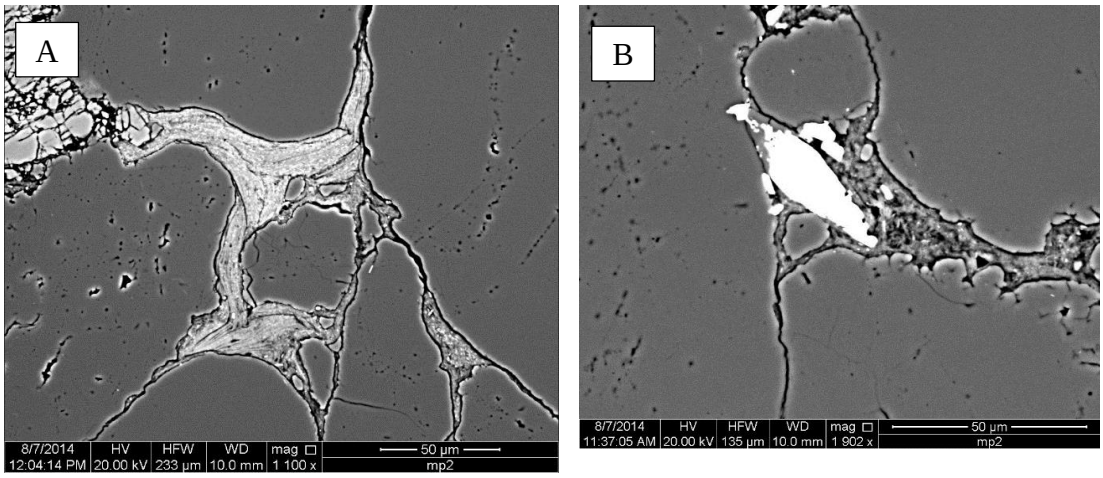

Figure 24: SEM backscattered electron images of the sandstone dikes. A) Replacement of biotite with iron-oxides (hematite) along cleavage planes. B) Near total replacement of detrital grain interpreted to be titanomagnetite (identified by EDS) by hematite.

Discussion

The magnetizations in the dikes are divided into different groups based on the ages of magnetizations derived from the APWP. ChRM I consists of sites and dikes that cluster near Proterozoic and Cambrian age reference poles (Hodych et al., 2004; Buchan, 2014). Component II is found in a cluster of sites and dikes that fall near the late Paleozoic portion of the APWP. Component III consists of sites that have

magnetizations younger than the late Paleozoic— dikes and sites that contain a Mesozoic or Cenozoic overprint. The streaked distributions seen in some dikes are interpreted as unresolved magnetic directions representing vector additions between Cenozoic-Modern or between Neoproterozoic/early Paleozoic and late Paleozoic magnetizations.

ChRM I

Dikes SSD-A, SSD3, MP2, SF, and site IT3 hold a magnetization in hematite based on the unblocking temperatures above 580°C, rock magnetic evidence, and the petrographic results. Petrographic analysis shows authigenic and detrital hematite in the dikes. Abundant pigment and specularite are seen throughout the matrix of the sandstone dikes. Detrital hematite, as well as replacement of detrital titanomagnetite by hematite is seen. It is not possible to identify which hematite grains are carrying ChRM I. It may be a combination of the authigenic and the detrital phases. Single-domain sized hematite blades <1μm occur within hematite-rimmed clays in the matrix (Fig. 23A), and may be the carriers of the magnetic remanence.

The unblocking temperatures are too high for the magnetization to be thermoviscous in origin (Pullaiah et al., 1976), and it is interpreted as a combination of a detrital remanent magnetization (DRM) and an early chemical remanent magnetization (CRM). There is no evidence for alteration by hydrothermal fluids above 650°C, which is the temperature the rocks would need to reach in order to thermoviscously reset the magnetization. While the authigenic hematite may have formed due to hydrothermal fluid alteration of the surrounding granites, the

temperatures were low (~200°C) (Spall, 1970). There are no field tests that can be performed to distinguish between a DRM and CRM in the dikes. The evidence for a DRM is the presence of probable detrital grains of hematite whereas the presence of authigenic hematite suggests that a CRM is also present.

ChRM I is "noisy" in many specimen orthogonal projections, as seen in the thermal demagnetization diagram for specimen SSD1-1 (Fig. 6), which shows linear decay but with some oscillation of the magnetization about the best-fit line. This noise can be explained by the presence of granitic fragments that were incorporated into the dike material during dike emplacement, (Fig. 20) or by a combination of a DRM and an early CRM. The presence of this noise explains the high-dispersion within sites (see Table 1) that contain ChRM I.

The VGP for ChRM I (Fig. 8) that plots at 13.9°S, 153.6°E, falls southwest of the APWP for North America as defined by Torsvik et al. (2012). The APWP for North America (Laurentia) is poorly defined for the Precambrian and early Paleozoic due to a lack of primary paleomagnetic poles of high quality during these times (Torsvik et al. 2012). The pole for ChRM I is similar to some other published poles (Hamilton et al., 2014; Hodych et al. 2004). The VGP for ChRM I and the VGP for the Neoproterozoic Long Range Dikes (19°S, 175°E; A_{95} = 18; summarized by Buchan, 2014) sampled in Newfoundland by Hodych et al. (2004) have significant overlap. The pole for ChRM I lies close to primary poles of the Long Range Dikes (Hodych et al., 2004), which were emplaced ~615 Ma. The error associated with ChRM I also overlaps primary poles from the Cambrian Long Mountain Granite in Oklahoma (Hamilton et al., 2014).

There is little to no evidence of rotation within the Pikes Peak batholith (Shallow, 1994). Spall (1970) notes that the main body of granite appears to be at or near its original attitude due to little displacement of overlying sedimentary rocks and the low angle of dip of unconformities. Spall (1970) concluded that no structural correction was needed for paleomagnetic data in his study area, which overlaps this study. An unpublished master's thesis (Shallow, 1994) provided a paleomagnetic analysis of the Pikes Peak Granite along the Rampart Range fault (a reverse fault east of the Ute Pass Fault, and north of the town of Woodland Park). Shallow (1994) determined that there was a primary magnetization in magnetite within the granite, and the pole position closely matched that of Spall (1970), therefore there was no rotation present. Geissman and Harlan (2002) make the same assumption that little to no rotation occurred within Pikes Peak Granite. They cite the similar finding of a primary TRM within the Pikes Peak Granite, held within magnetite, which matches Spall's (1970) pole, as well as other poles of similar age.

Spall (1970) reported that there are two phases of hematite within the Pikes Peak Granite. The first stage of hematite formed from deuteric alteration of the feldspars within the granite and occurred soon after crystallization. The second stage of authigenic hematite formation occurs along fractures in the granite, at some points enlarging the fractures due to its abundant formation. Hutchinson (1960) attributed this hematite formation to hydrothermal alteration, in agreement with Spall's (1970) conclusion.

Authigenic hematite is abundant in the dikes, occurring as pigment around grains, in altered micas, as overgrowths on detrital grains, as martite, and as detrital

grains. Several of these hematite types (pigment, replaced micas) are commonly found in other rocks and are attributed to weathering fluids (Creer, 1968; Parnell et al., 2000; Ricordel et al., 2007). This suggests that the inferred early CRM in the dikes could be related to weathering after emplacement of the dikes. Alternatively, the authigenic copper found in the dikes is likely associated with hydrothermal fluid flow responsible for deposition of metallic minerals within the Colorado Mineral Belt. These fluids flowed through the Pikes Peak Granite along lines of structural weakness as early as the Precambrian (Romberger, 1980).

ChRM I is inferred as Neoproterozoic to earliest Cambrian in age. Earlier researchers (Vitanage, 1954; Scott, 1963; Harms, 1965) have suggested infilling and/or injection from above into the Pikes Peak Granite, forming the dikes during Ancestral Rockies or Laramide deformation. Kost (1984) suggested that the dikes may be related to tectonic mechanisms associated with faulting and rifting within the Anadarko Basin in Oklahoma; the tectonic lineament trends to the northwest, and also originated along Precambrian zones of weakness. This association with tectonics related to the Oklahoma Aulacogen cannot be ruled out, as ChRM I lies close to the Cambrian portion of the APWP (Fig. 8).

Although mapped as Cambrian Sawatch (Temple et al., 2007), the likely sedimentary source of the dikes is a Neoproterozoic sand that has subsequently eroded (Temple, personal communication). The paucity of Neoproterozoic sediments within the present-day Front Range as well as the overprint of orogenies throughout the Paleozoic and Cenozoic (and possibly Proterozoic) makes the determination of the provenance of the dikes difficult.

The Uinta Mountain Group (UMG) sediments are one possible source; the sediments were deposited within a rift system associated with the break-up of Rodinia (Condie et al., 2001). The source of the UMG is identified as mixed Archean and Paleoproterozoic sources based on isotopic signatures (Condie, et al., 2001). A Neoproterozoic age for the dikes is corroborated by detrital zircon analysis of a subset of the dikes (Siddoway and Gehrels, 2014). As suggested by Siddoway et al. (2013), the break-up of Rodinia was occurring during this time, and tectonics associated with the extension may have opened fissures that were filled by a pre-Sawatch source (Temple, personal communication). Geochemical and petrographic analysis of the Uinta Mountain Group sandstones and shales shows that tectonic control of sediment deposition was associated with inter-continental rifting and the break-up of Rodinia (Ball and Farmer, 1998; Condie et al., 2001) during the Neoproterozoic.
During this activity, the dikes may have acquired a DRM or a CRM shortly after emplacement.

Component II

The late Paleozoic through early Triassic magnetizations that comprise the second grouping, component II, are found in dikes and within the Pikes Peak Granite near Pine, Colorado. Component II is similar in age to secondary magnetizations found within the Pikes Peak batholith (Spall, 1970; Shallow, 1984; Geissman and Harlan, 2002). This magnetization also resides in hematite and is interpreted as a CRM within the dikes and the granite.

Based on the pole positions (Fig. 8), component II was likely acquired during/post Ancestral Rockies orogenesis. Geissman and Harlan (2002) suggested that secondary porosity formed within the Pikes Peak Granite during exhumation and uplift associated with the Ancestral Rocky Mountains, and basinal fluid flow along unconformities is responsible for deposition of the authigenic hematite. Uplift of the Ancestral Rockies during the Pennsylvanian and associated basinal fluid flow along unconformities and pre-existing faults (such as the Ute Pass Fault) is a likely mechanism of remagnetization for the component II magnetization in MP1 and for TC2 dikes. This is consistent with many other late Paleozoic remagnetizations in North America (McCabe and Elmore, 1989; Elmore et al., 2012). Supergene weathering fluids are another possible model for acquisition of Component II, a mechanism of CRM acquisitions first discussed by Creer (1968). The late Permian/early Triassic was a period of relative tectonic quiescence, where much of the area that is now the Front Range was above sea-level, adjacent to the Transcontinental Arch (Maughan, 1980). The Permo-Triassic boundary was also a period of increased chemical weathering as seen in paleosols from Antarctica (Sheldon, 2006) as well as Sr and Nd isotope studies (Martin and Macdougall, 1995). In these conditions, a CRM may have been acquired by dike TC1, and the Pikes Peak Granite near Pine, Colorado.

Component III

Dikes (SSD 10), sites (IT2, IT5), and the Sawatch sandstone (SW), all hold component III in hematite with pole positions that are similar to Mesozoic-Cenozoic poles. These magnetizations are interpreted to be related to Laramide deformation.

Reactivation of faults along the present day Front Range may have provided conduits for remagnetizing fluids (Spall, 1970; Romberger, 1980).

Dike BC-D (sites BC3, BC4, BC9, and BC10), and dikes MP5, SSD6, MD, and CD, along with site IT6 all show streaked distributions on equal area projections. Many dikes and sites have streaked distributions as a result of multiple generations of hematite authigenesis associated with fluid flow from recurring tectonic movements along faults.

Dike BC1

Dike BC1 is treated separately from the clastic dikes. Not only is the origin of the magnetization within dike BC1 enigmatic, but the origins of the dike itself are also unclear. Dike BC1 is termed an intermediate composition igneous dike (Barry Weaver, personal communication). The presence of rounded quartz and apparent faint dust lines, however, raises questions about the origin of the rock. The percentage of feldspar within the dike is much higher than that in the surrounding clastic dikes, which contain less than 5% feldspar. The dark, fine-grained matrix appears igneous in origin, but is not present throughout the BC1 dike. BC1 holds a magnetization that is Cambrian or older in magnetite.

The BC1 dike has been interpreted as recording alteration by remagnetizing fluids, which resulted in the acquisition of a secondary magnetization of late Paleozoic age and held in hematite. Regardless of its origin, BC1 was remagnetized, possibly by the same process responsible for the secondary magnetizations within the clastic dikes, because the magnetizations are of similar age. The presence of multiple magnetizations in separate dikes—and multiple magnetizations present within the same dike—lend

credence to the supposition that the dikes were emplaced in the Neoproterozoic or early Cambrian and were subjected to remagnetizing fluids at later times.

The Pikes Peak Batholith was emplaced 1.09 Ga, and was not accompanied by regional metamorphism (Lovering and Goddard, 1950). The level of intrusion was shallow, and the batholith itself may have breached the surface in some areas (Tweto, 1980a). Post-intrusion, clastic materials were injected or flowed into fissures within the Pikes Peak Granite, forming the clastic dikes seen along the modern-day Front Range. Many mechanisms have been presented for clastic dike emplacement (e.g. Crosby, 1897; Vitanage, 1954; Harms, 1965; Siddoway, 2013). The absence of stratigraphic section representing 400 My of depositional history post-batholith intrusion (Tweto, 1980b) complicates determination of the age of emplacement of the dikes. The presence of ChRM I, a primary or early secondary magnetization, points to an initial emplacement age of Neoproterozoic-Cambrian, with subsequent remagnetizations during later tectonic activity.

Previous study of the dikes (Crosby, 1894; Vitanage, 1954; Harms, 1965) have provided estimation of the age of emplacement based on visual and petrographic comparison with the Cambrian Sawatch. Structural mapping of the areas where the clastic dikes are located shows that the mechanism of dike emplacement are tied to movement along the faults, which have been active since Precambrian time (Tweto, 1980a). Paleomagnetic analysis has shown that the dikes contain a magnetization that is Neoproterozoic/Cambrian. Therefore, the dikes must have been in place prior to (in the case of a CRM) or during (DRM) Neoproterozoic/Cambrian. Preservation of sediments

of this age in Colorado, and the tectonic processes associated with their deposition fills in a portion of the 400 My gap in the geologic history of Colorado.

Conclusion

Clastic dikes within Proterozoic Pikes Peak Granite along the present-day Front Range in Colorado were likely emplaced during the Neoproterozoic. Paleomagnetic evidence suggests a complex magnetization history within the dikes, beginning with a DRM/early CRM that was acquired ~615 Ma, followed by subsequent remagnetizations in the late Paleozoic, early Mesozoic, and Cenozoic. The primary/early secondary magnetization is interpreted as being acquired during either the break-up of Rodinia during the Neoproterozoic, or during rifting that began in the early Cambrian. Either of these tectonic settings may have opened fissures, allowing unconsolidated sands to either flow or inject into the underlying Pikes Peak Granite. A Neoproterozoic age for the clastic dikes agrees with detrital zircon data (Siddoway and Gehrels, 2014) that shows a correlation between Grenville-aged sediments and the dikes.

Secondary magnetizations were acquired during 1) the Ancestral Rockies orogeny (late Paleozoic), 2) re-activation of faults and the Front Range uplift that began during the Mesozoic, and 3) the Laramide orogeny during the Cenozoic. These magnetizations are CRMs, associated with fluid movement along faults and structure lineaments that have existed since Precambrian times, or possibly hematite authigenesis associated with weathering fluids.

The presence of multiple magnetizations within the clastic dikes confirms the complex tectonic history of present-day Front Range rocks. Emplacement of clastic

dikes in basement rocks occurred after deposition of both the Stoer and the Torridonian groups in Scotland (Dulin et al., 2005), a tectonic setting similar to that present during the Neoproterozoic in present-day western North America.

References

Bailey, R. C., and Halls, H. C., 1984, Estimate of the confidence in paleomagnetic directions derived from mixed remagnetization circle and direct observational data: Journal of Geophysics = Zeitschrift Fuer Geophysik, v. 54, no. 3, p. 174-182.

Ball, T. T., and Farmer, G. L., 1998, Infilling history of a Neoproterozoic intracontinental basin: Nd isotope provenance studies of the Uinta Mountain Group, Western United States: Precambrian Research, v. 87, p. 1-18.

Beacom, L. E., Anderson, T. B., and Holdsworth, R. E., 1999, Using basement-hosted clastic dikes as syn-rifting palaeostress indicators: an example from the basal Stoer Group, northwest Scotland: Geological Magazine, v. 136, no. 3, p. 301-310.

Buchan, K. L., 2014, Reprint of "Key paleomagnetic poles and their use in Proterozoic continent and supercontinent reconstructions: A review": Precambrian Research, v. 244, p. 5-22.

Condie, K. C., Lee, D., and Farmer, G. L., 2001, Tectonic setting and provenance of the Neoproterozoic Uinta Mountain and Big Cottonwood groups, northern Utah: constraints from geochemistry, Nd isotopes, and detrital modes: Sedimentary Geology, v. 141-142, p. 443-464.

Creer, K. M., 1968, Arrangement of the Continents during the Paleozoic Era: Nature, v. 219, no. 5149, p. 41-44.

Crosby, W. O., 1897, The Great Fault and Accompanying Sandstone Dikes of Ute Pass, Colorado: Science, v. 5, no. 120, p. 604-607.

Cross, W., 1894, Intrusive Sandstone Dikes in Granite: Geological Society of America Bulletin, v. 5, p. 225-230.

Dulin, S., Elmore, R. D., Engel, M. H., Parnell, J., and Kelly, J., 2005, Palaeomagnetic dating of clastic dykes in Proterozoic basement, NW Scotland: evidence for syndepositional faulting during deposition of the Torridonian: Scottish Journal of Geology, v. 41, p. 149-157.

Dulin, S., and Elmore, R. D., 2007, Paleomagnetism of the Weaubleau structure, southwestern Missouri, *in* Evans, K. R., ed., The sedimentary record of meteorite impacts, Volume 437, Geological Society of America, p. 55-64.

Elmore, R. D., and Dulin, S., 2007, New paleomagnetic age constraints on the Decaturville impact structure and Weaubleau structure along the 38th parallel in Missouri: Geophysical Research Letters, v. 34.

Elmore, R. D., Muxworthy, A. R., and Aldana, M., 2012, Remagnetization and chemical alteration of sedimentary rocks, *in* Elmore, R. D., Muxworthy, A. R., and Aldana, M., eds., Remagnetization and chemical alteration of sedimentary rocks, Volume 371: London, Geological Society of London.

Fisher, R., 1953, Dispersion on a Sphere: Proceedings of the Royal Society of London. Series A, Mathematical and Physical Sciences, v. 217, no. 1130, p. 295-305.

Freedman, D., Petronis, M., and Siddoway, C., 2013, Geomagnetic investigation of sandstone dikes of the Colorado Front Range, for determination of age and mode of emplacement, GSA-Rocky Mountain Section, Volume 44: Albuquerque, New Mexico, Geological Society of America, p. 73.

Geissman, J. W., and Harlan, S. S., 2002, Late Paleozoic remagnetization of Precambrian crystalline rocks along the Precambrian/Carboniferous nonconformity, Rocky Mountains: a relationship among deformation, remagnetization, and fluid migration: Earth and Planetary Science Letters, v. 203, p. 905-924.

Halls, H. C., 1976, A least-squares method to find a remanence direction from converging remagnetization circles: Geophysical Journal International, v. 45.2, p. 297-304.

Hamilton, M., Elmore, R.D., Weaver, B., and S.A. Dulin, 2014, Petrology and paleomagnetism of the Long Mountain Granite, Wichita Mountains, Oklahoma *in* Igneous and Tectonic History of the Southern Oklahoma Aulacogen; Oklahoma Geologic Survey vol. 38, p. 319-325.

Harms, J. C., 1965, Sandstone Dikes in Relation to Laramide Faults and Stress Distribution in the Southern Front Range, Colorado: Geological Society of America Bulletin, v. 76, p. 981-1002.

Hedge, C. E., Houston, R. S., Tweto, O. L., Peterman, Z. E., Harrison, J. E., and Reid, R. R., 1986, The Precambrian of the Rocky Mountain Region: Correlation of Precambrian rocks of the United States and Mexico, Volume U.S.G.S Professional Paper 1321-A,.

Heslop, D., Dekkers, M. J., Kruiver, P. P., and Oorschot, I. H. M. v., 2002, Analysis of isothermal remanent magnetization acquisition curves using the expectation-maximization algorithm: Geophysical Journal International, v. 148, p. 58-64.

Hodych, J. P., Cox, R. A., and Kosler, J., 2004, An equatorial Laurentia at 550 Ma confirmed by Grenvillian inherited zircons dated by LAM ICP-MS in the Skinner Cove volcanics of western Newfoundland: implications for inertial interchange true polar wander: Precambrian Research, v. 129, p. 93-113.

Hutchinson, R. M., 1960, Structure and Petrology of North End of the Pikes Peak Batholith, Colorado: Guide to the Geology of Colorado, v. Rocky Mountain Association of Geologists, p. 170.

Kent, J. T., 1982, The Fisher-Bingham Distribution on the Sphere: Journal of the Royal Statistical Society, v. 44, no. 1, p. 71-80.

Kirschvink, J. L., 1980, The least-squares line and plane and the analysis of paleomagnetic data: Geophysical Journal of the Royal Astronomical Society, v. 62, no. 3, p. 699-718.

Kost, L. S., 1984, Paleomagnetic and petrographic study of Sandstone Dikes and the Cambrian Sawatch Sandstone, Eastern Flank of the Southern Front Range, Colorado [M.S.: University of Colorado, 190 p.

Kruiver, P. P., Dekkers, M. J., and Heslop, D., 2001, Quantification of magnetic coercivity components by the analysis of acquisition curves of isothermal remanent magnetization: Earth and Planetary Science Letters, v. 189, p. 269-276.

Lovering, T. S., & Goddard, E. N.,1950, *Geology and ore deposits of the Front Range, Colorado*. US Government Printing Office.

Lowrie, W., 1990, Identification of ferromagnetic minerals in a rock by coercivity and unblocking temperature properties: Geophysical Research Letters, v. 17, no. 2, p. 159-162.

Martin, E. E., and Macdougall, J. D., 1995, Sr and Nd isotopes at the Permian/Triassic boundary: A record of climate change: Chemical Geology, v. 125, p. 73-99.
Maughan, E. K., 1980, Permian and Lower Triassic Geology of Colorado, *in* Kent, H. C., and Porter, K. W., eds., Colorado Geology: Denver Colorado, Rocky Mountain Association of Geologists, p. 103-110.
McCabe, C., and Elmore, R. D., 1989, The occurance and origin of Late Paleozoic remagnetization in the sedimentary rocks of North America: Reviews of Geophysics, v. 27, no. 4, p. 471-494.
McFadden, P. L., and McElhinny, M. W., 1988, The combined analysis of remagnetization circles and direct observations in paleomagnetism: Earth and Planetary Science Letters, v. 87, no. 1-2, p. 161-172.
Parnell, J., Baron, M., Davidson, M., Elmore, R. D., and Engel, M., 2000, Dolomitic breccia veins as evidence for extension and fluid flow in the Dalradian of Argyll: Geologic Magazine, v. 137, no. 4, p. 447-462.
Peters, C., and Dekkers, M. J., 2003, Selected room temperature magnetic parameters as a function of mineralogy, concentration and grain size: Physics and Chemistry of the Earth, v. 2, p. 659-667.
Pullaiah, G., Irving, E., Buchan, K. L., and Dunlop, D. J., 1975, Magnetization changes caused by burial and uplift. : Earth and Planetary Science Letters, v. 28, p. 133-143.
Ricordel, C., Parcerisa, D., Thiry, M., Moreau, M. G., and Gomes-Gras, D., 2007, Triassic magnetic overprints related to albitization in granites from the Morvan massif (France): Palaeogeography, Palaeoclimatology, Palaeoecology, v. 251, p. 268-282.
Romberger, S. B., 1980, Metallic Mineral Resources of Colorado, *in* Kent, H. C., and Porter, K. W., eds., Colorado Geology: Denver Colorado, Rocky Mountain Association of Geologists, p. 225-236.
Scharer, U., and Allegre, C. J., 1982, Uranium-lead system in fragments of a single zircon grain: Nature, v. 295, p. 585-587.
Scott, G. R., 1963, Bedrock Geology of the Kassler Quadrangle: Geological Survey Professional Paper
Shallow, J. M., 1994, A paleomagnetic examination of the hanging wall of the Rampart Range Fault, Front Range, Colorado. M.S.: University of Colorado, 87 p.
Sheldon, N. D., 2006, Abrupt chemical weathering increase across the Permian-Triassic boundary: Palaeogeography, Palaeoclimatology, Palaeoecology, v. 231, p. 315-321.
Siddoway, C., Petronis, M., and Rosales, M., 2009, New Insights into Emplacement Mechanisms and Geotectonic Context for Sandstone Dikes Hosted by Proterozoic Granite, Front Range, Colorado: Abstracts AAPG Annual Convention.
Siddoway, C., Myrow, P., and Diaz, E. F., 2013, Stratas, Structures, and Enduring Enigmas: A 125th Anniversary appraisal of Colorado Springs geology. Field Guide, Geological Society of America Meeting 2013.
Siddoway, C., and Gehrels, G. E., 2014, Basement-hosted sandstone injectites of Colorado: A vestige of the Neoproterozoic revealed through detrital zircon provenance analysis: Lithosphere, v. L390-1.

Smith, D. R., Noblett, J., Wobus, R. A., Unruh, D., and Chamberlain, K. R., 1999, A review of the Pikes Peak batholith, Front Range, central Colorado: A "type example" of A-type granitic magmatism: Rocky Mountain Geology, v. 34, no. 2, p. 289-312.

Spall, H., 1970, Palaeomagnetism of the Pikes Peak Granite, Colorado: Geophysical Journal of the Royal Astronomical Society, v. 21, p. 427-440.

Temple, J., Madole, R., Keller, J., and Martin, D., 2007, Geologic Map of the Mount Deception Quadrangle, Teller and El Paso Counties, Colorado: Colorado Geological Survey.

Torsvik, T. H., Voo, R. V. d., Preeden, U., Niocaill, C. M., Steinberger, B., Doubrovine, P. V., Hinsbergen, D. J. J. v., Domeier, M., Gaina, C., Tohver, E., Meert, J. G., McCausland, P. J. A., and Cocks, L. R. M., 2012, Phanerozoic polar wander, palaeogeography and dynamics: Earth-Science Reviews, v. 114, p. 325-368.

Tweto, O., 1980a, Precambrian Geology of Colorado, *in* Kent, H. C., and Porter, K. W., eds., Colorado Geology: Denver, Colorado, Rocky Mountain Association of Geologists, p. 37-46.

Tweto, O., 1980b, Tectonic History of Colorado, *in* Kent, H. C., and Porter, K. W., eds., Colorado Geology: Denver, Colorado, Rocky Mountain Association of Geologist, p. 5-10.

Vitanage, P. W., 1954, Sandstone Dikes in the South Platte Area, Colorado: The Journal of Geology, v. 62, no. 5, p. 493-500.

Yonkee, W. A., Dehler, C. D., Link, P. K., Balgord, E. A., Keeley, J. A., Mayes, D. S., Wells, M. L., Fanning, C. M., and Johnston, S. M., 2014, Tectono-stratigraphic framework of Neoproterozoic to Cambrian strata, west-central U.S.: Protracted rifting, glaciation, and evolution of the North American Cordilleran margin: Earth-Science Reviews, v. 136, p. 59-95.

Zijderveld, J. D. A., 1967, A.C. Demagnetization of rocks: Analysis of results, *in* Collison, D. E., K.M.Creer, and Runcorn, S. K., eds., Methods in Paleomagnetism: New York, El Sevier Science, p. 254-286.

Chapter 2: Remagnetization of Zebra Dolomite within the Basin and Range Province, southern Nevada

Abstract

Zebra dolomites within the Devonian Guilmette Formation in the southern Basin and Range Province, Nevada, are the focus of a paleomagnetic study to determine timing of formation. Zebra dolomite has formed in close stratigraphic proximity and within the Alamo Breccia in the Delamar Range. The zebra dolomite is made up of alternating bands of white and black dolomite, with saddle dolomite being a common constituent. The zebra dolomite and associated host rock contain a characteristic remanent magnetization (ChRM) that resides in magnetite and was acquired during the late Triassic. The ChRM was also found within clasts of the Alamo Breccia. $^{87}Sr/^{86}Sr$ values for the zebra dolomite are elevated compared to Devonian seawater values, suggesting the dolomite formed from externally derived fluids. The presence of a late Triassic magnetization indicates that the zebra dolomite can be no younger than late Triassic, regardless of the mechanism of zebra dolomite formation. The ChRM is interpreted as a chemical remanent magnetization (CRM) based on the maximum unblocking temperatures for the ChRM (520ºC) and low burial temperatures. The CRM was acquired when the zebra dolomite formed from brines, which were likely mobilized during the Triassic Sonoma orogeny.

Introduction

Hydrothermal zebra dolomite occurs in carbonates throughout the Basin and Range province as well as other structural provinces of the western United States (Diehl

et al., 2010; Vandeginste, 2005). The origins of zebra dolomite remain poorly understood (Vandeginste, 2005; Merino et al., 2006), although most hypotheses invoke a hydrothermal fluid flow mechanism of deposition, commonly associated with deposition of metals or with tectonic activity.

Diehl et al. (2010) studied zebra dolomites in the Basin and Range province of Nevada and California. Hydrothermal zebra dolomite is inferred to form during migration of warm (90-200°C) basinal brines that were also responsible for deposition of Mississippi Valley Type (MVT) and sedimentary exhalative (SEDEX) ore mineralization. Therefore, the age of the zebra dolomites is coeval with deposition of ore mineralization (Diehl et al., 2010). Absolute age dating was not performed, and the age was inferred from the association of zebra dolomite with ore mineralization and the assumption that the same processes formed both. Determining the absolute timing of zebra dolomite formation would provide an improved understanding of their origin. Absolute dating of zebra dolomite formation has been difficult.

Hydrothermal fluid migration is responsible for remagnetization of carbonate rocks, with many studies focusing on paleomagnetic analysis to determine timing of hydrothermal events (e.g., Elmore et al., 2012). In this study, zebra dolomite and host rocks of the Delamar Range, Mt. Irish, and Hancock Summit of Nevada (Fig. 1) were sampled in order to determine timing of zebra dolomite formation and associated hydrothermal events using paleomagnetic analysis.

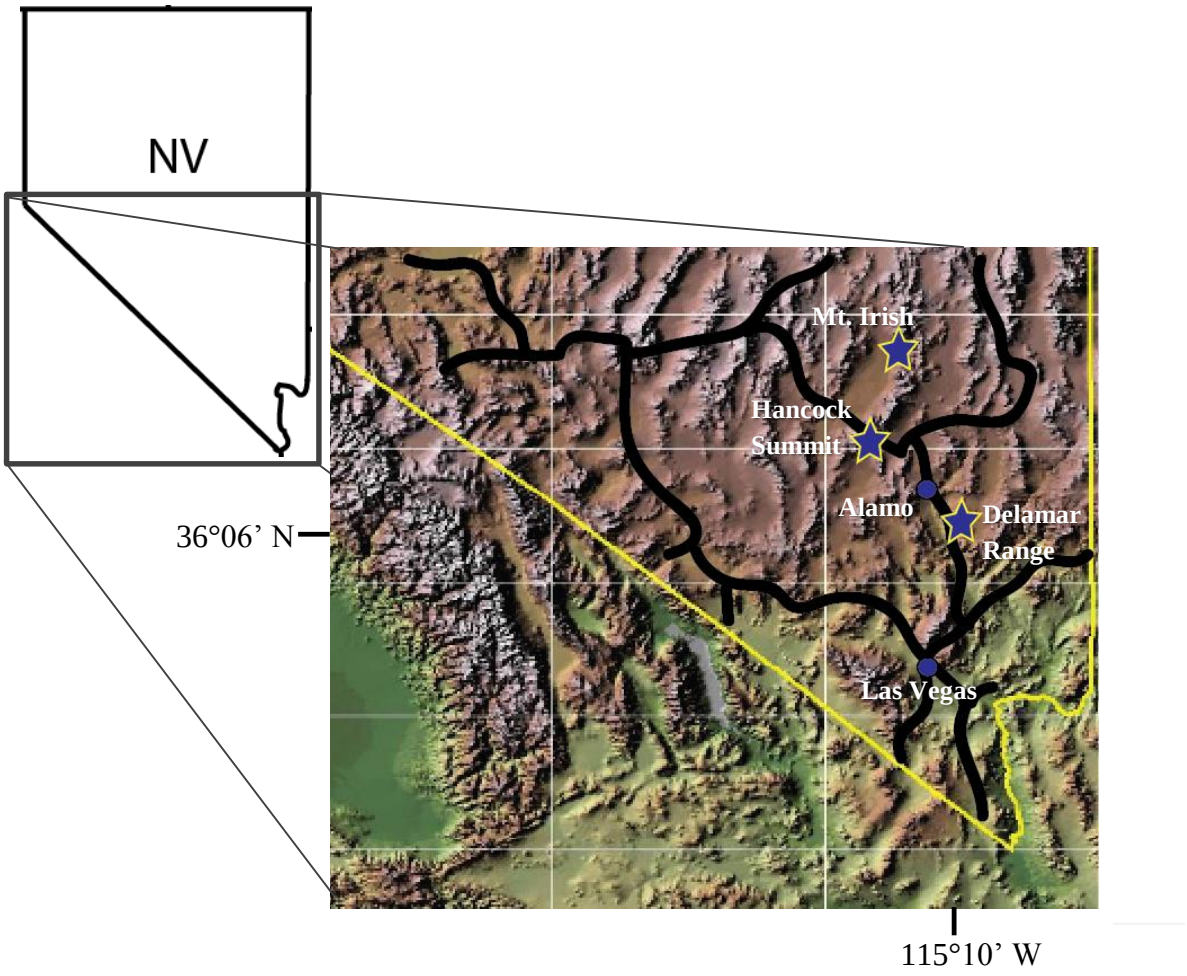

Figure 1: Location of study areas in southern Nevada. Inset shows topographic profile of the Basin and Range Province (mod. from http://fas.org/irp/imint/docs/rst/Sect6-/Sect6_8.html). Sampling locations are marked with stars. Hancock Summit and Mt. Irish are located in the Pahranagat Range.

Geologic setting and previous work

The kinematic and tectonic formation of zebra dolomite is complex, with many different theories for the genesis of the zebra texture. The formation of the zebra texture

is generally attributed to (relatively) hot brines, from fluid inclusion analyses comparing host and zebra dolomites (Diehl et al., 2010). Prevailing views of zebra dolomite formation link migration of hot brines with dissolution of host limestone. The hot brines cause dolomitization and/or ore mineralization in addition to dissolution of the host carbonate, leaving a void space where zebra dolomite subsequently precipitates (Leach et al., 2005; Emsbo, 2009). Merino et al. (2006) proposed that this mechanism is faulty, and that zebra rhythmites and associated zebra breccia textures form by self-reorganization of dolomites, with the zebra "veins" growing at the expense of the surrounding rock, creating stylolites to accommodate the transport of material displaced during precipitation of the zebra dolomite. Vandeginste et al. (2005) suggested zebra dolomite precipitates by brine movement driven along microcracks created by compressional stresses. Extensional tectonic stresses have also been invoked as a mechanism of zebra dolomite formation; as pressure is relieved on faults during extension, mineralizing fluids flow, causing precipitation of zebra dolomite (Heijlen et al., 2003).

Diehl et al. (2010) provided a comprehensive treatment of zebra dolomites associated with ore mineralization throughout Nevada, far western Utah, and near Death Valley in southeastern California. In most cases, the zebra dolomite was found in association with mineral deposits—sedimentary exhalative (SEDEX) and Mississippi Valley Type (MVT) were the most common. Diehl et al. (2010) sampled zebra dolomites in Cambrian-Mississippian host dolostones to determine cause of formation and possible relation to the age of the host rocks. The timing of zebra formation is epigenetic—younger than the host rock—in all cases, although direct dating of

recrystallization was not accomplished (Diehl et al., 2010). The zebra dolomite was interpreted as hydrothermal in origin, and was deposited by hot brines (<200°C) that flowed along pre-existing faults re-activated during both extensional and compressional tectonic events and orogenesis (Diehl et al., 2010).

This study focuses on zebra dolomite within the Delamar Range, Mt. Irish, and Hancock Summit, in Lincoln County, Nevada (Fig. 2). Mineralization of ore grade is not associated with zebra dolomite at Hancock Summit, however the ghost town of Delamar lies within the Delamar Range. The town of Delamar was associated with a productive gold mine that operated until early in the 20th century (www.ghosttowns.com/states/nv/delamar). Silver was mined near the flanks of Mt. Irish and many abandoned mines occur throughout the Mt. Irish Range.

Cenozoic extensional processes formed the Basin and Range province of Nevada (Stewart, 1980); the structural trends are roughly north-south trending mountain ranges bounded by normal faults, of which the Delamar Range is an example. Hancock Summit is the highest summit within the Pahranagat Range, and is the type locality for the Alamo Breccia. The Mt. Irish Range also contains zebra dolomite that is stratigraphically above the Alamo Breccia.

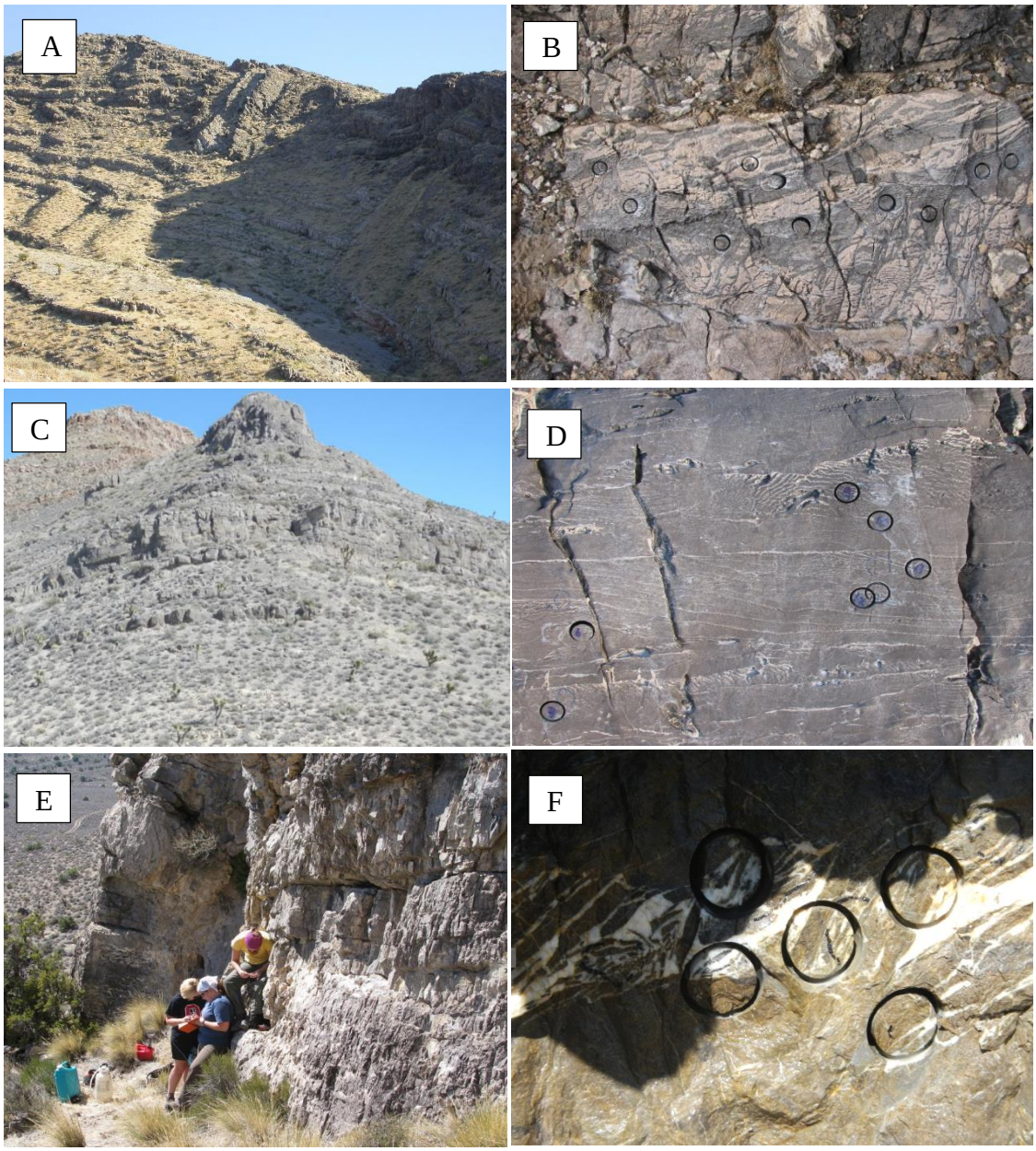

Figure 2: Sampling locations and representative zebra dolomite pictures from each area. Cores are 2.5cm in diameter. A) Delamar Range Guilmette section. The chaotic blocks at the top of the canyon represent megaclasts of the Alamo Breccia. B) Delamar Range zebra dolomite (DZ), concordant to bedding. C) Hancock Summit. D) Zebra dolomite is "patchy" and not as stratigraphically widespread as in the Delamar Range. E) Mt. Irish. F) The zebra dolomite frequently appears brecciated at Mt. Irish.

The zebra dolomite in the three sampling localities are within the Devonian Guilmette Formation. The Alamo Breccia, which is interpreted to have formed due to a late Devonian bolide impact on the shallow carbonate shelf of western Nevada (Warme, 1998), is the middle member of the Guilmette. The breccia is 50m thick in the Delamar Range, 100m at Mt. Irish, and 100m at Hancock Summit.

The Guilmette Formation is a thick succession of black limestone and dolostone that formed on the shallow shelf during the mid-to-late Devonian (Givetian-Frasnian). The limestone was dolomitized during late diagenesis (Elrick, 1986). During the mid-Paleozoic, the Antler orogeny affected deposition of the carbonate platform (Gillett and Karlin, 2004) and created a compressional stress regime throughout the area. Ancestral Rockies uplift during the late Paleozoic created high-angle thrust faults and associated basins in northern and central Nevada (Gillett and Karlin, 2004). The Permo-Triassic Sonoma orogeny next affected Nevada, which created a compressional regime that formed as a result of accretion of an island-arc along the western edge of the carbonate platform (Wyld, 1991). The Sevier orogeny during the late Cretaceous created thrust belts trending NE across southern Nevada into Utah, which coincided with the paleocontinental margin during that time (Gillett and Karlin, 2004). The Cenozoic brought extensional tectonic stresses and created the present-day Basin and Range province (Stewart, 1980).

Gillett and Karlin (2004) conducted a paleomagnetic study on middle Cambrian-upper Pennsylvanian miogeoclinal carbonate strata throughout the Basin and Range in Nevada, Utah, Arizona, and California. They found a pervasive late Paleozoic-Triassic remagnetization, held in magnetite, throughout the study area. The low-inclination

magnetization was interpreted as a chemical remanent magnetization (CRM) that formed from migration of orogenic fluids during the late Paleozoic/early Triassic Sonoma orogeny, during the Ancestral Rockies orogeny, or by burial diagenetic processes (Gillett and Karlin, 2004).

Evans et al. (2012) provided a comprehensive paleomagnetic analysis of the Alamo Breccia member of the Guilmette Formation at Hancock Summit and Mt. Irish. Two magnetic components occur within and surrounding the breccia at both localities. A syn-tilting intermediate temperature component, in pyrrhotite, that is Cretaceous to Paleogene in age, and a pre-tilting higher-temperature component, in magnetite, that is Pennsylvanian to Permian in age. The magnetizations are similar to those found by Gillett and Karlin (2004), and are interpreted as CRMs related to externally derived fluids, which is supported by elevated $^{87}Sr/^{86}Sr$ values within the Guilmette Formation.

Vertical axis rotation resulted from Cenozoic extension of the Basin and Range throughout the study area. The southern Delamar Range had negligible vertical axis rotation and was used as a non-rotated reference location when determining the extent of block rotations (Hudson et al., 1998). Hancock Summit and Mt. Irish are likely to have experienced small (<10°) counterclockwise rotation about a vertical axis during extension in the Cenozoic. This interpretation is consistent with paleomagnetic data (Gillett and Karlin, 2004; Evans et al., 2012).

Methods

Zebra dolomite within one canyon in the Delamar Range was sampled for paleomagnetic analysis. All samples of zebra dolomite at Delamar are designated sites

DZ. The zebra dolomite was sampled both within and below the Alamo breccia. Sites DR2, G9, and G21 are hosted in the Guilmette Formation. At Hancock Summit, zebra dolomite is sparsely dispersed throughout the Alamo Breccia. Four sites were sampled, but the specimens were widely spaced, with 10-14 specimens collected per site (HS). One site—HS1—had anomalously high natural remanent magnetization (NRM) intensities of >76 mA/M, and was deemed altered by lightning. At Mt. Irish, 8 sites were collected in zebra dolomite that appeared brecciated (as described by Diehl et al., 2010) in nature. Only 2 sites of 8 collected at Mt. Irish yielded a stable ancient magnetization.

Paleomagnetic samples were collected using a gasoline powered modified chainsaw with a stainless steel coring device that extracts 2.5cm diameter cores. Cores were oriented in the field using a Brunton compass and inclinometer. Once in the laboratory, cores were cut to standard 2.2cm specimens. The natural remanent magnetization (NRM) was measured in a shielded room using a 2G Enterprises cryogenic magnetometer with DC squids. Specimens were then subjected to stepwise thermal demagnetization (NRM-600°C in 20°C steps) using an ASC Thermal Demagnetizer. A pilot set of specimens (14) were subjected to two low temperature demagnetization (LTD) treatments in liquid nitrogen and warmed in a zero field to remove a magnetization held in multi-domain (MD) magnetite (Dunlop and Argyle, 1991) before thermal demagnetization. These specimens had companion specimens that were cut from the same core and were only subjected to thermal demagnetization. The results from each set of specimens were compared.

Thermal demagnetization data were plotted as orthogonal projection diagrams (Zijderveld, 1967) and analyzed using principal component analysis (Kirschvink, 1980) to determine the magnetic components within each sample. A minimum of five demagnetization steps were used to pick the components. Mean angular deviations (MAD) of 15° or less were deemed acceptable, though most samples have a MAD angle of less than 10°. Means were computed using Fisher (1953) statistics, and the mean was corrected to remove Cenozoic tilting of the beds. This mean direction was used to determine a pole position that was compared to the APWP for North America (Torsvik et al., 2012).

Five representative specimens were imparted with an isothermal remanent magnetization (IRM) at room temperature using an ASC Scientific impulse magnetizer to determine magnetic mineralogy. Specimens were first subjected to alternating field (AF) demagnetization to remove the remanent magnetizations. An IRM was then imparted in a stepwise fashion from 0 to 2500mT. The specimens were subjected to a second AF demagnetization and subsequently imparted with three perpendicular IRMs (120mT, 500mT, and 2500mT). The specimens were then thermally demagnetized in a stepwise fashion to yield tri-axial decay curves (Lowrie, 1990).

Over 50 thin sections of zebra dolomite and host Guilmette carbonate were analyzed using transmitted light microscopy and reflected light microscopy to identify opaque minerals. Scanning electron microscope (SEM) analysis of thin sections and rock samples supplemented the thin section analysis. The SEM analysis was completed using an environmental scanning electron microscope (FEI Quanta 200) with energy dispersive capabilities at the University of Oklahoma Mewbourne College of Earth and

Energy IC3 lab. One sample was sent for analysis on a Raman mass spectrometer and a streamline map was made of a sample of zebra dolomite from the Delamar Range. Data was collected with a 50x objective on a Renishaw inVia spectrometer using a 532nm excitation source at 10% power and 0.5 μm step size. Spectra were background corrected and noise filtered prior to multicomponent analysis.

Light bands of zebra dolomite were microsampled for $^{87}Sr/^{86}Sr$ analysis. Strontium isotopic analysis was performed at the University of Texas at Austin, following the methods described by Gao et al. (1992). Analysis of $^{87}Sr/^{86}Sr$ isotopic ratios are used to determine if the rocks have been altered by radiogenic fluids. The mean $^{87}Sr/^{86}Sr$ value of NBS 987 = 0.710269 ± 0.0012 was measured and then normalized relative to NBS 987 = 0.71014 and compared to coeval seawater values for the Devonian (McArthur et al., 2001).

Results and Interpretations

Delamar Range

The Delamar Range zebra dolomites were sampled within the Guilmette Formation, below and within the lower Alamo Breccia. The Delamar Range zebra dolomite exhibits a rythymite-like habit as described by Merino et al. (2006), where the alternating band of black and white dolomite are similar in thickness, and they occur throughout a large stratigraphic interval (~200m) within the canyon (Fig. 3). The zebra dolomite occurs concordant to bedding, similar to that described by Diehl et al. (2010) in eastern Nevada.

Thermal demagnetization at low temperatures (<200°C) removes a northerly and steep down component in many specimens (Fig. 4), which is interpreted as the Modern viscous remanent magnetization (VRM). At higher temperatures, the zebra dolomite and surrounding host rock (both Guilmette carbonate and Alamo Breccia) in the Delamar Range hold a stable ancient magnetization. The characteristic remanent magnetization (ChRM) has southerly declinations and shallow inclinations and is removed between 250-520°C (Table 1). Shown in figure 4A-D are orthogonal projection diagrams for zebra dolomite specimens and surrounding host dolostone specimens. Figure 4E is the equal are plot of specimen directions. The results from the zebra dolomite (DZ) are similar to the host carbonate (DR2, G9, G21; Table 1). The ChRM is interpreted to reside in magnetite based on unblocking temperatures below 580°C.

One DZ specimen contains a northerly declination, which is interpreted as the antipode to the ChRM. Figure 4C shows an orthogonal projection diagram showing the reversal, which is removed from 460-560°C. The northerly ChRM direction is seen on figure 4E. The antipode to the northerly direction was included when calculating a mean direction for the zebra dolomites. Since only one specimen contains this northerly direction a reversal test was not feasible.

Mean directions were calculated for both the zebra dolomite and the host Guilmette carbonate; the VGPs for the mean directions are similar (Fig. 5; Table 1). The mean stratigraphic direction of the ChRM in the zebra dolomite, corrected for Cenozoic extensional tilting, has a declination of 163.1°, with an inclination of -14.6° ($k = 30.3$, $\alpha_{95} = 5.1°$; Table 1).

Site DZ only has 50% of the specimens with the ChRM. Many of the specimens without the ChRM have low NRM intensities and only contain the VRM. In approximately 30% of the specimens the demagnetization points on the orthogonal projections move to the southeast quadrant, supporting the presence of the ChRM, but do not display linear decay at higher temperatures.

The two LTD treatments of the pilot specimens changed the NRM values by 11% (std. dev. = 7.3) with 12 showing a decrease and 2 increasing in intensity. Comparison of the thermal demagnetization results from the LTD and non- LTD treated specimens did not show any significant differences. LTD treatment did not appear to affect the ChRM in the specimens.

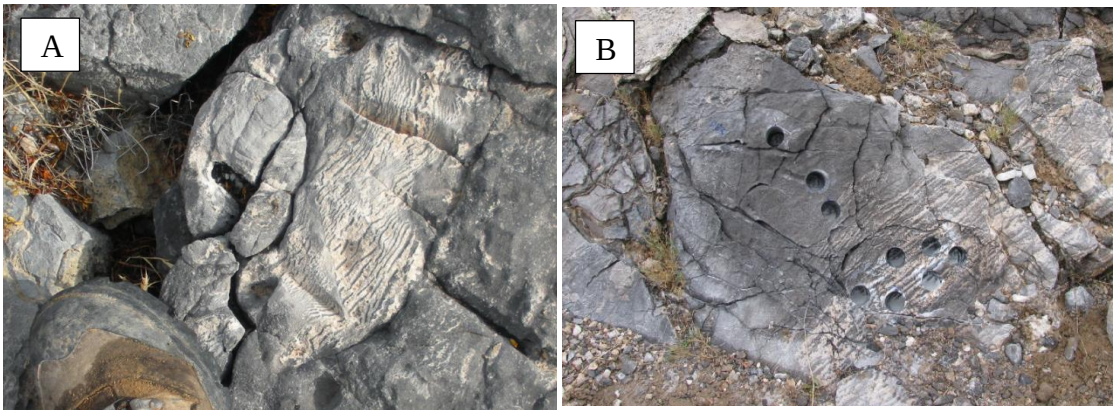

Figure 3: Zebra dolomite in the Delamar Range A) and B). Note the "rhythmite" appearance of the nearly equally spaced black and white bands of the dolomite.

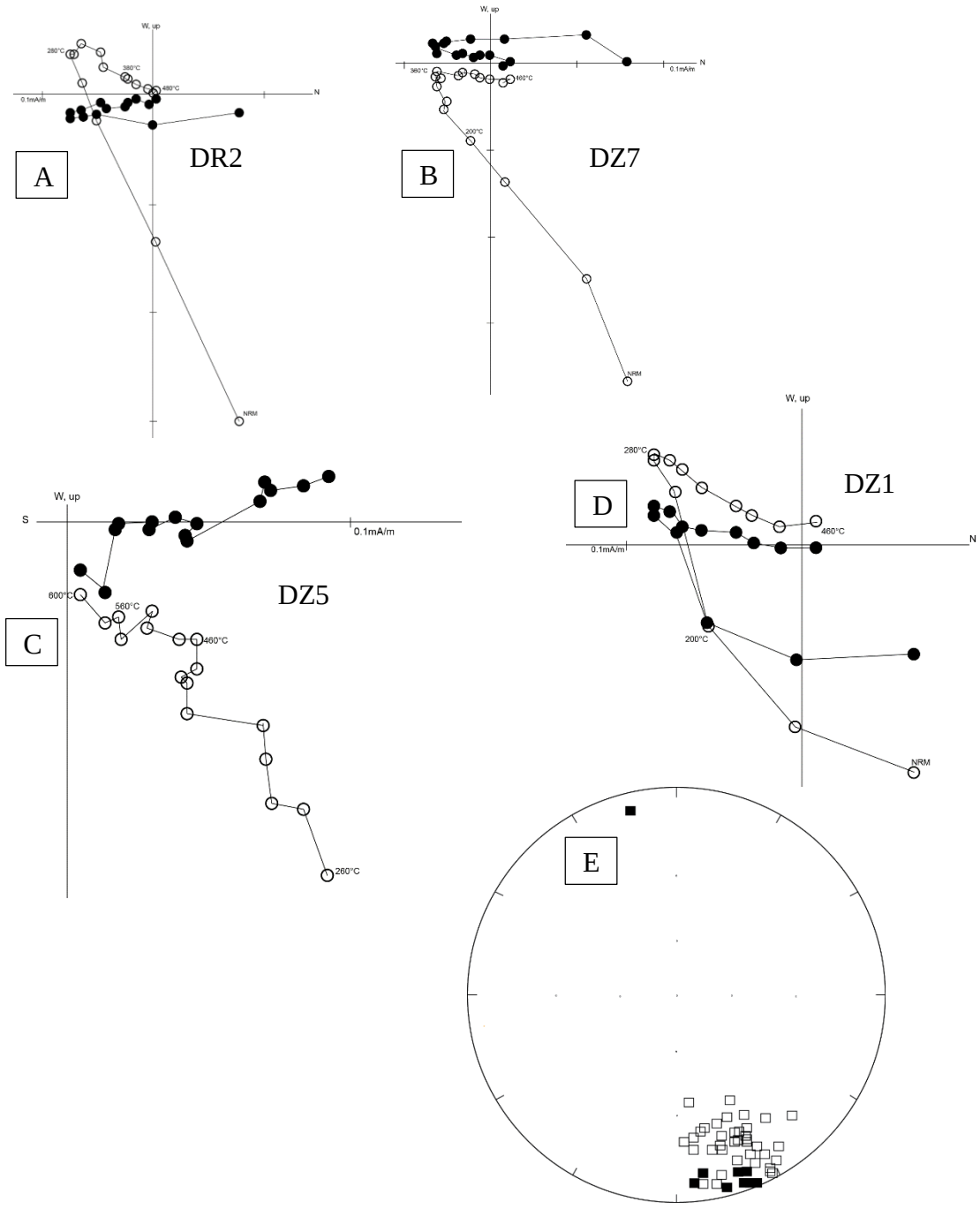

Figure 4: Orthogonal projection diagrams of host A) and B) Guilmette carbonate and C) and D) zebra dolomite in the Delamar Range. The closed (open) symbols represent the horizontal (vertical) component of the magnetization. Within all samples, a Modern VRM is removed up to ~220°C. E) Equal area plot of specimen directions of all samples that hold the ChRM in the Delamar Range. Closed (open) circles represent positive (negative) inclinations. The northerly ChRM direction is show; the antipode was used to calculate all statistics.

Site	Strike/Dip	N/N$_0$	Geo		*k*	α95	Strat		VGP	VGP	d_p(°)	d_m(°)
			D(°)	*I(°)*			*D(°)*	*I(°)*	lat(°N)	lon(°E)		
Delamar Range												
DZ	186/42	28/63	178.9	-26.1	30.3	5	163.1	-14.6	56.6	96.6	2.6	5.1
DR2		6/7	167.2	-25.5	238.4	4.3	155.4	-7.2				
G9		7/8	165.1	-23.3	91.9	6.3	155.3	-4.3				
G21		8/13	173.9	-23.9	33.7	9.7	161.2	-10				
Mean host	*186/42*	*21/28*	*169*	*-24.2*	*59.4*	*4.2*	*157.6*	*-7.3*	50.8	102	2.1	4.2
Mt. Irish												
MI6		10/12	163.7	-17.5	112.3	4.6	151.2	-15.7				
MI9		3/6	162.9	-22.4	98.2	12.5	147.3	-18.8				
Mean	148/40	*13/18*	*163.5*	*-18.7*	*110.1*	*4*	*150.3*	*-16.4*	50.3	114.7	2.1	4.1
Hancock Summit												
HS3	013/36	3/11	137.2	29.1	50.5	17.5	134.3	-4.7	35.4	125.9	8.8	17.5
HS2		38	318.4	31.9	44.28	3.5	342.6	61.4				

Table 1: Paleomagnetic data of all sites of Guilmette carbonate and zebra dolomite. Dec and Inc for geographic (in situ) and stratigraphic (corrected) are shown, as well as the strike/dip of the structural correction that was applied. N/N_o represents the number of samples used to calculate the mean with respect to the number of samples measured in total; precision parameter, k, represents grouping; α_{95} represents 95% cone of confidence around pole; virtual geomagnetic pole (VGP) latitude and longitude were calculated from the stratigraphic dec and inc; d_p/d_m represent minor/major ellipse axis of the α95 cone of confidence.

The mean direction in the zebra dolomite is similar to late Paleozoic/Triassic directions found throughout Nevada (Gillett and Karlin, 2004). Gillett and Karlin (2004) determined that the tilting post-dated the acquisition of the Paleozoic aged magnetizations throughout Nevada. Although there is no tilt test, it is likely that the ChRM was acquired prior to Cenozoic Basin and Range extension. The mean of the zebra dolomite specimen directions (stratigraphic) was used to calculate a pole position. The calculated pole is at 56.6°N, 96.6°E (d_p = 2.6°, d_m = 5.1°) and lies close to the late

Triassic portion of the apparent polar wander path (APWP) for North America (Fig. 5). The host Guilmette carbonate also holds the ChRM, and the calculated pole lies close to that of the zebra dolomite at 50.8°N, 102°E (d_p = 2.1°, d_m = 4.2°)

Mt. Irish

The zebra dolomite at the Mt. Irish sampling locality does not resemble the rhythmite-like zebra dolomites seen at Delamar. The zebra dolomite appears brecciated (Fig. 6), similar to that found at outcrops described by Diehl et al. (2010) in northern Nevada. The dolomites occur above the Alamo Breccia in this locality. MI6 is within the highly mineralized zones of zebra dolomite; MI6 appears mineralized with white dolomite streaks in-between darker host dolomite and also brecciated zebra dolomite. MI9 is darker host Guilmette dolomite stratigraphically above the zebra dolomite sites.

Thermal demagnetization removes the Modern VRM at temperatures below 200°C in most specimens (Fig. 7A-B). The ChRM is removed by 480-500°C in most samples; the remanent magnetization is interpreted to be held in magnetite. The ChRM has a southeasterly declination, 150.3°, and a shallow inclination, -16.4° (k = 100, α_{95} = 4°; Figure 7C; Table 1).

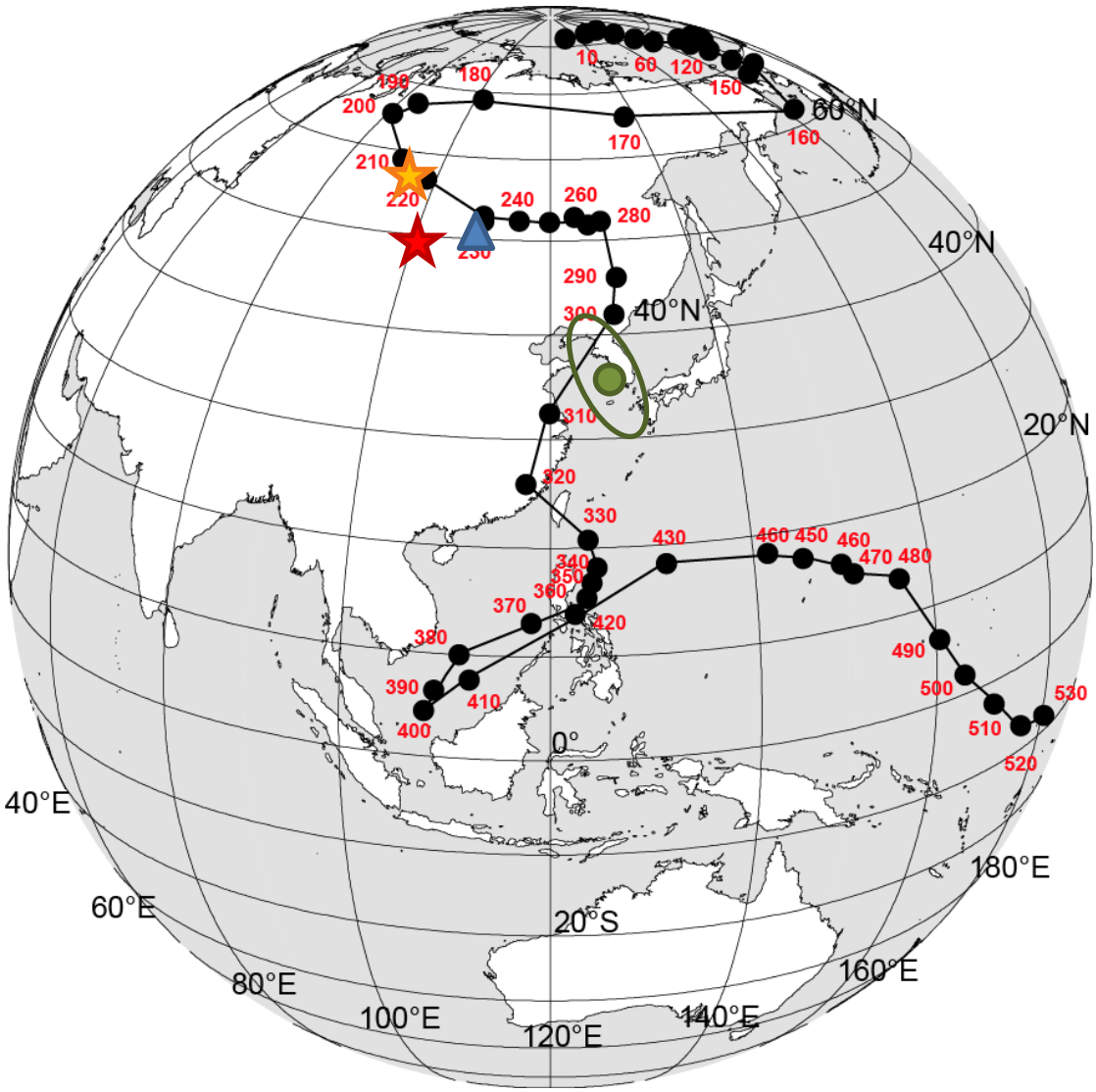

Figure 5: Apparent polar wander path for North America (Torsvik et al., 2012). The orange star represents the ChRM from the zebra dolomite and the red star represents the mean of the host rock in the Delamar Range. The blue triangle represents the ChRM from the zebra dolomite and host carbonate at Mt. Irish. Error ellipse is too small to be shown. The green circle and associated error ellipse represents the ChRM from Hancock Summit. Hancock Summit has likely experienced counterclockwise rotation, which when corrected would bring the ChRM near the VGP calculated from the other two sampling locations.

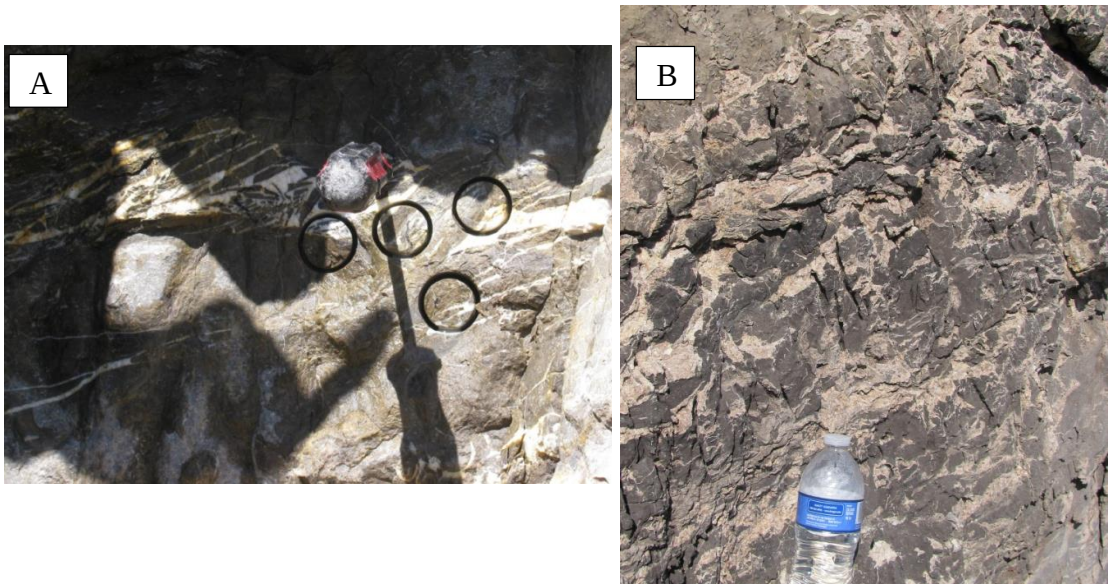

Figure 6: Zebra dolomite at Mt. Irish. A) “Brecciated” appearing zebra dolomite. B) “Brecciated” and rhythmite zebra dolomite. Cores are 2.5cm across.

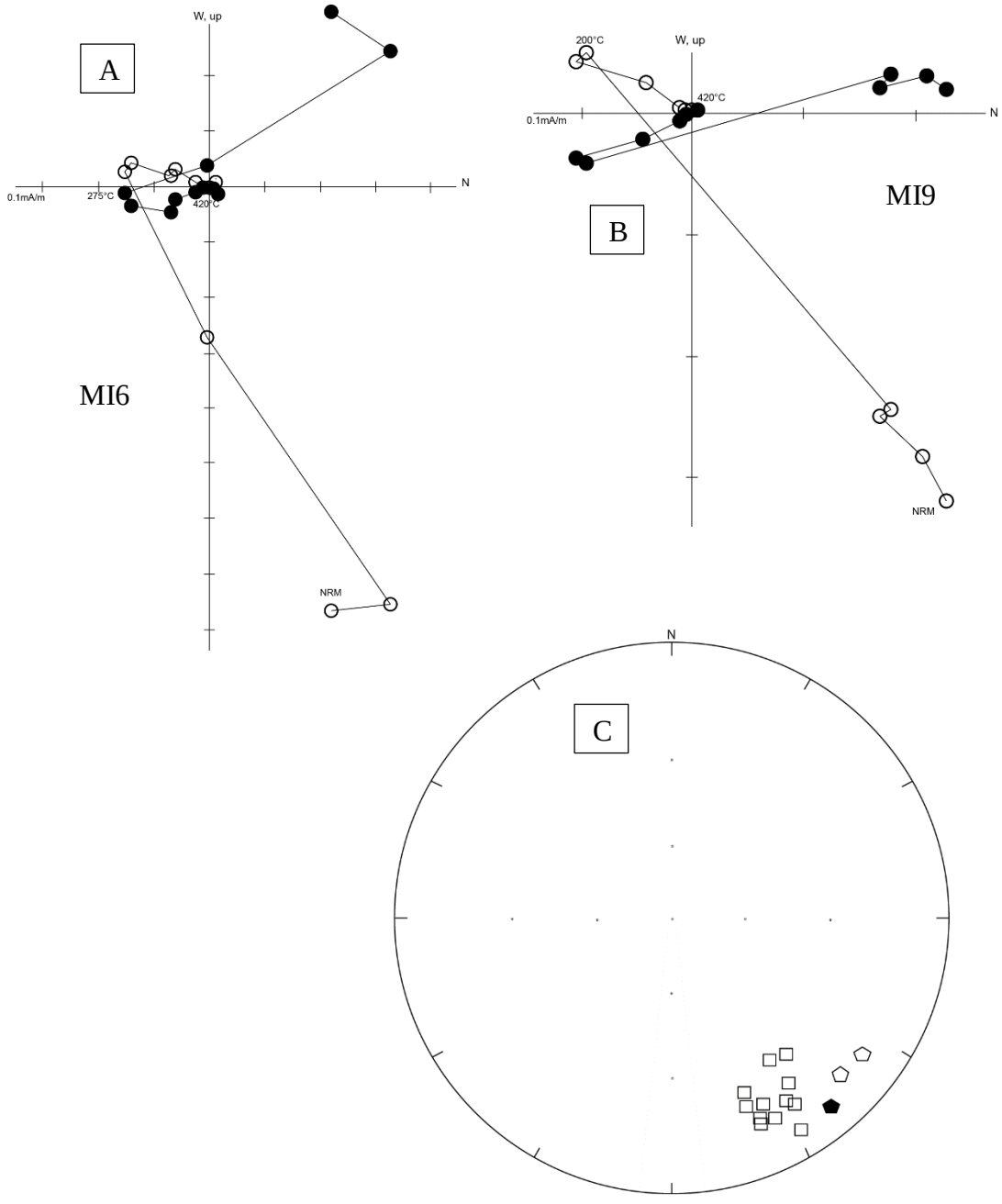

Figure 7: Orthogonal projections diagrams from A) zebra dolomite and B) host grey carbonate at Mt. Irish. Closed (open) symbols represent horizontal (vertical). C) Equal area plot showing specimen directions from Mt. Irish (squares) and Hancock Summit (pentagons). Closed (open) symbols represent positive (negative) inclinations.

Site MI8, shows a different magnetic component that is more easterly and more steep (Dec = 112.8°; Inc = -48.4°; k = 265.4; α95 = 3.4°) than is seen in the zebra dolomites. MI9 lies above the topmost beds that can be identified as the Alamo Breccia. This bed appears to be highly mineralized, but without the definitive rhythmite structure of the other zebra dolomites sampled. The bedding here also appears slightly contorted. The mean direction of this component was used to calculate a VGP, which fell well off of the APWP for North America. The NRM intensity at this site is also anomalously high (>17 mA/m) and is interpreted to have been affected by lightning (Butler, 1992).

The Alamo Breccia at Mt. Irish lies stratigraphically below the zebra dolomite. Evans et al. (2013) report a high-temperature magnetic component similar to that seen in the zebra dolomite within and above the breccia. This component is also held in magnetite. This ChRM within and above the Alamo Breccia at Mt. Irish (averaged data from Evans et al. (2012): Dec = 159.3°, Inc = -28.8°) is the same as seen in the zebra dolomite in that location (Dec = 150.3°, Inc = -16.4°).

A VGP was calculated for the zebra dolomite at Mt. Irish, and plots at 50.3°N, 114.7°E (d_p = 2.9°, d_m = 24.5°; Fig. 5). The age of the magnetization is late Triassic, and is the same age as the magnetization within the zebra dolomite in the Delamar Range.

Hancock Summit

The zebra dolomite at Hancock Summit is found within the Guilmette Formation, stratigraphically below the Alamo Breccia. The zebra dolomite at this location is not as extensive as that found in the Delamar Range, but is patchy, like that seen at Mt. Irish. Unlike Mt. Irish, the zebra dolomite displays the small scale black and white rhythmite structure (Fig. 8).

Thermal demagnetization removes a Modern VRM below 200°C in most samples. At intermediate temperatures, a magnetic component with a northwesterly and steep down inclination (Dec = 342.6°; Inc = 61.4°; k =44.28; α95 = 3.5°; Table 1) was present in all but three of the specimens. This component is the same as the intermediate temperature (IT) component found by Evans et al. (2012) from above, below, and within the Alamo Breccia at Hancock Summit. The sites sampled below the breccia (HSB) by Evans et al. (2012) almost exclusively contained this component with unblocking temperatures ranging from 320-500°C, this magnetization is interpreted by Evans et al. (2012) to be held in pyrrhotite and magnetite. The zebra dolomites sampled below the breccia that hold this component also have unblocking temperatures that range from 360-480°C, suggesting the same magnetic mineralogy.

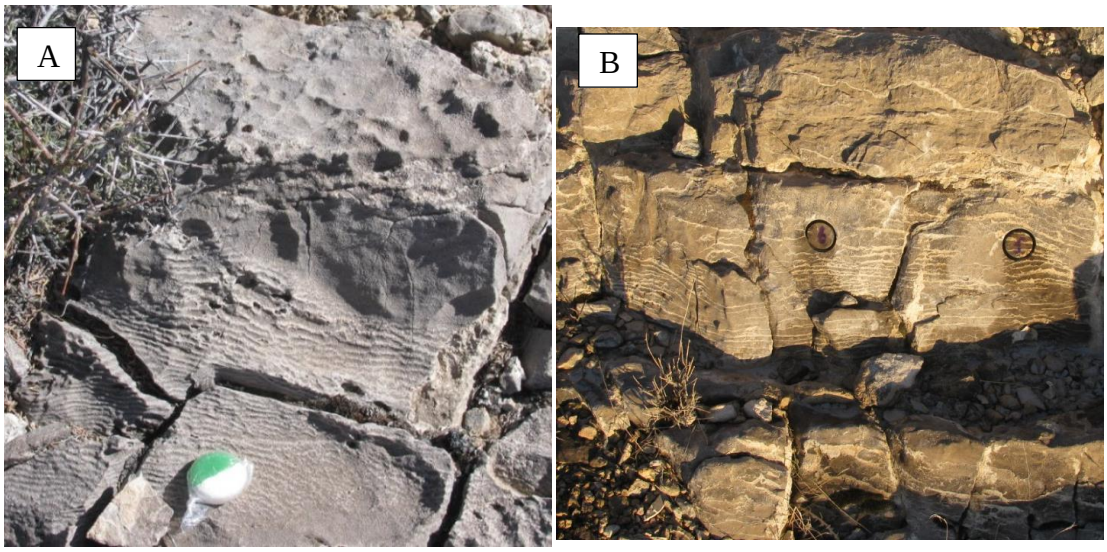

Figure 8: A) and B) Zebra dolomite at Hancock Summit. Cores are 2.5cm in diameter.

Three specimens from zebra site HS3 contain a ChRM (Fig. 9) with southeasterly declinations and shallow inclinations (Dec = 134.3°, Inc = -4.7°, N = 3, k = 50.5, α_{95} = 17.5°; Table 1; Fig. 5; Fig 7C). It is interpreted to reside in magnetite based on unblocking temperatures of 480-500°C. It is similar to the high-temperature component (HT) found within the Alamo Breccia at Hancock Summit by Evans et al. (2012). The VGP reported by Evans et al. (2012) for the HT component (similar to the zebra dolomite ChRM) is Pennsylvanian in age. Some question remains as to whether a small amount (<10°) of vertical axis rotation may have occurred in the Pahranagat Range (Hudson et al., 1998), in which case the age of the magnetization may be as young as the early Triassic.

An inclination-only tilt test was performed (due to possibility of block rotation) on the HT component found in the Alamo Breccia at Hancock Summit and Mt. Irish by Evans et al. (2012). The results yielded a best-grouping at 100% un-tilting, suggesting

that the magnetization was acquired pre-tilting, as also shown by Gillett and Karlin (2004).

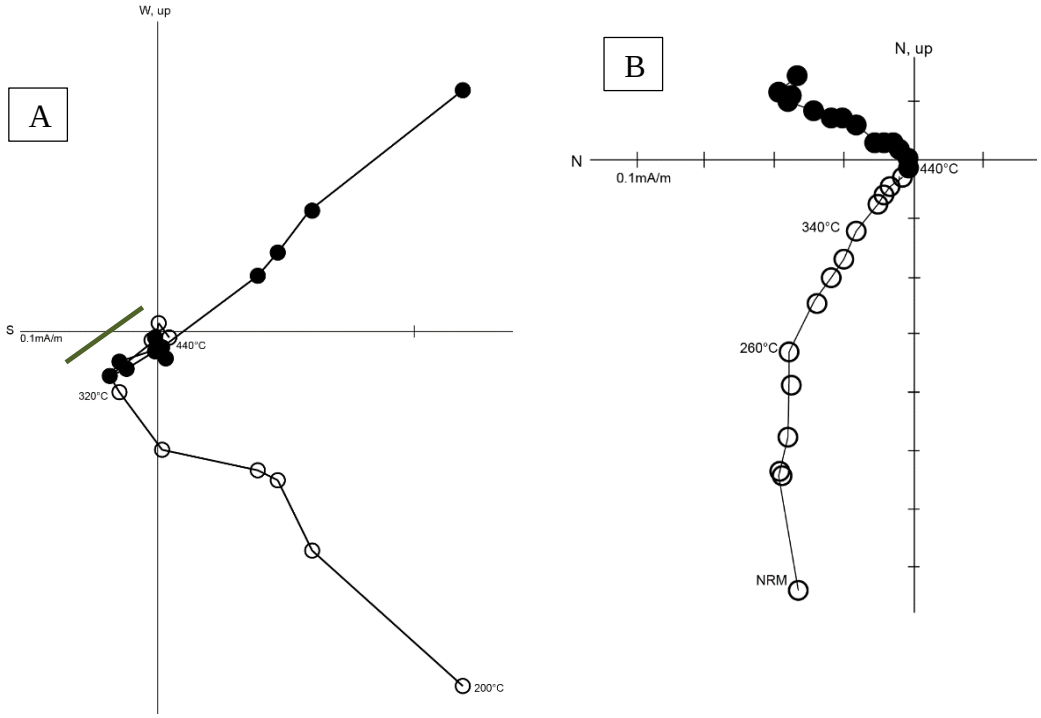

Figure 9: Orthogonal projection diagrams of zebra dolomite from Hancock Summit. A) HS3-7 is one of three specimens that holds the ChRM at high temperatures, identical to the "HT" component found by Evans et al. (2012) at Hancock Summit; the ChRM is outlined in green. B) HS2-8 is a zebra dolomite specimen that does not hold the ChRM, but holds the "IT" component found by Evans et al. (2012).

Petrographic and SEM Results

Nineteen thin sections of the zebra dolomite and associated host rock were examined from the three study localities. The zebra dolomites are made up of alternating bands of white and black dolomites, with saddle dolomite being a common constituent (Fig. 10). The banding is not manifest in thin section under plane polarized light, and a diffused light source must be used to identify the dark and light banding textures.

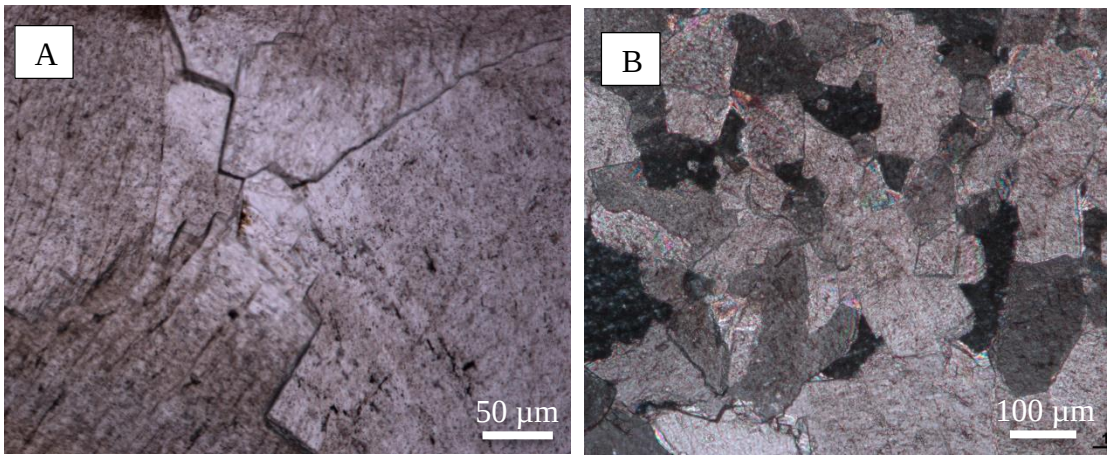

Figure 10: Photomicrographs of zebra dolomite A) and B) in CPO. The zebra dolomite commonly shows the curved surfaces which indicate saddle dolomite. The color banding is not manifest in thin section.

Reflective light microscopy showed small, scattered reflective grains seen between the dolomite rhombs, with no preferential orientation (i.e. light or dark bands). The grains are interpreted as magnetite based on morphology. Some alteration of magnetite by hematite is seen within the dolomite, although it is rare. Figure 11A shows a reflective magnetite grain that is rimmed by hematite. In figure 11B, the internal red reflection can be seen in the hematite alteration rim. Although present, the hematite is not interpreted to be a carrier of the remanent magnetization. Authigenic quartz was found in between dolomite grains in the Delamar Range. The quartz is doubly terminated (Fig 12). This further indicated the presence of diagenetic alteration of the carbonates by fluid migration.

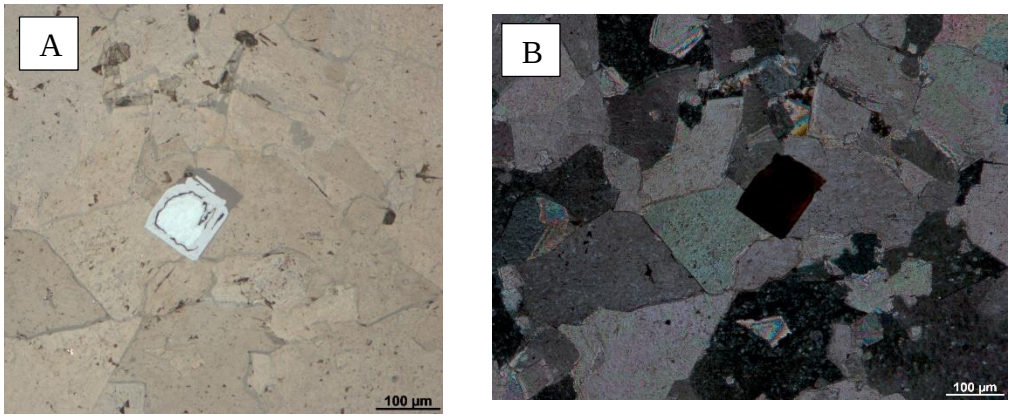

Figure 11: Magnetite grain altering to hematite. A) Reflective light showing magnetite grain with alteration rim and hematite replacement. B) CPL image showing red internal reflections of hematite.

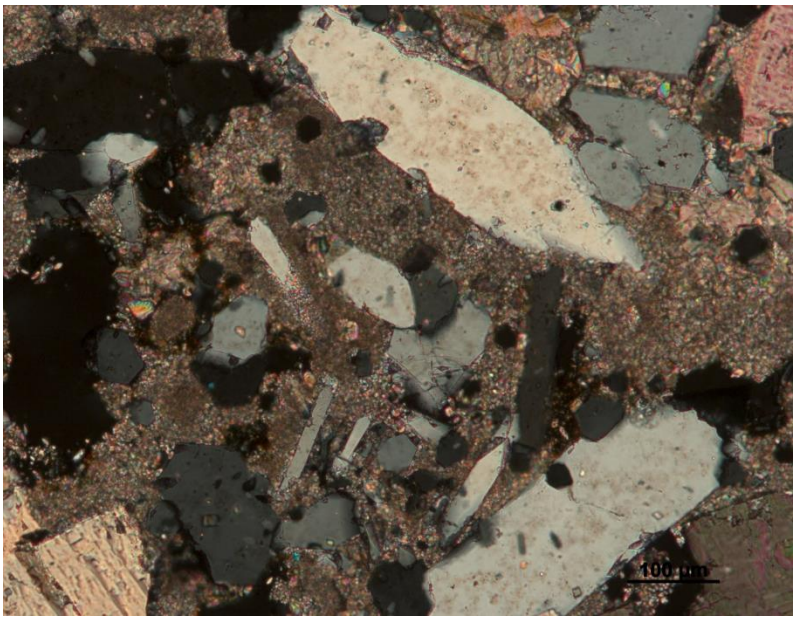

Figure 12: Doubly terminated quartz in between dolomite rhombs. The presence of these crystals indicates fluid migration in the interstitial spaces of the rock at post-deposition.

Scanning electron microscopy was used to determine the habit of the magnetic remanence carriers. The magnetization within the zebra dolomites is weak—on the order of 0.08mA/m or less—and the paucity of large magnetic grains made identification difficult. Energy dispersive spectroscopy (EDS) detected no high concentrations of iron, and there appeared to be no preferential iron oxide habit (such as preferential differentiation in the light vs. the dark bands).

Raman mass spectrometry measurements were made on one specimen, DZ7-7, from the Delamar Range. Figure 13 is a spectral map of the zebra dolomite with shaded areas representing different elemental signatures. The spectral map shows a magnetite and goethite signature, which is nearly identical to synthetic magnetite and goethite spectral signatures (Swindle, 2014).

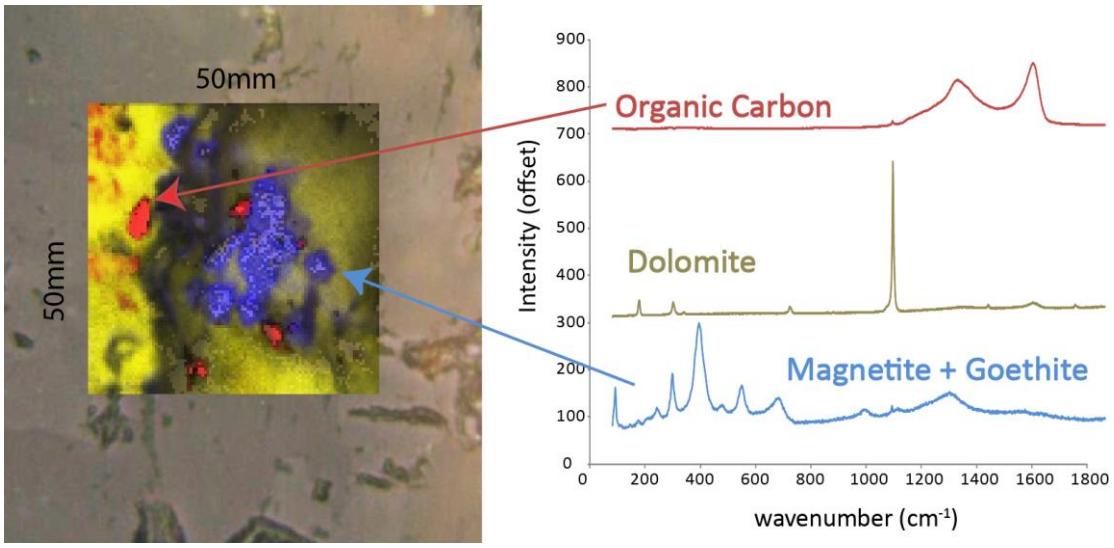

Figure 13: Raman mass spectrometer spectral map of zebra dolomite from the Delamar Range. Spectra were background corrected and noise filleted prior to multicomponent analysis. Red ovals are likely organic carbon inclusions. Blue area is a combination of magnetite and goethite.

Rock magnetic studies

IRM acquisition experiments performed on the zebra dolomites shows that the specimens are mostly saturated by 2500mT. The IRM acquisition curve from a representative DZ specimen from the Delamar Range (Fig. 14A) does not level out as is seen in HS4 (Fig. 14B), the zebra dolomite from Hancock Summit. This suggests that in this location there may be a higher coercivity component present (some hematite was seen petrographically [Fig. 11]) in this location. Although there may be a higher coercivity component present, all the ChRMs are interpreted to be held in magnetite due to the low unblocking temperatures (below 520°C) of the magnetizations. This interpretation is also supported by tri-axial decay of the IRM, which reveals that a low coercivity component is the highest intensity magnetic phase in the zebra dolomite samples (Fig. 14C, 14D).

Isotopic signatures

$^{87}Sr/^{86}Sr$ isotope values for the zebra dolomite and the Alamo Breccia within the Delamar Range are shown in figure 15. The values of all the zebra dolomites within the Delamar Range are elevated with respect to Devonian coeval seawater values, suggesting that externally derived fluids altered the entire carbonate section at the Delamar Range and Hancock Summit. These results are consistent with Evans et al. (2013) who found that within the Alamo Breccia at Hancock Summit the carbonates were enriched in ^{87}Sr with respect to Devonian seawater values. This led to the conclusion that at Hancock Summit the entire sequence was altered by externally derived fluids.

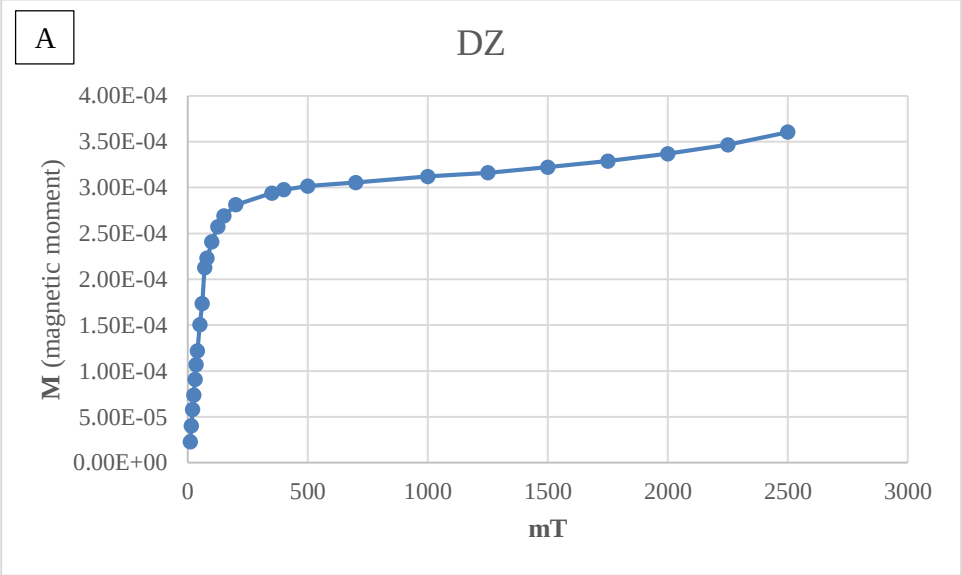
A
DZ
4.00E-04
3.50E-04
3.00E-04
2.50E-04
2.00E-04
1.50E-04
1.00E-04
5.00E-05
0.00E+00
M (magnetic moment)
0
500
1000
1500
2000
2500
3000
mT

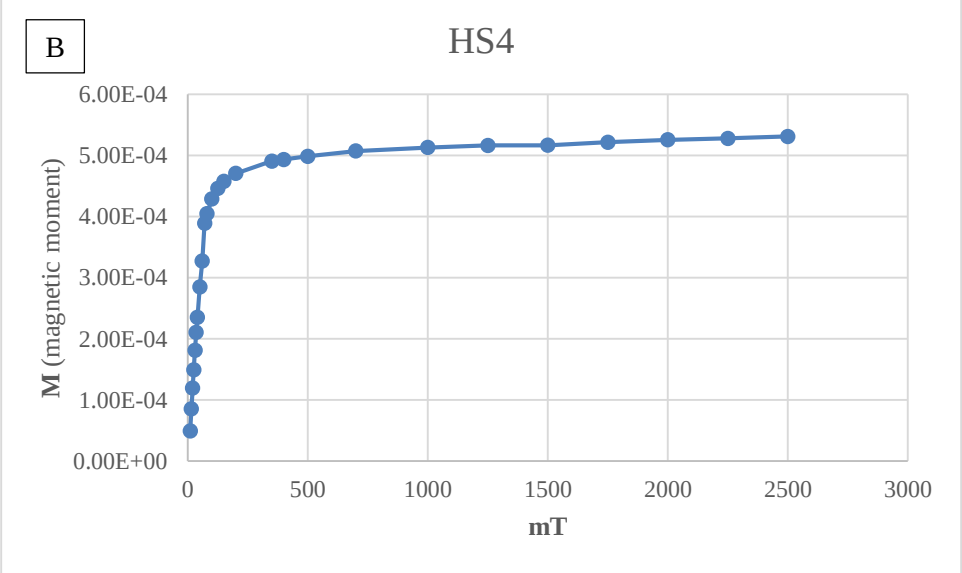
B
HS4
6.00E-04
5.00E-04
4.00E-04
3.00E-04
2.00E-04
1.00E-04
0.00E+00
M (magnetic moment)
0
500
1000
1500
2000
2500
3000
mT

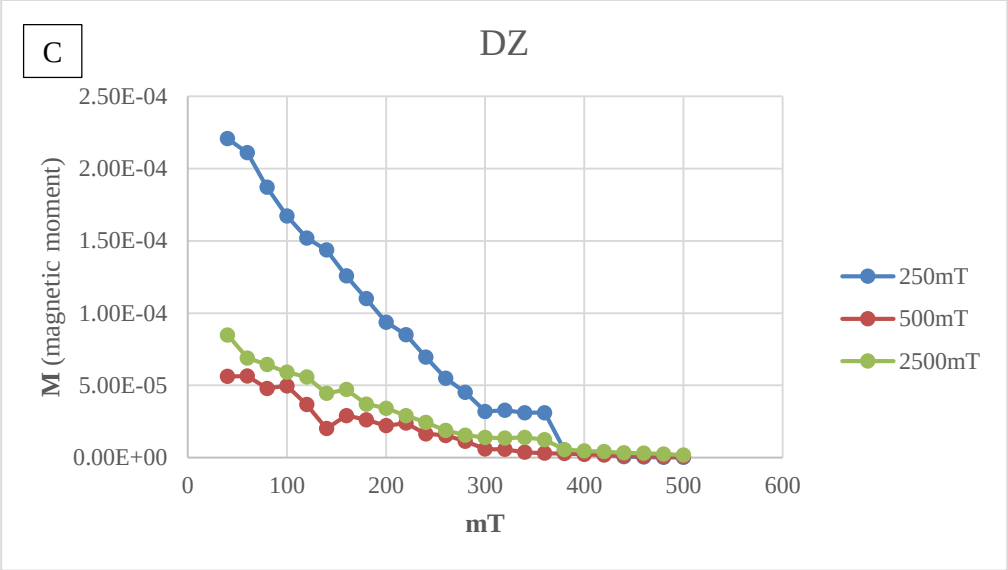

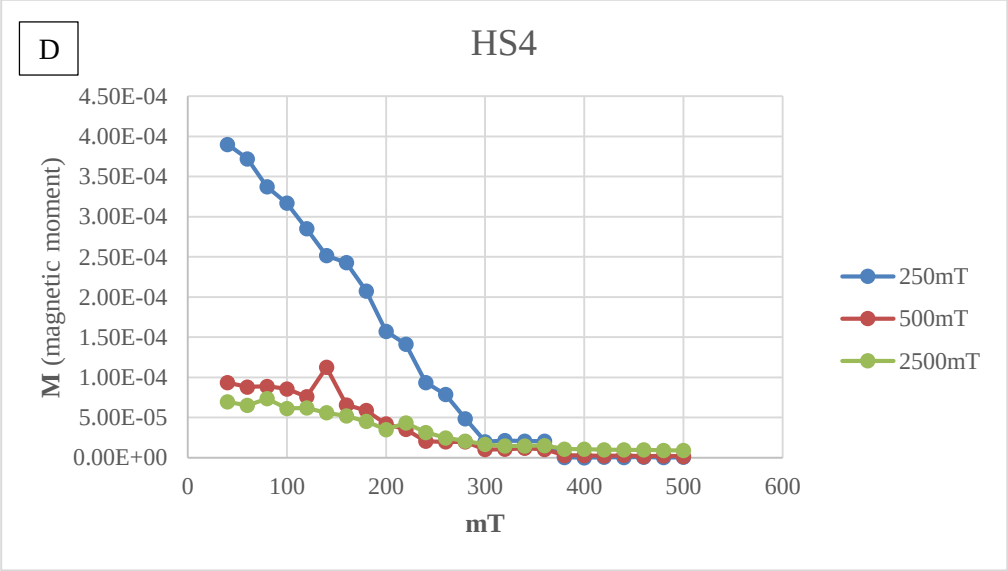

Figure 14: IRM acquisition curves of zebra dolomite from A) Delamar Range and B) Hancock Summit. Acquisition curves are mostly saturated by 2.5T showing that a low coercivity mineral is the main magnetic phase present. Thermal tri-axial decay of the IRM for zebra dolomites in C) Delamar Range and D) Hancock Summit confirm the presence of a low coercivity mineral as the dominant magnetic phase. All magnetization is decayed by 460°C in these specimens.

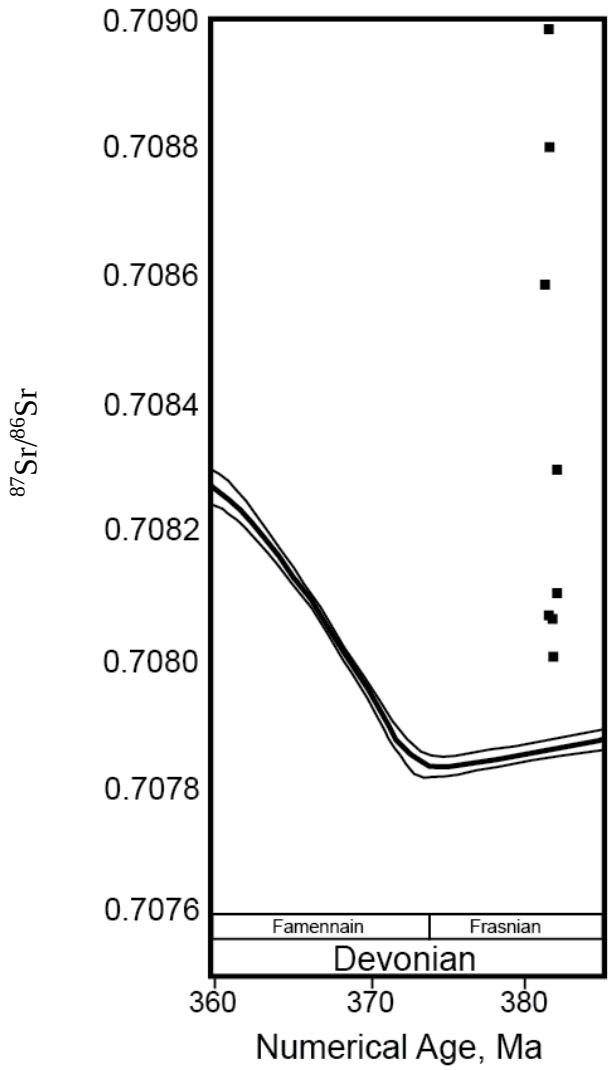

Figure 15: Coeval $^{87}Sr/^{86}Sr$ values for Devonian seawater (McArthur et al., 2001). The squares represent zebra dolomite samples from the study areas. All zebra dolomites show elevated $^{87}Sr/^{86}Sr$ values, indicating alteration by radiogenic fluids. (Figure mod. from Evans et al., 2012)

Discussion

A ChRM residing in magnetite is seen in both zebra dolomite and surrounding host rock in zebra dolomites throughout southern Nevada. Burial temperatures for the Alamo Breccia and the Guilmette Formation were less than 200°C based on a CAI Index of 3.0 (personal communication, Jared Marrow, 2008). Based on the relatively low burial temperatures, and the time-temperature relaxation time curves for single domain (Pullaiah et al., 1975) and multidomain (Kent, 1985; Middleton and Schmidt, 1982) magnetite, the southerly and shallow ChRM is interpreted as a CRM.

At Mt. Irish, a ChRM residing in magnetite is present within zebra dolomites and breccias. The ChRM within the mineralized zebra rocks has a VGP that plots on the late Triassic portion of the APWP, within the error of the ChRM found at the Delamar Range. The entirety of the Guilmette Formation at Mt. Irish has been remagnetized. The similarity in age of the CRMs at Mt. Irish and Delamar suggest that the same fluids that precipitated (or remagnetized) the zebra dolomite were also responsible for the remagnetization in the Guilmette Formation at Mt. Irish. The magnetization within the zebra dolomite at Hancock Summit is the same magnetization reported by Evans et al. (2012) within the Alamo Breccia at this locality. Only three samples contain a ChRM that is southerly and shallow; the VGP for this magnetization plots on the late Pennsylvanian portion of the APWP. There is evidence for as much as 10° of rotation at Hancock Summit (Hudson et al., 1998), and when rotated the pole for Hancock Summit may be as young as Triassic. If this is the case, then the same orogenic fluids

responsible for the remagnetization or creation of the zebra dolomite at both Mt. Irish and at the Delamar Range may have also affected the entire Guilmette section at Hancock Summit.

The remaining zebra samples at Hancock Summit all have a northwesterly and moderate to steep inclinations. This is the same component found as Evans et al. (2012) IT component. Evans et al. (2012) performed a fold test on the IT component found in the Alamo Breccia at Hancock Summit and at Mt. Irish. The result was a syn-tilting magnetization, which would agree with a Cenozoic age of magnetization acquisition. Since only three of the zebra dolomite samples at Hancock Summit contain the ChRM, it is likely that most of the zebra dolomite was remagnetized during the Cenozoic.

The ChRM in the zebra dolomite at all three locations is interpreted as a CRM that was acquired during hydrothermal fluid flow along pre-existing weaknesses during the Triassic Sonoma Orogeny. Elevated $^{87}Sr/^{86}Sr$ values confirm that the Guilmette was altered by externally derived fluids. Fluids were driven eastward, onto the shelf, causing a widespread remagnetization of rocks throughout eastern Nevada (Gillett and Karlin, 2004). Gillett and Karlin (2004) invoke this tectonic even as a viable mechanism for the remagnetization they found. The only agreement in the scientific literature on the formation of zebra dolomite is the presence of fluids which cause either recrystallization or reorganization of the host dolostones, and the warm orogenic fluids associated with the Sonoma Orogeny may have caused formation of zebra dolomites in the host Guilmette Formation.

The habit of the zebra dolomites is similar to other hydrothermal zebra dolomites reported throughout the Basin and Range (Diehl et al., 2010; Vandeginste,

2005). As previously mentioned, the mechanism by which zebra dolomites form is interpreted as deposition due to movement of hot brines (Vandeginste, 2005; Diehl et al., 2010) through host dolomites. Merino et al. (2006) also describe zebra dolomite rhythmites and breccias as developing in stress regimes that create unique conditions that force self-reorganization of the host dolomites into rhythmic black and white striped zebra dolomites. All cases of zebra dolomite formation are associated with alteration by fluids. The presence of a wide-spread CRM within the zebra dolomites in the study area and elevated $^{87}Sr/^{86}Sr$ values suggest that warm, radiogenic fluids flowed through the carbonates, possibly precipitating the zebra dolomite as well as locking in a magnetization at the time of fluid flow. The CRM could date the formation of the zebra dolomite or a subsequent remagnetization event.

The presence of this widespread late Triassic-age CRM within Paleozoic carbonates throughout the Basin and Range records a large scale secondary magnetization event. The timing of zebra dolomite formation within these carbonates is not known; the CRM provides a time-constraint on the age of the zebra dolomite. It cannot yet be ruled out that this event was responsible for alteration within host carbonates that created zebra dolomite. The further study of zebra dolomite within host carbonates of different ages will yield further insight into the timing of zebra dolomite formation with respect to deposition of the host and also to understand mechanisms of secondary magnetizations within the Basin and Range Province.

Conclusions

The age of the magnetization within the zebra dolomite and the surrounding host dolomite records a fluid flow event that dates or proceeds the formation of zebra dolomite. Regardless of the mechanism of zebra dolomite formation, whether it was crystallized into void spaces (Diehl et al., 2010), formed in association with fluid flow along pre-existing microcracks (Vandegestine et al., 2005), or crystallized at the expense of the host dolomite (Merino et al., 2006), the magnetization provides an age constraint on its formation. The CRM in the Guilmette Formation that is associated with zebra dolomite is of reversed polarity and resides in magnetite. The zebra dolomite contains elevated $^{87}Sr/^{86}Sr$ values suggesting the dolomite formed from externally derived fluids. The CRM was acquired during the late Triassic most likely due to alteration associated fluid flow triggered by the Triassic Sonoma Orogeny.

References

Butler, R. F., 1992, Paleomagnetism: Magnetic Domains to Geologic Terranes: Tucson, AZ.

Diehl, S. F., Hofstra, A. H., Koenig, A. E., Emsbo, P., Christiansen, W., and Johnson, C., 2010, Hydrothermal Zebra Dolomite in the Great Basin, Nevada--Attributes and Relation to Paleozoic Stratigraphy, Tectonics, and Ore Deposits: Geosphere, v. 6, no. 5, p. 663-690.

Dunlop, D. J., and Argyle, K. S., 1991, Separating multidomain and single-domain-like remanences in pseudo-single-domain magnetites (215-540nm) by low-temperature demagnetization: Journal of Geophysical Research, v. 96, p. 2007-2017.

Elmore, R. D., Muxworthy, A. R., and Aldana, M., 2012, Remagnetization and chemical alteration of sedimentary rocks, *in* Elmore, R. D., Muxworthy, A. R., and Aldana, M., eds., Remagnetization and chemical alteration of sedimentary rocks, Volume 371: London, Geological Society of London.

Elrick, M., 1986, Depositional and Diagenetic HIstory of the Devonian Guilmette Formation, Southern Goshute Range, Elko County, Nevada [M.S.: Oregon State University, 119 p.

Emsbo, P., 2009, Geologic criteria for the assessment of sedimentary exhalative (sedex) Zn-Pb-Ag deposits: U.S. Geological Survey.

Evans, S. C., Elmore, R. D., Dennie, D., and Dulin, S. A., 2012, Remagnetization of the Alamo Breccia, Nevada: Geological Society, London, Special Publications, v. 371.

Fisher, R., 1953, Dispersion on a Sphere: Proceedings of the Royal Society of London. Series A, Mathematical and Physical Sciences, v. 217, no. 1130, p. 295-305.

Gao, G., Elmore, R. D., and Land, L. S., 1992, Geochemical constraints on the origin of calcite veins and associated limestone alteration, Ordovician Viola Group, Arbuckle Mountains, Oklahoma, U.S.A.: Chemical Geology, v. 98, p. 257-269.

Gillett, S. L., and Karlin, R. E., 2004, Pervasive late Paleozoic-Triassic remagnetization of miogeoclinal carbonate rocks in the Basin and Range and vicinity, SW USA: regional results and possible tectonic implications: Physics of the Earth and Planetary Interiors, v. 141, p. 95-120.

Hamilton, M., Elmore, R.D., Weaver, B., and S.A. Dulin, 2014, Petrology and paleomagnetism of the Long Mountain Granite, Wichita Mountains, Oklahoma *in* Igneous and Tectonic History of the Southern Oklahoma Aulacogen; Oklahoma Geologic Survey vol. 38, p. 319-325.

Heijlen, W., Muchez, P., Banks, D. A., Schneider, J., and Kucha, H., 2003, Carbonate-hosted Zn-Pb deposits in Upper Silesia, Poland; origin and evolution of mineralizing fluids and contraints on genetic models: Economic Geology, v. 98, no. 5, p. 911-932.

Hudson, M. R., Rosenbaum, J. G., Gromme, C. S., Scott, R. B., and Rowley, P. D., 1998, Paleomagnetic evidence for counterclockwise rotation in a broad sinistral shear zone, Basin and Range province, southeastern Nevada and southwestern Utah, *in* Faulds, J. E., and Stewart, J. H., eds., Accommodation Zones and

Transfer Zones: The Regional Segmentation of the Basin and Range Province, Geological Society of America Special Paper 323, p. 149-180.
Kent, D.V. 1985. Thermoviscous remagnetization in some Appalachian limestones. Geophysical Research Letters, 12, 805-808.
Kirschvink, J. L., 1980, The least-squares line and plane and the analysis of paleomagnetic data: Geophysical Journal of the Royal Astronomical Society, v. 62, no. 3, p. 699-718.
Leach, D. L., Sangster, D. F., Kelley, K. D., Large, R. R., Garven, G., Allen, C. R., Gutzmer, J., and Walters, S., 2005, Sediment-hosted lead-zinc deposits; a global perspective: Economic Geology, v. One Hundreth Anniversary Volume, 1905-2005, p. 561-607.
Lowrie, W., 1990, Identification of ferromagnetic minerals in a rock by coercivity and unblocking temperature properties: Geophysical Research Letters, v. 17, no. 2, p. 159-162.
McArthur, J. M., Howarth, R. J., and Bailey, T. R., 2001, Strontium isotope stratigraphy: Lowess version 3: best fit to the marine Sr-Isotope curve for 0-509 Ma and accompanying look-up table from deriving numerical age: The Journal of Geology, v. 109, p. 155-170.
Merino, E., Canals, A., and Fletcher, R. C., 2006, Genesis of self-reorganized zebra textures in burial dolomites: Displacive veins, induced stress, and dolomitization: Geologica Acta, v. 4, no. 3, p. 383-393.
Middleton, M. F., and Schmidt, P. W., 1982, Paleothermometry of the Sydney Basin: Journal of Geophysical Research: Solid Earth, v. 87, no. B7, p. 5351-5359.
Pullaiah, G., Irving, E., Buchan, K. L., and Dunlop, D. J., 1975, Magnetization changes caused by burial and uplift. : Earth and Planetary Science Letters, v. 28, p. 133-143.
Stewart, J. H., 1980, Regional tilt patterns of late Cenozoic basin-range fault blocks, western United States: Geological Society of America Bulletin, v. 91, p. 460-464.
Swindle, A. L., Madden, A., Cozzarelli, I., and Benamara, M., 2014, Size-dependant reactivity of magnetite nanoparticles: a field-laboratory comparison: Environmental Science and Technology, v. 48, no. 19.
Torsvik, T. H., Voo, R. V. d., Preeden, U., Niocaill, C. M., Steinberger, B., Doubrovine, P. V., Hinsbergen, D. J. J. v., Domeier, M., Gaina, C., Tohver, E., Meert, J. G., McCausland, P. J. A., and Cocks, L. R. M., 2012, Phanerozoic polar wander, palaeogeography and dynamics: Earth-Science Reviews, v. 114, p. 325-368.
Vandeginste, V., Swennen, R., Gleeson, S. A., Ellam, R. M., Osadetz, K., and Roure, F., 2005, Zebra dolomitization as a result of focused fluid flow in the Rocky Mountains Fold and Thrust Belt, Canada: Sedimentology, v. 52, p. 1067-1095.
Warme, J., 1998, Anatomy of an anomaly; the Devonian catastrophic Alamo impact breccia, Nevada: AAPG Bulletin, v. 84, no. 11, p. 1881-1882.
Wyld, S. J., 1991, Permo-Triassic tectonism in volcanic arc sequences of the Western U.S. Cordillera and implications for the sonoma orogeny: Tectonics, v. 10, no. 5, p. 1007-1017.

Zijderveld, J. D. A., 1967, A.C. Demagnetization of rocks: Analysis of results, *in* Collison, D. E., K.M.Creer, and Runcorn, S. K., eds., Methods in Paleomagnetism: New York, El Sevier Science, p. 254-286.

Chapter 3: Paleomagnetism as a tool for dating unconformity surfaces and the implications for recording climate change

Abstract

The Permian-Triassic boundary has been interpreted as representing a shift to Triassic greenhouse conditions and increased weathering; this shift may be recorded in altered crystalline basement rocks which occur at unconformity surfaces and contain Permian-Triassic secondary magnetizations in Europe and North America. Determining the geographical extent of this hypothesized weathering surface will aid in understanding if enhanced weathering conditions were present and how widespread they were the Permo-Triassic boundary. Ricordel et al. (2007) documented early Triassic age secondary magnetizations throughout mainland Europe. The magnetizations are held in authigenic hematite, which precipitated during interaction of basement rock with weathering fluids. To test if this hypothesis extends into Scotland and North America, samples of basement rocks at unconformities were collected from several areas to determine if a similar magnetization is widespread. Samples of basement rocks with overlying Permo-Triassic (P-T) sediments were collected in Oklahoma, Colorado, and Scotland. The Long Mountain Granite in central Oklahoma is a reddened granite that becomes grey/green at depth. The red granite holds a stable magnetization in hematite; the age of the magnetization is ~295 Ma (paleopole: 44.9°N, 124.9°E). In west-central Scotland, reddened Dalradian schist overlain by upper Permian sandstone also holds a stable magnetization in hematite. The magnetization was acquired ~270 Ma (VGP: 52.7°N, 160.5°E). In western Colorado, reddened crystalline basement rocks which are overlain by Triassic redbeds in Unaweep Canyon

do not contain stable magnetizations, despite hematite precipitation along joints in the granite, which indicates that fluids penetrated the basement. At Byers Canyon in north-central Colorado, the Jurassic Morrison Formation overlies reddened Precambrian granite that also does not hold a stable magnetization at the unconformity surface. These findings indicate that early Triassic magnetizations like those recorded in mainland Europe are not pervasive throughout Pangea. Local climatic variables (such as atmospheric CO_2 fluctuations) and local tectonic influences during the Permian may be responsible for the older secondary magnetizations recorded in Oklahoma and Scotland. The lack of secondary magnetization that is P-T in age in Colorado indicates that the climate conditions, and therefore weathering processes, at the P-T boundary may have been more localized and variable.

Introduction

In recent years there has been a resurgence of interest in characterizing the origins of Permo-Triassic aged secondary magnetizations in granitoid rocks throughout Europe (Franke et al., 2010; Parcerisa et al., 2010; Ricordel et al., 2007). There is also some evidence that such secondary magnetizations of this age also occur worldwide (Hamilton et al., 2014; Parnell et al., 2000; Torsvik, 1984), and are commonly associated with sedimentary cover that unconformably overlies crystalline basement rock. These remagnetizations are attributed to supergene weathering fluids that can deeply permeate (~200m) basement rocks and trigger authigenic hematite formation (e.g., Parcerisa et al., 2010; Ricordel et al., 2007). These reddened granite surfaces

therefore represent the paleo-topography at the time of hematite authigenesis/magnetization acquisition.

The identification of paleosurfaces is an important input to geodynamic modeling as well as paleoclimate applications. The weathering-induced alteration of many granitoid rocks throughout western Europe is leading to a better understanding of the early Triassic paleogeography, a necessary input when modeling continental evolution (Franke et al., 2010). The Permo-Triassic boundary marks a global shift to a greenhouse environment; if increased weathering began to occur at this time period, then the alteration of granitoid rocks due to these weathering fluids dates a paleoclimatic shift.

This study aims to determine if the inferred wide-spread climate shift during the transition from early Permian icehouse conditions to late Permian/early Triassic greenhouse conditions is recorded on a global scale in the paleomagnetic record. Creation of authigenic hematite, particularly in basement rocks at unconformity surfaces, has been reported in many locations (e.g., Creer, 1968; Parnell et al., 2000; Ricordel et al., 2007; Franke et al., 2010); a comprehensive investigation of more of these surfaces will give a clearer geographic picture of the widespread, or localized, nature of the weathering-related phenomenon. This investigation summarizes results from the Long Mountain Granite in Oklahoma, and presents new data from Scotland and Colorado, focusing on reddened basement rock that is overlain by Permian or Triassic sediments to determine if the acquisition of Permo-Triassic aged magnetization is widespread, and therefore relatable to transitional long-term icehouse to greenhouse conditions that occurred at the Permo-Triassic boundary.

Previous Work and Geologic Setting

The role of weathering fluids as a mechanism for remagnetization was first suggested by Creer (1968). Late Paleozoic remagnetizations were identified in North America and Europe, which were both situated near the equator during the late Paleozoic. Rocks of the same age in eastern Russia, which was at high latitudes during the late Paleozoic, were apparently not remagnetized. This led Creer (1968) to hypothesizes that a wetter and warmer equatorial climate was responsible for the remagnetization of equatorial rocks during the late Paleozoic.

The formation of hematite associated with weathering fluids is commonly accompanied by albitization of underlying basement rock (Parcerisa et al., 2010; Ricordel et al., 2007). This process, known also as sodium metasomatism, has been described elsewhere, without regards to mechanism. Engvik et al. (2008) described albitization of granitic and mafic rocks in southeastern Norway, which are also associated with a reddening by hematite within the igneous units. Wang (1992) described reddening of Carboniferous sandstones in Northern Ireland, associated with weathering fluids that created secondary porosity during late Carboniferous-early Permian uplift. The widespread nature of this albitization in basement rocks as well as the reddening of rocks, and the significance of the phenomenon is not well understood.

Ricordel et al. (2007) report that the hematization that accompanies the albitization of basement rocks in the Morvan massif and other locations in Poland, Morocco, and Spain (Parcerisa, personal communication; Fig. 1), holds an ancient stable magnetization. These magnetizations, which are Triassic and contain both normal

and reversed directions (C. Franke, personal communication), were locked in during growth of authigenic hematite from paleoweathering fluids. These magnetizations are only present in the upper 200m of the basement, and diminish with depth (Franke et al., 2010). The abundance of Permo-Triassic-aged magnetization throughout mainland Europe (reported by Ricordel et al., 2007) and new data from the Morvan massif and Catalonia (Franke et al., 2010) that report early Triassic aged magnetizations lead to the conclusion that the magnetizations define a widespread paleotopographic surface that was affected by oxidizing weathering fluids during the Permo-Triassic. Magnetizations of similar age have been identified in Scotland (Parnell et al., 2000) as well as southern Oklahoma (Hamilton et al., 2014), and are associated with the "reddening" of granite due to authigenic hematite precipitation by weathering fluids.

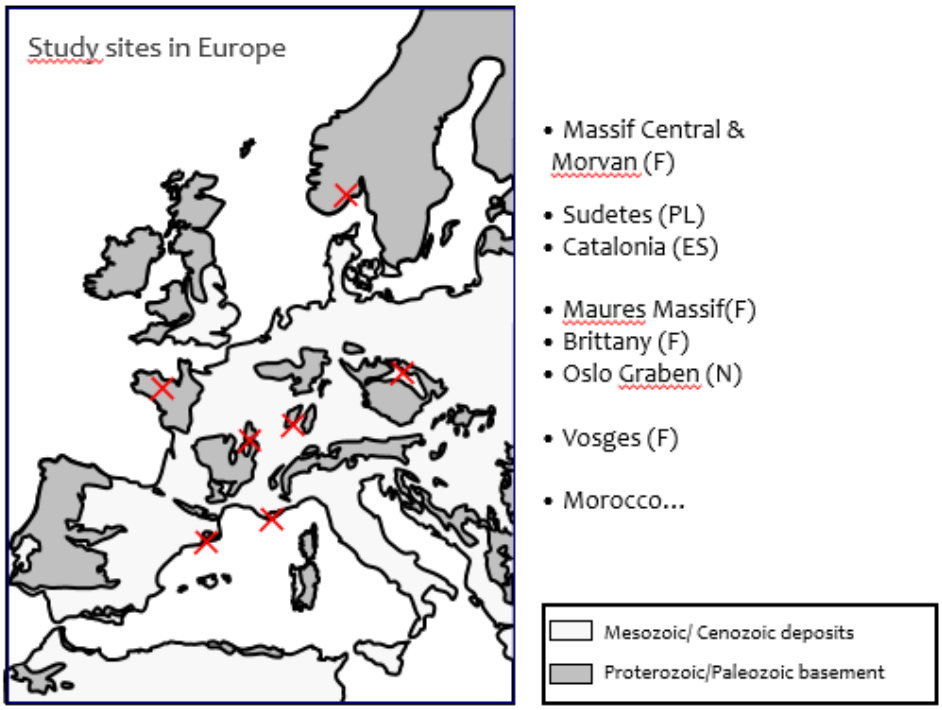

Figure 1: European study areas were late Permain/early Triassic-aged magnetizations (held in hematite) are associated with reddened basement rocks. Figure from (Parcerisa, 2013).

The Long Mountain Granite, a granitic sill within the Wichita Mountains in southern Oklahoma, is an altered reddened granite. Quarrying operations have exposed green, unaltered granite at depth. Hamilton et al. (2014) found a secondary magnetization residing in hematite within the red granite, and a primary magnetization in magnetite within the green granite (Fig. 2). Whole rock geochemical analysis shows that the iron for hematite formation was sourced from the granite itself—there is no change in wt % Fe between the green and the red granite (Hamilton et al., 2014). The magnetization residing in the hematite is of early Permian age, and is interpreted as a chemical remanent magnetization (CRM) that was acquired from oxidizing weathering fluids when the Long Mountain Granite was exposed at the surface (Hamilton et al., 2014).

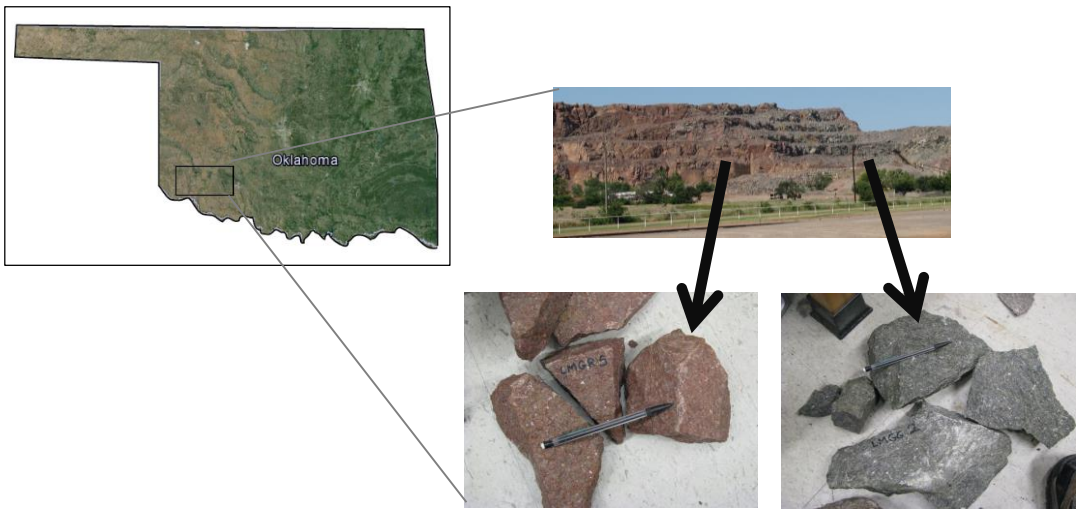

Figure 2: Long Mountain Granite quarry, located in the Wichita Mountains of southwest Oklahoma. The inset picture shows the red granite at the surface (left) and the green granite (right) exposed by quarrying operations.

In Scotland, reddened Neoproterozoic Argyll Group schists (within the Dalradian Supergroup) crop out along the coast, south of the town of Tarbert (Fig. 3). Parnell et al. (2000), reported the presence of a CRM residing in hematite in dolomite veins and within Dalradian schist in Argyll, Scotland. The CRM contains both normal and reversed directions (Parnell et al., 2000). The age of hematite formation is late Permian-early Triassic and is interpreted to form from oxidizing weathering fluids (Parnell et al., 2000). Permo-Triassic New Red Sandstone beds that nonconformably overlie basement in the area contain a similar magnetization but relatively unaltered grey Dalradian schist does not contain a stable magnetization (Parnell et al., 2000).

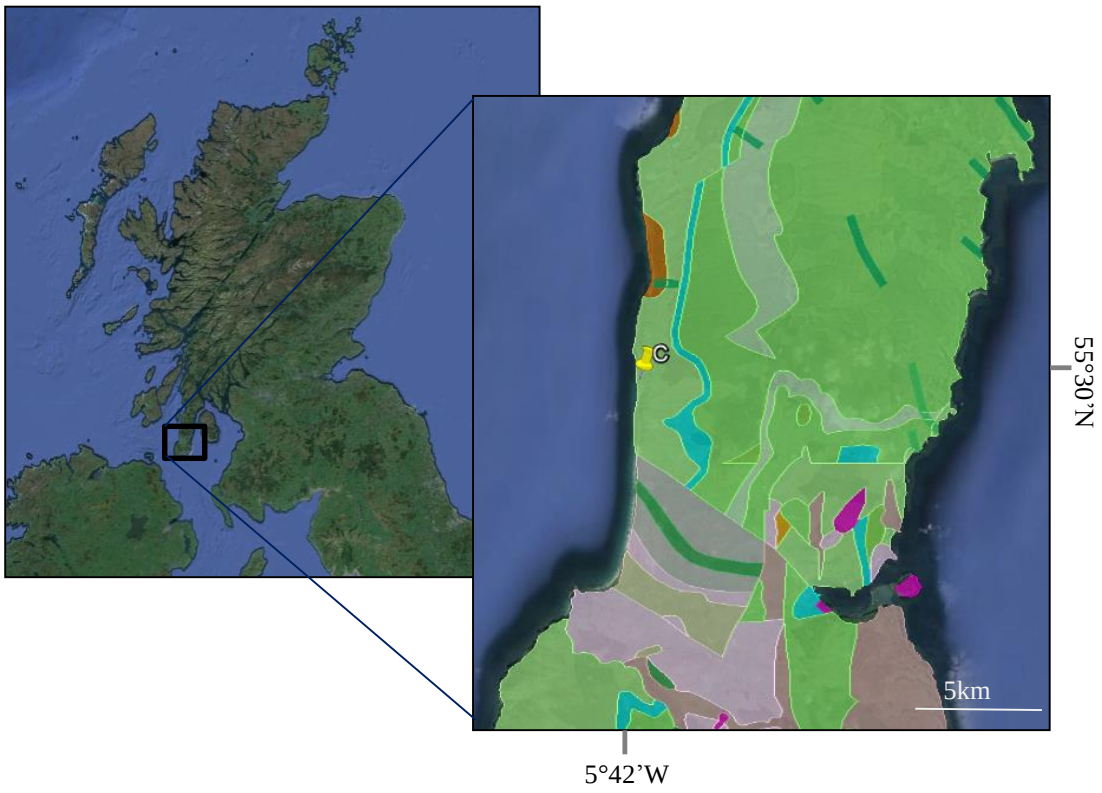

Figure 3: Map of Scotland, with geologic map inset showing sampling location (C). The green represents the Proterozoic Dalradian Supergroup basement rocks, the brown north of the sampling location represents Permian New Red Sandstone outcrops. *Reproduced with the permission of the British Geological Survey ©NERC. All rights Reserved.*

Byers Canyon is located between Hot Sulphur Springs and Kremmling, in Grand County Colorado (Fig. 4). Byers Canyon is in the structural province of Middle Park Colorado, which is a highly faulted and discontinuous province with structural lineaments inherited from the Ancestral Rocky Mountain and Laramide orogenies (Chronic, 1980). The sulphur springs that are the town’s namesake flow along the fault network near the canyon. The Middle Park and North Park basins are fault bounded, with Mesozoic and younger sedimentary rocks forming the floor of the synclinal basin, and Precambrian rocks thrust over the sediments at the edges of the basin (Tweto,

1957). The crystalline basement rock within Byers Canyon is reddened, although with a patchy distribution, with nonconformably overlying Jurassic sandstones of the Morrison Formation.

Unaweep Canyon lies south of the western slope town of Grand Junction, in Mesa County, Colorado (Fig. 4). This area of Colorado is situated on the Uncompahgre Plateau, which is an area of the larger Colorado Plateau that experienced uplift from the late Mesozoic though Miocene (Chronic, 1980). The origin and age of the canyon itself are debated. The prevailing theory is that Unaweep was carved by either the ancestral Gunnison River or the Colorado River (Spencer and Patchett, 1997; Pederson et al., 2002) associated with uplift of the Uncompahgre Plateau in the Cenozoic. An alternate theory is that the ancestral Gunnison River merely exhumed Unaweep Canyon, and the origins of the canyon formation are associated with tectonism during Ancestral Rocky Mountain orogenesis in the late Paleozoic (Soreghan et al., 2007). Despite the age of canyon formation, Unaweep remains a canyon that was carved into Precambrian crystalline basement rocks, and is overlain nonconformably by the sedimentary Triassic Chinle Formation. The crystalline basement is weathered and reddened at the unconformity surface.

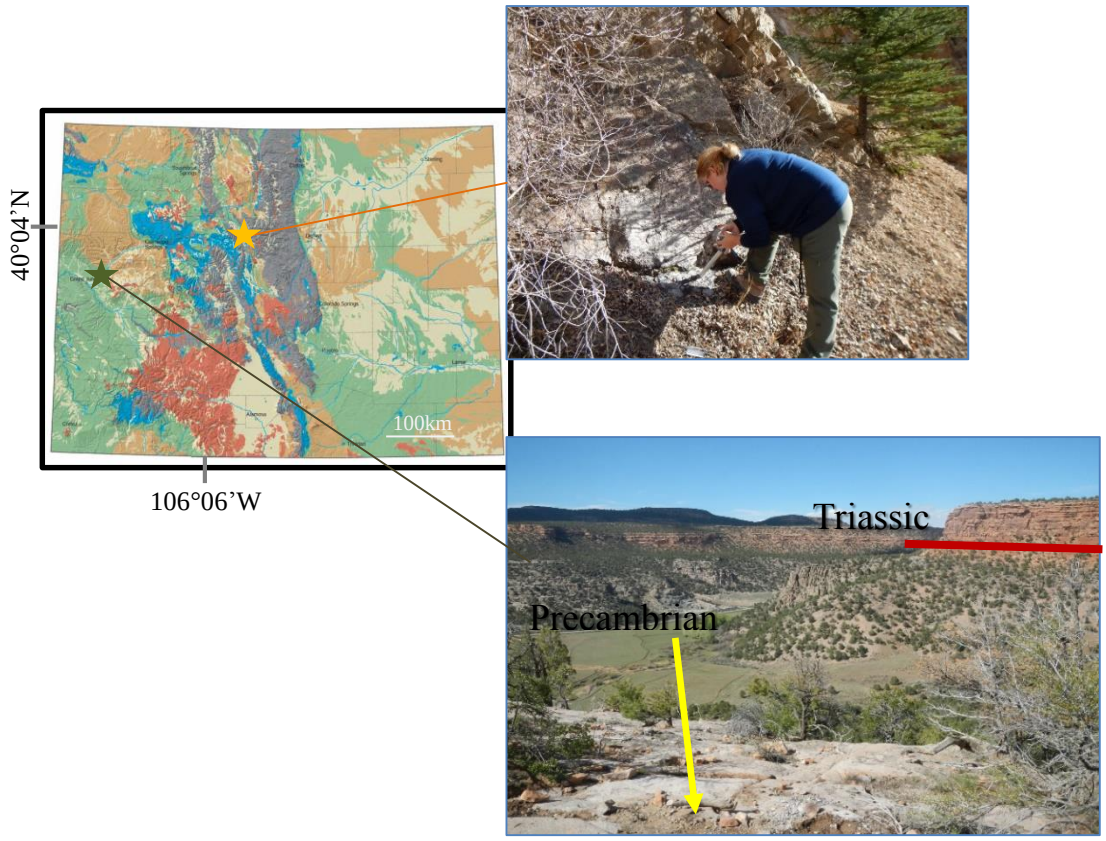

Figure 4: Geologic map of Colorado. Orange star is Byers Canyon, located in the Middle Park, Colorado. Green star is Unaweep Canyon, situated on the edge of the Colorado Plateau.

Methods

At each unconformity surface in Scotland, Unaweep Canyon, and Byers Canyon, sites consisting of 8-10 specimens per site were drilled within the basement rock. The specimens from Scotland were collected to test the previous results from the reddened schist; the previous study focused on characterizing the magnetization in dolomite veins (Parnell et al., 2000). Paleomagnetic samples were collected using a

gasoline powered modified chainsaw with a stainless steel coring device that extracts 2.5cm diameter cores. Cores were oriented in the field using a Brunton compass and inclinometer. Once in the laboratory, cores were cut to standard 2.2cm specimens. The natural remanent magnetization (NRM) was measured in a shielded room using a 2G Enterprises cryogenic magnetometer with DC squids. Specimens were then subjected to stepwise thermal demagnetization (100-600°C in 20°C steps) using an ASC Thermal Demagnetizer.

Thermal demagnetization data were plotted as orthogonal projection diagrams (Zijderveld, 1967) and analyzed using principal component analysis (Kirschvink, 1980) to determine the magnetic components within each sample. For Scotland data, mean angular deviations (MAD) of 11° or less were deemed acceptable, though most samples have a MAD angle of less than 9°. Means were computed using Fisher (1953) statistics and the means were combined with previous data (Parnell et al., 2000) to determine a mean of means. This mean direction was used to determine a pole position that was compared to the APWP for Europe (Torsvik et al., 2012).

A total of ten thin sections were analyzed using transmitted light microscopy and reflected light microscopy to identify opaque minerals. Scanning electron microscope (SEM) analysis of thin sections and rock samples supplemented the thin section analysis. The SEM analysis was completed using an environmental scanning electron microscope (FEI Quanta 200) with energy dispersive capabilities at the University of Oklahoma Mewbourne College of Earth and Energy IC3 lab.

Results and Interpretations

Scotland

Reddened schists of the Dalradian Supergroup were sampled along the western coast, south of the town of Tarbert and north of Campbeltown, on the Kintyre Peninsula, Scotland. Two sites (C4 and C5) were sampled for a total of 19 specimens. Thermal demagnetization of the schist removed one component that is southerly with a moderate up inclination (Fig. 5; Table 1). The magnetization decayed by 680°C in all samples. An average of 20% of decay of the remanent magnetization was above 580°C, and the magnetization is interpreted to reside in hematite based on unblocking temperatures. No modern viscous remanant magnetization was seen in any of the reddened schist samples.

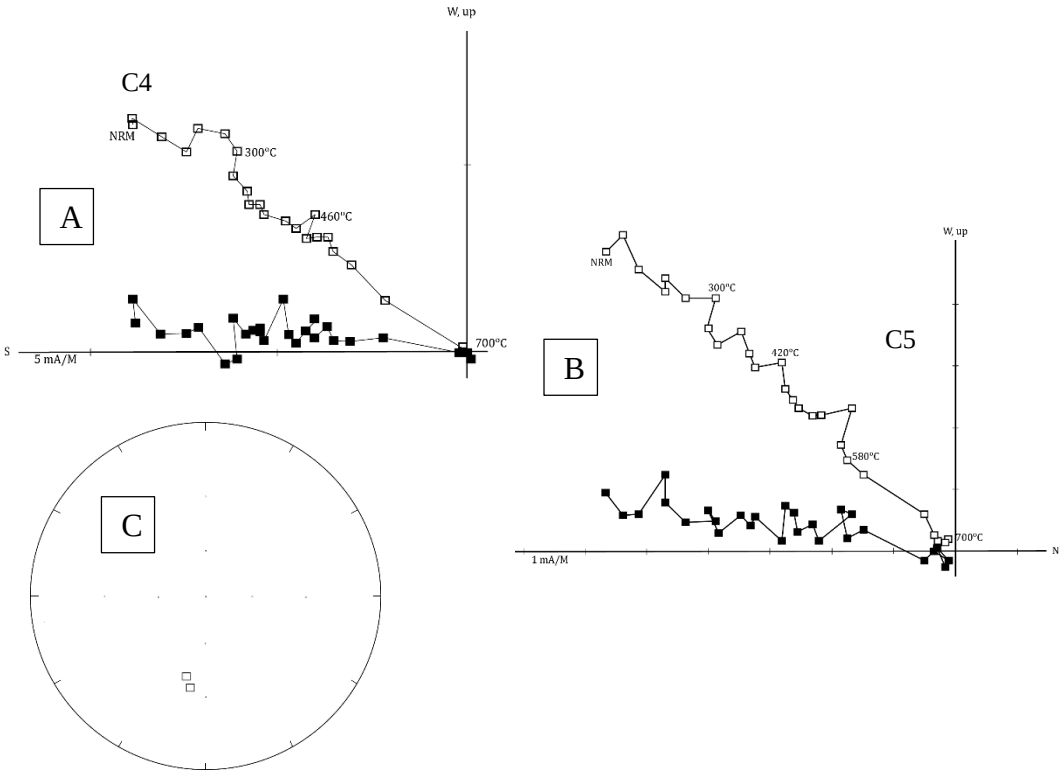

Figure 5: A) and B) Orthogonal projection diagrams of reddened Dalradian schist. C) Equal area projection showing the site means.

The data for the two sites were combined with previously published data from the reddened schist just south of the study area (Parnell et al., 2000) to determine a mean of the characteristic remanent magnetization (ChRM) (Fig. 6; Table 1). The mean for the reddened schist is Dec = 188°, inc = -35.5°, N = 28, k = 76.8, α_{95} = 10.6°. These data are similar to data from the nonconformably overlying Permo-Triassic New Red Sandstones sampled south of the current study area (Fig. 6; Table 1). The VGP for the ChRM is plotted on figure 7, and lies at 58.6°N, 163.4°E (d_p = 7.1°, d_m = 12.3°), on the mid-Permian portion of the APWP at ~270 Ma.

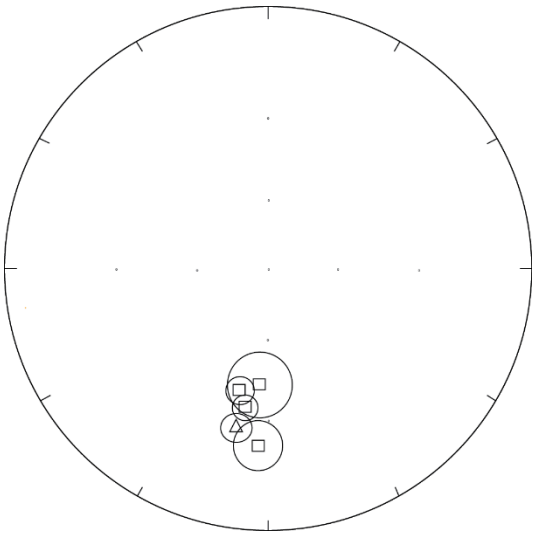

Figure 6: Equal area showing the means for each schist site (squares) from this study and from Parnell et al. (2000) and for the sandstone (triangle). Open symbols represent negative inclinations.

Site	*Dec (°)*	*Inc (°)*	*N/N$_o$*	*k*	*α95*	*VGP lat (°N)*	*VGP long (°E)*	*d$_p$(°)*	*d$_m$(°)*
C4	189.4	-35.2	7/7	176.4	4.6				
C5	193.7	-40.1	11/11	97.8	4.6				
B2*	183.8	-23.6	6/6	62.6	7.8				
B3*	185.6	-43	4/4	47	12				
Mean	*188*	*-35.5*		*76.8*	*10.6*	*58.6*	*163.4*	*7.1*	*12.3*
AH2*	191.8	-29.1	13/14	158	4.9	55	154	3	5.4

Table 1: Site statistics for Dalradian schist and New Red Sandstone (AH2). *Data from previous study (Parnell et al., 2000). Declination and inclination (°) for magnetic directions. N/N_o represents the number of samples used to calculate the mean with respect to the number of samples measured in total; precision parameter, k, represents grouping; α_{95} represents 95% cone of confidence around pole; virtual geomagnetic pole (VGP) latitude and longitude were calculated from the dec and inc; d_p/d_m represent minor/major ellipse axis of the α95 cone of confidence.

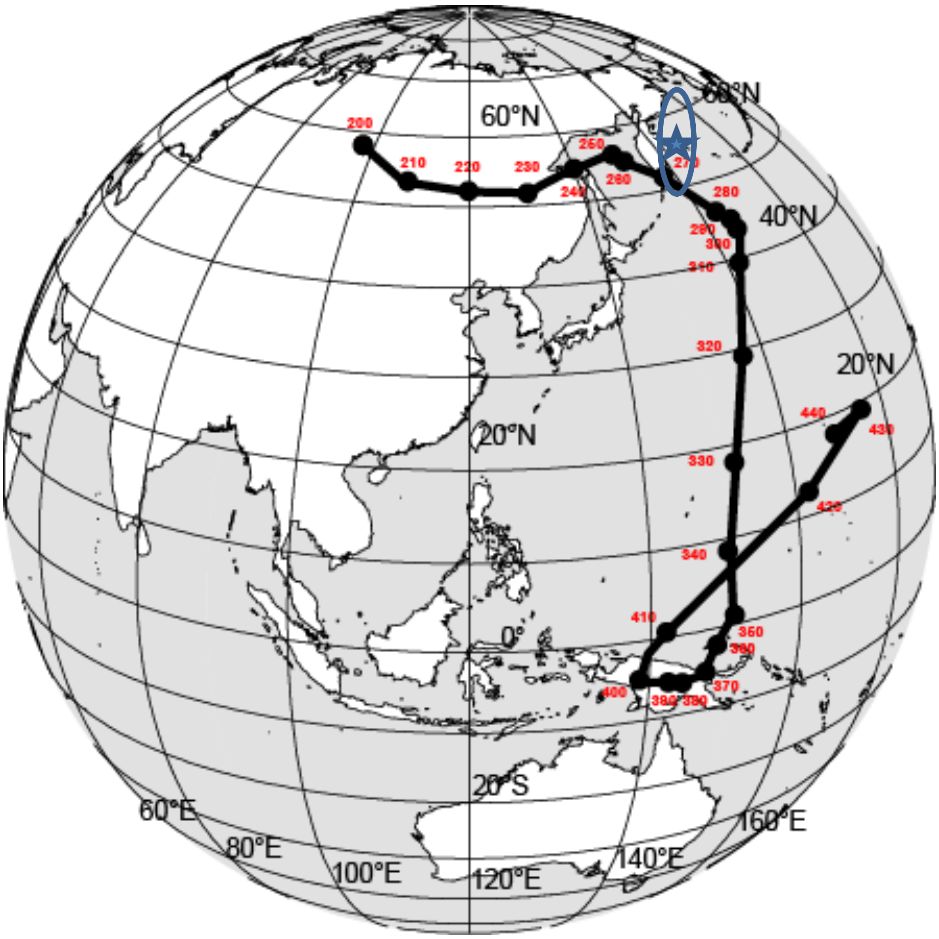

Figure 7: Apparent Polar Wander Path for Europe (Torsvik et al., 2012). The star represents the VGP for the reddened schist.

Colorado

Fifteen sites, with an average of 8-10 specimens per site, were drilled in Unaweep Canyon within the Precambrian crystalline basement beneath the unconformity surface. Five sites from Unaweep Canyon were drilled with a drill press from oriented slabs that were collected. Samples were taken along Divide Road, which climbs from the bottom of the canyon up through the Mesozoic cover rocks that cap the canyon. The sites were selected to sample the unconformity surface, and also to

vertically transect below the unconformity to assess whether or not the magnetization changed with depth.

Thermal demagnetization of many specimens removed a magnetization with northerly declinations and steep positive inclinations below 200°C, interpreted as the viscous remanent magnetization that records the Modern magnetic field direction. Further stepwise demagnetization revealed a complex magnetization up to 700°C (Fig. 8). Some samples showed linear decay whereas other samples showed curved trajectories and multiple components. Although there were stable ancient magnetizations in many specimens, there were no groupings of similar specimen directions within any sites at Unaweep Canyon. Figure 8 shows the equal area plot of specimen directions that held a stable magnetization. No pervasive Triassic direction or other direction is present in the specimens. This may be because the magnetization is complicated by non-linear decay within many specimens which is interpreted to be caused by overlapping components.

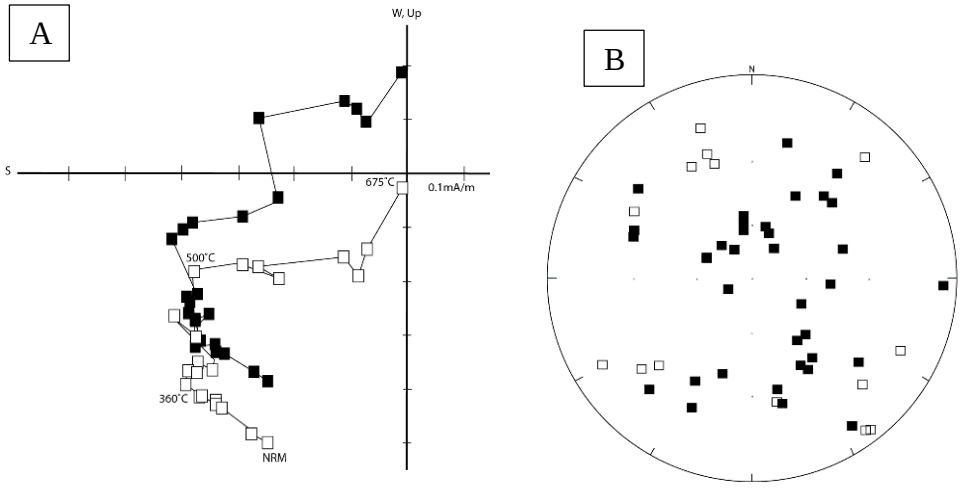

Figure 8: Orthogonal projection diagram (right) from the reddened granite at the unconformity surface at Unaweep Canyon. The equal area plot (left) shows that although several specimens contained a stable magnetic component, there was no grouping.

Four sites were drilled at Byers Canyon. Stepwise thermal demagnetization does not reveal a stable remanent magnetization in the basement rocks at the unconformity at this location (Fig. 9). The NRM of the basement rocks is 0.9mA/m, no VRM is present and decay is unstable within the specimens. The rocks at the unconformity surface have likely been affected by fluid flow and movement along Ancestral Rockies and Laramide faults that are adjacent to the sampling location.

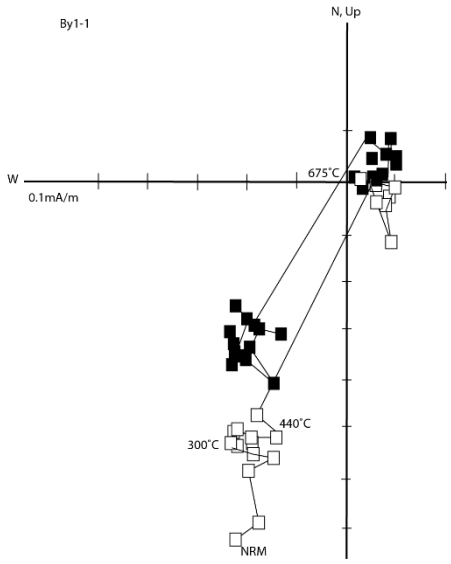

Figure 9: Orthogonal projection diagram of the reddened basement rock at Byers Canyon. No stable magnetic components could be determined from the data.

Petrography

Hematite is the ubiquitous magnetic mineral at all the unconformity surfaces. The Dalradian schist in Scotland has abundant specularite and pigment hematite (Fig. 10). Previous rock magnetic studies (Parnell et al., 2000) confirm that hematite is the

carrier of the CRM in these rocks. Authigenic hematite is also abundant at the other locations (Fig. 11).

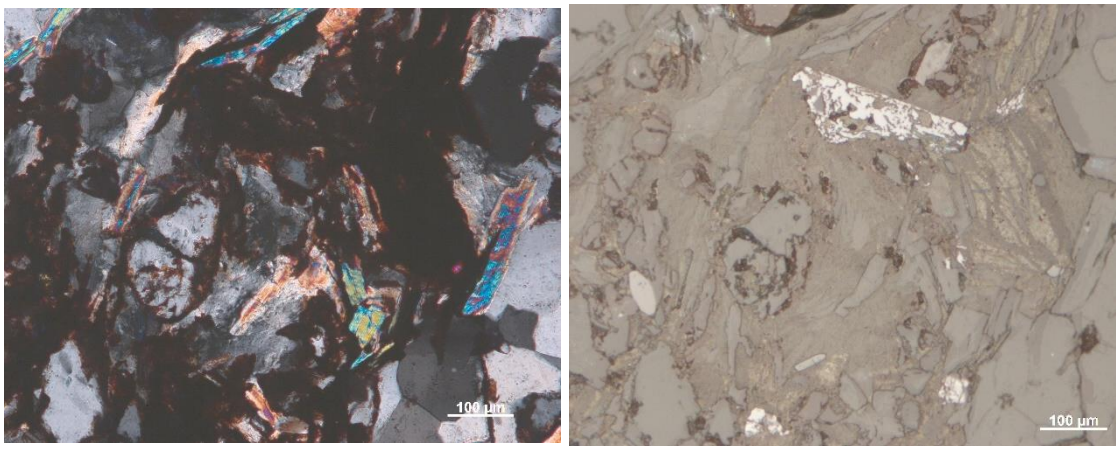

Figure 10: CPL (left) and reflected light (right) photomicrographs of reddened Dalradian schist in Scotland. The hematite is seen altering pre-existing grains, likely biotite.

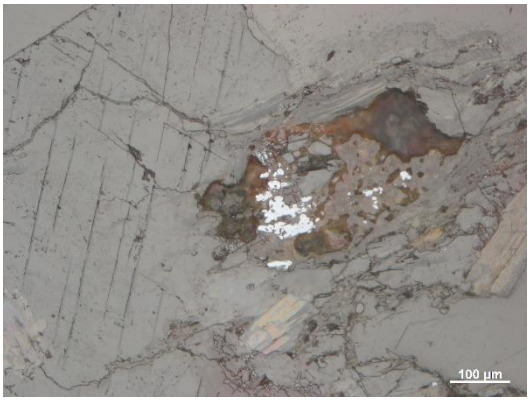

Figure 11: Reflected light photomicrograph of basement rock from Byers Canyon, showing the presence of hematite altering feldspar.

Discussion

At unconformity surfaces in Scotland, a late Permian magnetization residing in hematite is found, which is consistent with previously reported results from reddening at unconformities within the Dalradian Supergroup (Parnell et al., 2000) near the study area. The southerly ChRM that has moderate inclination is interpreted as a CRM that is carried in hematite. Fluid inclusion data from quartz within the Dalradian schist near the sampling area shows that the rocks were heated during burial to no more than 115°C (Parnell et al., 2000). These low burial temperatures rule out a thermoviscous origin for the remanent magnetization.

Reddening of both basement rocks (Parnell et al., 2000) and sedimentary cover rocks (Smith et al., 1974; Wang et al., 1992) throughout Scotland have been reported. Studies by Ricordel et al. (2007) and Franke et al. (2010) report reddened basement rock throughout mainland Europe that possess ChRMs in hematite that are late Permian-early Triassic. The presence of this alteration away from mainland Europe shows that the climatic conditions responsible for the event may have been widespread, or locally similar. The origin of the hematite in all of the studies (Wang et al., 1992; Parnell et al., 2000; Ricordel et al., 2007; Franke et al., 2010) is from oxidizing weathering fluids that permeate cover rock and basement rock at shallow depths.

This increased oxidation is attributed to widespread increased chemical weathering during the late Permian into the early Triassic (Martin and Macdougall, 1995). This increase in chemical weathering mirrors an increase in atmospheric CO_2, which continued to rise through the end of the Permain (Berner, 2001; Montanez et al., 2007). As orogenesis throughout Pangea slowed during the end Permian, a lack of

available fresh silicate rocks for weathering also increased atmospheric CO_2 (Kidder and Worsley, 2004). Paleosols from Antarctica (Sheldon, 2006) as well as Sr and Nd isotope studies (Martin and Macdougall, 1995) indicate an increase in chemical weathering at or near the Permo-Triassic boundary.

Based on the results from Colorado, the increase in chemical weathering that occured as earth entered into a greenhouse climate is not ubiquitous in terms of the paleomagnetic signal. In addition, when plotted on the CO_2 curve by Montanez et al. (2007), the age of the CRMs for Scotland and Long Mountain show no correlation with CO_2 levels. The CRM for Long Mountain was acquired during a time of relatively low atmospheric CO_2. Conversely, the CRM from Scotland was acquired during a time of relatively high CO_2. If the model of CRM acquisition is correct, then there are other variables that create the conditions for hematite authigenesis from supergene weathering fluids.

The hypothesized global increase in chemical weathering has many localized complexities, which may explain the lack of an increased chemical weathering signature in basement rocks that were sampled in Colorado. Riebe et al. (2006) state that tectonic influences are much stronger than climatic ones in accelerating chemical weathering rates. Increased precipitation and localized seasonality (Guiterrez, 2005) will greatly affect the rate of weathering at a particular location. Localized elevation differences will enhance (high terrain) weathering or decrease (low terrain) chemical weathering rates (Riebe et al., 2006). The effects of climate on hematite authigenesis in red beds (Sheldon, 2005) have been questioned, and that certain climate conditions (i.e. increased weathering) may not be the only reason for reddening. Sheldon (2005)

strongly cautioned against unilateral development of a red bed model, and emphasizes the need to understand the local environmental variables that cause creation of hematite within the red beds.

These localized differences may explain the lack of a stable remanent magnetization that is Permo-Triassic in age within what appear to be similar tectonic environments. Within Unaweep Canyon and Byers Canyon, there are reddened basement rocks at an unconformity surface overlain by Mesozoic strata. There are many stable magnetizations present within the Precambrian basement rocks in Unaweep Canyon, but the magnetizations are complex, with many showing unresolvable vector addition between components. In Byers Canyon there are large thrust faults from Ancestral Rocky Mountains and Laramide orogenesis (Tweto, 1957). These faults may have acted as foci for migration of basinal orogenic fluids, which may have altered magnetizations that were held in the rocks prior to tectonic movement. The entire province of Middle Park is highly faulted and structurally complex (Tweto, 1957), which decreases the likelihood of preserving pre-orogenic magnetizations.

The original hypothesis that hematite authigenesis occurs at weathering surfaces due to alteration of the basement rock by supergene weathering fluids is valid (e.g. Parnell et al., 2000; Ricordel et al., 2007). The absence of a stable magnetization at some weathering surfaces (Byers Canyon, Unaweep Canyon) does not disprove the mechanism, but suggests that other factors (i.e. local elevation) may be responsible for retaining magnetic remanence. This hypothesis will be further tested, and numerous possibilities exist for investigation. Preliminary sampling at the Great Unconformity near Durness in northern Scotland reveals that metamorphic basement holds a Cambrian

aged magnetization. Reddened basement rocks in Nevada at the Great Unconformity are also being investigated. More data may further elucidate the mechanisms of magnetization acquisition at unconformity surfaces and the paleoclimatic implications of hematite authigenesis.

Conclusions

Although more work is needed, initial results suggest that the original hypothesis of an abrupt climatic shift at the Permo-Triassic boundary that would result in increased oxidized weathering fluids globally may be more complicated than originally thought. Permian-aged magnetizations are preserved in basement rocks in Scotland and in Oklahoma and yet are absent (or altered) in basement rocks of Colorado. It is likely that local tectonic and local weather and/or climate influences may be stronger drivers of chemical weathering than atmospheric CO_2 levels. This does not disprove that an abrupt global climate shift occurred during the late Permian/early Triassic, but does suggest that careful study of localized environmental variables are needed to fully understand the effects of climate on chemical weathering and the acquisition of magnetization associated with the precipitation of iron oxides at unconformity surfaces.

References

Berner, R.A., Kothavala, X., 2001. GEOCARBIII: a revised model of atmospheric CO_2 over Phanerozoic time. American Journal of Science 301, 182-204.

Chronic, H., 1980, Roadside geology of Colorado, Mountain Press Publishing Company.

Creer, K. M., 1968, Arrangement of the Continents during the Paleozoic Era: Nature, v. 219, no. 5149, p. 41-44.

Engvik, A. K., Putnis, A., Fitzgerald, J. D., and Austrheim, H., 2008, Albitization of granitic rocks: the mechanism of replacement of oligoclase by albite: The Canadian Mineralogist, v. 46, p. 1401-1415.

Fisher, R., 1953, Dispersion on a Sphere: Proceedings of the Royal Society of London. Series A, Mathematical and Physical Sciences, v. 217, no. 1130, p. 295-305.

Franke, C., Thiry, M., Gomez-Gras, D., Jelenska, M., Kadzialko-Hofmokl, M., Lagroix, F., Parcerisa, D., Spassov, S., Szuszkiewicz, A., and Turniak, K., 2010, Paleomagnetic age constraints and magneto-mineralogic implications for the Triassic paleosurface in Europe: Gephysical Research Abstracts, v. 12, no. EGU General Assembly.

Gutierrez, M., 2005, Developments in Earth Surface Processes, *in* Jr., J. F. S., ed., Climatic Geomorphology, ElSevier, p. 760.

Hamilton, M., Elmore, R.D., Weaver, B., and S.A. Dulin, 2014, Petrology and paleomagnetism of the Long Mountain Granite, Wichita Mountains, Oklahoma *in* Igneous and Tectonic History of the Southern Oklahoma Aulacogen; Oklahoma Geologic Survey vol. 38, p. 319-325.

Kidder, D. L., and Worsley, T. R., 2004, Causes and consequences of extreme Permo-Triassic warming to globally equable climate and relation to the Permo-Triassic extinction and recovery: Palaeogeography, Palaeoclimatology, Palaeoecology, v. 203, p. 207-237.

Kirschvink, J. L., 1980, The least-squares line and plane and the analysis of paleomagnetic data: Geophysical Journal of the Royal Astronomical Society, v. 62, no. 3, p. 699-718.

Martin, E. E., and Macdougall, J. D., 1995, Sr and Nd isotopes at the Permian/Triassic boundary: A record of climate change: Chemical Geology, v. 125, p. 73-99.

Montanez, I. P., Tabor, N. J., Niemeier, D., DiMichele, W. A., Frank, T. D., Fielding, C. R., Isbell, J. L., Birgenheier, L. P., and Rygel, M. C., 2007, CO2-Forced climate and vegetation instability during late Paleozoic deglaciation: Science, v. 315, no. 87-91.

Parcerisa, D., Thiry, M., and Schmitt, J. M., 2010, Albitisation related to the Triassic unconformity in igneous rocks of the Morvan Massif (France): Internation Journal of Earth Science (Geologische Rundschau), v. 99, no. 3, p. 18.

Parcerisa, D., Franke, C., and Fabrega, C., 2013, Implications from Paleomagnetic Age Constraints and Petrology Analyses on the Reconstruction of the Triassic Paleosurface in Europe-Examples from Catalonia and the Polish Sudetes: American Geophysical Union Fall Meeting Abstracts, v. 1, no. 2013.

Parnell, J., Baron, M., Davidson, M., Elmore, R. D., and Engel, M., 2000, Dolomitic breccia veins as evidence for extension and fluid flow in the Dalradian of Argyll: Geologic Magazine, v. 137, no. 4, p. 447-462.

Pederson, J. L., Mackley, R. D., and Eddleman, J. L., 2002, Colorado Plateau uplift and erosion evaluated using GIS: GSA Today, v. 12, no. 8, p. 4-10.

Ricordel, C., Parcerisa, D., Thiry, M., Moreau, M. G., and Gomes-Gras, D., 2007, Triassic magnetic overprints related to albitization in granites from the Morvan massif (France): Palaeogeography, Palaeoclimatology, Palaeoecology, v. 251, p. 268-282.

Riebe, C. S., Kirchner, J. W., Granger, D. E., and Finkel, R. C., 2001, Strong tectonic and weak climatic control of long-term chemical weathering rates: Geology, v. 29, no. 6, p. 511-514.

Sheldon, N. D., 2005, Do red beds indicate paleoclimatic conditions?: A Permian case study: Palaeogeography, Palaeoclimatology, Palaeoecology, v. 228, p. 305-319.

Sheldon, N. D., 2006, Abrupt chemical weathering increase across the Permian-Triassic boundary: Palaeogeography, Palaeoclimatology, Palaeoecology, v. 231, p. 315-321.

Smith, D. B., Bunstrom, R. G. W., Manning, P. I., Simpson, S., and Shotton, F. W., 1974, A Correlation of Permian Rocks in the British Isles: Journal of the Geological Society of London, v. 130, p. 1-45.

Soreghan, G. S., Sweet, D. E., Marra, K. R., Eble, C. F., Soreghan, M. J., Elmore, R. D., Kaplan, S. A., and Blum, M. D., 2007, An Exhumed Late Paleozoic Canyon in the Rocky Mountains: The Journal of Geology, v. 115, p. 473-481.

Spencer, J. E., and Patchett, P. J., 1997, Sr isotope evidence for a lacustrine origin for the upper Miocene to Pliocene Bouse Formation, lower Colorado River trough, and implications for timing of Colorado Plateau uplift: Geological Society of America Bulletin, v. 109, p. 767-778.

Torsvik, T. H., 1984, Palaeomagnetism of the Foyers and Strontian granites, Scotland: Physics of the Earth and Planetary Interiors, v. 36, p. 163-177.

Torsvik, T. H., Voo, R. V. d., Preeden, U., Niocaill, C. M., Steinberger, B., Doubrovine, P. V., Hinsbergen, D. J. J. v., Domeier, M., Gaina, C., Tohver, E., Meert, J. G., McCausland, P. J. A., and Cocks, L. R. M., 2012, Phanerozoic polar wander, palaeogeography and dynamics: Earth-Science Reviews, v. 114, p. 325-368.

Tweto, O., 1957, Geologic Sketch of Southern Middle Park, Colorado, Guidebook to the Geology of the North and Middle Parks Basin, Colorado, Rocky Mountain Association of Geologists.

Wang, W. H., 1992, Origin of reddening and secondary porosity in Carboniferous sandstones, Northern Ireland, *in* Parnell, J., ed., Basins on the Atlantic Seaboard: Petroleum Geology, Sedimentology and Basin Evolution, Volume 62: London, Geological Society of London, p. 243-254.

Zijderveld, J. D. A., 1967, A.C. Demagnetization of rocks: Analysis of results, *in* Collison, D. E., K.M.Creer, and Runcorn, S. K., eds., Methods in Paleomagnetism: New York, El Sevier Science, p. 254-286.